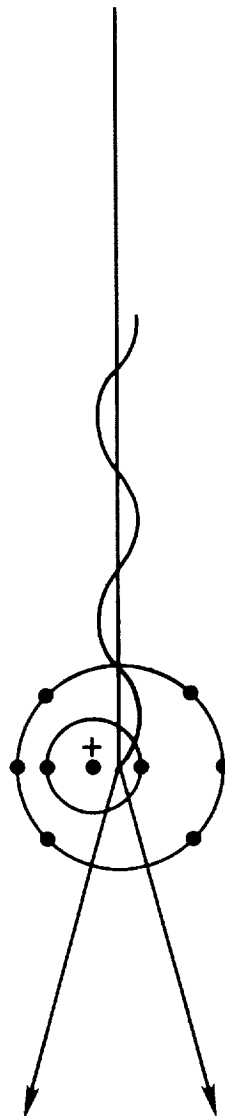


N91-14098

WORKSHOP ON COSMOGENIC NUCLIDE PRODUCTION RATES



7

4

7

4

**WORKSHOP ON
COSMOGENIC NUCLIDE PRODUCTION RATES**

**Edited by
Peter A. J. Englert
Robert C. Reedy
Rolf Michel**

**Held at
The University of Vienna
Vienna, Austria
July 25-26, 1989**

**Sponsored by
Lunar and Planetary Institute
San Jose State University
and
The University of Vienna**

Lunar and Planetary Institute 3303 NASA Road 1 Houston, Texas 77058-4399

LPI Technical Report Number 90-05

Compiled in 1990 by the
LUNAR AND PLANETARY INSTITUTE

The Institute is operated by Universities Space Research Association under Contract NASW-4066 with the National Aeronautics and Space Administration.

Material in this document may be copied without restraint for library, abstract service, educational, or personal research purposes; however, republication of any portion requires the written permission of the authors as well as appropriate acknowledgment of this publication.

This report may be cited as:

Englert P. A. J., Reedy R. C., and Michel R., eds. (1990) *Workshop on Cosmogenic Nuclide Production Rates*. LPI Tech. Rpt. 90-05. Lunar and Planetary Institute, Houston. 124 pp.

Papers in this report may be cited as:

Author A. A. (1990) Title of paper. In *Workshop on Cosmogenic Nuclide Production Rates* (P. A. J. Englert, R. C. Reedy, and R. Michel, eds.), pp. xx-yy. LPI Tech. Rpt. 90-05. Lunar and Planetary Institute, Houston.

This report is distributed by:

ORDER DEPARTMENT
Lunar and Planetary Institute
3303 NASA Road 1
Houston, TX 77058-4399

Mail order requestors will be invoiced for the cost of shipping and handling.

Contents

Preface	10 MIT
Program	70 MIT
Workshop Summary	110 MIT
Abstracts	
Isotope Production by Solar and Galactic Cosmic Rays: Experimental Depth Profiles and Model Calculations <i>N. Bhandari</i>	19 ⁵¹
Studies of the Cosmic Ray Induced Gamma-Emission at Planetary Surfaces Using Monte-Carlo Techniques in Respect of the Mars Observer Mission <i>G. Dage, P. Cloth, P. Dragovitsch, D. Filges, and J. Brückner</i>	24 ⁵²
Cross Sections for Long-Lived Radionuclides from High Energetic Charged-Particle-Induced Reactions <i>B. Dittrich, U. Herpers, R. Bodemann, M. Lüpke, R. Michel, H. J. Hofmann, and W. Wölfli</i>	28
INC Model Calculation of Cosmogenic Nuclide Production in Stony Meteorites <i>M. Divadeenam, T. A. Gabriel, O. W. Lazareth, M. S. Spergel, and T. E. Ward</i>	36
Applications of the Hermes Code System in Meteoritics <i>P. Dragovitsch, P. Cloth, G. Dage, D. Filges, and R. Michel</i>	39
Simulation of the GCR Irradiation of Meteoroids: Unification of Experimental and Theoretical Approaches <i>P. Dragovitsch and the Cologne Collaboration</i>	44
Simulation Experiments for Cosmogenic Nuclide Production Rates <i>P. A. J. Englert</i>	47
A Model for the Production of Cosmogenic Nuclides in Chondrites <i>T. Graf, H. Baur, and P. Signer</i>	49
Composition Dependence of Cosmogenic Nuclide Production Rates <i>G. F. Herzog</i>	51
Saturated ²⁶ Al in Stony Meteorites <i>J. E. Keith, H. R. Heydegger, and K. E. Kavana</i>	53
Cosmogenic Nuclide Production in Extraterrestrial Objects <i>D. Lal</i>	55
Status of Charged Particles and Neutrons Induced Nuclear Reactions Leading to Stable and Radioactive Isotopes <i>B. Lavielle</i>	60

Cross Sections of Neon and Krypton Isotopes Produced by Neutrons <i>B. Lavielle, H. Sauvageon, and P. Bertin</i>	65
Exposure Ages and Long-Term Variations of the Cosmic Ray Flux <i>K. Marti</i>	70
Simulation of Cosmogenic Nuclide Production <i>J. Masarik and P. Povinec</i>	71
Prediction of Thin-Target Cross Sections of Neutron-Induced Reactions up to 200 MeV <i>R. Michel and H. Lange</i>	76
Thin-Target Cross Sections for the Production of Cosmogenic Nuclides by Charged-Particle-Induced Reactions <i>R. Michel, R. Bodemann, M. Lüpke, U. Herpers, and B. Dittrich</i>	81
Monte Carlo Modelling of the Production of Cosmogenic Nuclides in Extraterrestrial Matter by Galactic Cosmic Ray Particles <i>R. Michel, P. Dragovitsch, G. Dagge, P. Cloth, and D. Filges</i>	86
^{10}Be and ^{26}Al in Metal and Stone Phases of Meteorites <i>H. Nagai, M. Honda, M. Imamura, K. Kobayashi, and H. Ohashi</i>	91
Depth Profiles of Radionuclide Production in Solids with 2-D Geometry <i>K. Nishiizumi, R. C. Reedy, and J. R. Arnold</i>	96
Cosmogenic-Nuclide Production Rates Calculated Using Particle Fluxes and Cross Sections <i>R. C. Reedy</i>	98
Production Rates of Cosmogenic Planetary Gamma Rays <i>R. C. Reedy and P. A. J. Englert</i>	100
Cross Sections for Galactic-Cosmic-Ray-Produced Nuclides <i>R. C. Reedy, K. Nishiizumi, and J. R. Arnold</i>	102
A New Semi-Empirical Formula for Spallation and Fragmentation Reactions Induced by High Energy Protons <i>H. Sauvageon</i>	104
Production Rates of Noble Gases in Meteorites -- A Review <i>L. Schultz</i>	109
Evolution of Meteoritic Bodies in Space <i>G. K. Ustinova, V. A. Alexeev, and A. K. Lavrukina</i>	111
Cosmogenic Radionuclide Production Rates in Meteorites <i>S. Vogt</i>	112
Study of High Energy Particle Propagation Inside Solid Matter and Derivation of Cosmogenic Nuclide Production Rates in Iron Meteorites <i>B. Zanda</i>	119
List of Workshop Participants	123

OMIT TO
P. 19

Preface

This report documents the Workshop on Cosmogenic Nuclide Production Rates held at the Institute of Geochemistry of The University of Vienna, Vienna, Austria, on July 25-26, 1989. The workshop was cosponsored by the Lunar and Planetary Institute, San Jose State University, and The University of Vienna. The conveners were Dr. Peter A. J. Englert of the San Jose State University, Dr. Rolf Michel of the University of Hannover, and Dr. Robert C. Reedy of the Los Alamos National Laboratory, with technical support headed by Dr. Christian Koeberl of The University of Vienna and Ms. Pamela Jones of the Lunar and Planetary Institute.

In 1984 the Workshop on Cosmogenic Nuclides (published as Lunar and Planetary Institute Technical Report Number 86-06, edited by Robert C. Reedy and Peter Englert, 1986) was held in Los Alamos, New Mexico, USA, and demonstrated that this 40-year-old field of studies of the effects of cosmic-ray bombardment of small and large bodies of the solar system is still very active. Recent improvements in experimental techniques and theoretical understanding, together with new materials being investigated and new scientific applications of cosmogenic nuclides, have caused a revival of this field of science. However, the large variety of applications makes it impossible to deal with all the different aspects of the interactions of cosmic rays with matter within a two-day workshop. Therefore, the present workshop was restricted to work involving extraterrestrial materials.

The main questions still to be answered by investigating cosmogenic nuclides in extraterrestrial matter are those involving the spectral distribution, composition, and intensity of solar and galactic cosmic rays over timescales of up to 10^9 years, as well as the irradiation histories of small and large bodies of the solar system. These questions can only be answered by untangling the cosmic-ray record in the irradiated objects. There is really no other way to adequately receive information about many aspects of the past other than by studying cosmogenic nuclides, and after 40 years of investigation the final answers are not yet known. Production rates of cosmogenic nuclides are the key quantities for any interpretation of the observed abundances of cosmogenic nuclides. Therefore, this workshop was dedicated to cosmogenic nuclide production rates.

The original excitement about being able to derive, for example, cosmic-ray exposure ages has long been overcome by the struggle for the improvement of the cosmogenic-nuclide-based dating methods. Many problems are not yet solved. Extensive meteorite, terrestrial, and extraterrestrial sample analyses, sophisticated simulation experiments, and model calculations are employed to refine our understanding of cosmogenic nuclide production rates. Subjects of continuing studies are primarily the influence of the chemical composition and the effects of shielding on the production rates. This workshop surveyed the present status of experimental measurements of extraterrestrial samples, of terrestrial simulation experiments, of the various theoretical models for the interpretation of cosmogenic-nuclide abundances, and, last but not least, of the requirements of nuclear data for a reliable theoretical interpretation. It provided an opportunity for researchers to discuss open questions, to define the future needs of

experimental and theoretical work, and to arrange collaborations and consortia.

There were 42 registered participants from 10 countries at the Workshop on Cosmogenic Nuclide Production Rates. Two groups from Eastern Europe could not attend the workshop but submitted written contributions. At the 2-day workshop, there were 18 oral presentations, 8 posters, and a panel discussion summarizing and closing the workshop. Presentations in the four scientific sessions consisted of several invited presentations and contributed papers. The contributed papers were roughly divided equally between oral and poster presentations. The invited oral presentations focused on different aspects of the problem and served as introductions to various subjects. The eight posters were an important part of the workshop. Poster presenters were given the opportunity to present key points in a short (about three minutes with one "visual") oral presentation without discussion immediately preceding one of two poster sessions. There was ample time to view posters during coffee breaks. There were no parallel sessions.

The presentations were divided into discussion topics. The following general topic areas were used: (1) measured cosmogenic noble gas and radionuclide production rates in meteorite and planetary surface samples, (2) cross-section measurements and simulation experiments, and (3) model calculations: interpretation of sample studies and simulation experiments.

During the first day, experimental measurements on cosmogenic nuclides in extraterrestrial materials were mainly dealt with, while the second day was dedicated to terrestrial simulation experiments, measurements and predictions of cross sections, and model calculations. In addition to discussions after each talk, there was a panel at the end of the workshop. Panel members presented

their summaries of the workshop to initiate further discussion by all participants. After the panel and general discussion, the participants departed by bus for the workshop social event at a "Heuriger" (a Viennese wine tavern).

Information and ideas presented at the workshop will help us to obtain more accurate cosmogenic nuclide production rates in order to address many questions, such as the possible exposure-age differences among petrologic types in the ~8-Ma exposure-age peak of the H-chondrites and the problem of unraveling complex exposure histories of meteorites and planetary surfaces. The workshop's presentations and discussions should help to clarify (1) which production rates are considered to be sufficiently well studied, (2) which chemistry and shielding correction methods are satisfactory, (3) where improvements have to be made, and (4) how to proceed in order to solve identified problems.

We wish to thank all participants of the workshop, especially those who agreed to present invited papers and those who contributed papers on the workshop's theme and/or participated in the discussion at the workshop. They all made the workshop a success. We are especially grateful to P. A. J. Englert, U. Herpers, K. Nishiizumi, and J. R. Arnold for serving as session chairs and for keeping the program on schedule. We also wish to thank J. R. Arnold, F. Begemann, P. Eberhardt, G. F. Herzog, and D. Lal for serving on the panel and leading the lively discussion at the end of the workshop. We want to thank all sponsoring agencies, especially the Lunar and Planetary Institute, Houston, USA, and the Institute of Geochemistry, The University of Vienna, Austria, for technical, logistical, and financial assistance. Very special thanks go to C. Koeberl (Institute of Geochemistry, The University of Vienna) and P. Jones (Program Services Department, Lunar and Planetary

Institute, Houston) for invaluable help with the organization and to their many assistants whose help was crucial in preparing for and running the workshop. Thanks also to Joan Shack and others in the Publications Services Department of the Lunar and Planetary Institute for preparing the abstract volume and this report.

Peter A. J. Englert
San Jose, California

Robert C. Reedy
Los Alamos, New Mexico

Rolf Michel
Hannover, Federal Republic of Germany

Program

Tuesday morning, 25 July 1989

Registration and small welcome party

SESSION I
Chairman: P. A. J. Englert

Welcome, opening remarks, workshop ground rules

L. Schultz*
Production Rates of Noble Gases in Meteorites - A Review

K. Marti*
Exposure Ages and Long-Term Variations of the Cosmic Ray Flux

Tuesday afternoon, 25 July 1989

SESSION II
Chairman: U. Herpers

K. Nishiizumi*, R. C. Reedy, and J. R. Arnold
Depth Profiles of Radionuclide Production in Solids with 2π Geometry

S. Vogt*
Cosmogenic Radionuclide Production Rates in Meteorites

Brief oral presentations of posters

R. C. Reedy, K. Nishiizumi, and J. R. Arnold
Cross Sections for Galactic-Cosmic-Ray-Produced Nuclides

R. Michel, R. Bodemann, M. Lüpke, U. Herpers, and B. Dittrich
Thin-Target Cross Sections for the Production of Cosmogenic Nuclides by Charged-Particle-Induced Reactions

R. Michel and H. Lange
Prediction of Thin-Target Cross Sections of Neutron-Induced Reactions up to 200 MeV

B. Lavielle, H. Sauvageon, and P. Bertin
Cross Sections of Neon and Krypton Isotopes Produced by Neutrons

Coffee break/poster session

G. F. Herzog*
Composition Dependence of Cosmogenic Nuclide Production Rates

H. Nagai, M. Honda*, M. Imamura, K. Kobayashi, and H. Ohashi
Cosmogenic Be-10 and Al-26 in Metal and Stone Phases of Meteorites

*Denotes speaker

J. E. Keith*, H. R. Heydegger, and K. E. Kavana
Saturated ^{26}Al in Stony Meteorites

D. Lal*
Cosmogenic Nuclide Production in Extraterrestrial Objects

Wednesday morning, 26 July 1989

SESSION III
Chairman: K. Nishiizumi

B. Lavielle*
Status of Charged Particle and Neutron Induced Nuclear Reactions Leading to Stable and Radioactive Isotopes

B. Dittrich*, U. Herpers, R. Bodemann, M. Lüpke, R. Michel, H. J. Hofmann, and W. Wölfli
Cross Sections for Long-Lived Radionuclides from High Energetic Charged-Particle-Induced Reactions

H. Sauvageon*
A New Semi-Empirical Formula for Spallation and Fragmentation Reactions Induced by High Energy Protons

Brief oral presentations of posters

P. Dragovitsch, P. Cloth, G. Dagge, D. Filges, and R. Michel
Applications of the Hermes Code System in Meteoritics

M. Divadeenam, T. A. Gabriel, O. W. Lazareth, M. S. Spergel, and T. E. Ward
(presented by R. C. Reedy)
INC Model Calculation of Cosmogenic Nuclide Production in Stony Meteorites

G. Dagge, P. Cloth, P. Dragovitsch, D. Filges, and J. Brückner
Studies of the Cosmic Ray Induced γ -Emission at Planetary Surfaces Using Monte-Carlo Techniques in Respect of the Mars Observer Mission

R. C. Reedy and P. A. J. Englert
Production Rates of Cosmogenic Planetary Gamma Rays

Coffee break/poster session

P. A. J. Englert*
Simulation Experiments for Cosmogenic Nuclide Production Rates

P. Dragovitsch* and the Cologne Collaboration
Simulation of the GCR Irradiation of Meteoroids: Unification of Experimental and Theoretical Approaches

Wednesday afternoon, 26 July 1989

SESSION IV
Chairman: J. R. Arnold

T. Graf*, H. Baur, and P. Signer
A Model for the Production of Cosmogenic Nuclides in Chondrites

R. C. Reedy*
Cosmogenic-Nuclide Production Rates Calculated Using Particle Fluxes and Cross Sections

R. Michel*, P. Dragovitsch, G. Dagge, P. Cloth, and D. Filges
Monte Carlo Modelling of the Production of Cosmogenic Nuclides in Extraterrestrial Matter by Galactic Cosmic Ray Particles

Coffee break/poster session

B. Zanda*
Study of High Energy Particle Propagation Inside Solid Matter and Derivation of Cosmogenic Nuclide Production Rates in Iron Meteorites

N. Bhandari*
Isotope Production in Chondrites by Cosmic Rays: Experimental Depth Profiles and Model Calculations

Panel discussion (J. R. Arnold, F. Begemann, P. Eberhardt, G. F. Herzog, and D. Lal)
and general discussion

10/10/10

Workshop Summary

The Workshop on Cosmogenic Nuclide Production Rates was well focused, with the various aspects of research leading to production rates well covered. In keeping with the workshop's focus, not much was said about specific applications. A new review paper by S. Vogt, G. F. Herzog, and R. C. Reedy (*Rev. Geophys.*, in press) briefly surveys cosmogenic nuclide production rates but concentrates on many applications of cosmogenic nuclides, including several types of unusual samples such as cosmic spherules and meteoritic grains irradiated ~4.6 Ga ago.

Very little was said about the related areas of tracks and thermoluminescence (TL), which are also produced by cosmic rays. While TL was mentioned as possibly providing information about radiation effects, the interpretation of most TL data has not been very quantitative. It was agreed that measurements of the tracks made by heavy cosmic-ray nuclei are valuable in unfolding exposure histories and should be done on many of the samples used for cosmogenic-nuclide studies. However, it was also noted that very few researchers now measure cosmic-ray tracks and that there is a need for more researchers to measure them in conjunction with cosmogenic nuclides.

There were no major "breakthroughs" or revolutionary new ideas presented on production rates, as might be expected for a mature area of research. Much good work was reported that has resulted in improving production rates. The production rates for spallogenic nuclides in the Moon were felt to be in fairly good shape. Most of the work has concentrated on stony meteorites, mainly ordinary chondrites. One workshop participant noted that "meteorites are complicated things" that need to be studied with a "variety of tools," one of those "tools" being cosmogenic nuclides. Relatively little work has been done on iron and stony-iron meteorites, which tend to have been overlooked during the last few decades.

Many of the comments made during the workshop are given below under specific research topics. There was a consensus that the agreement between predicted production rates and measurements has been fairly good and the quality of production rates is improving. However, it was agreed that there is much to do to get production rates that are good enough to address many problems that are not now satisfactorily being answered. Some workshop participants commented that production rates should be less concerned with fitting old data and more with making predictions for new

meteorites under investigation. Others noted that most models are flexible enough that they can predict (although sometimes not very well) many new cases. Several participants pointed out the need to plan ahead, both for new types of samples (such as samples returned from Mars and volatile-rich comets) and for other cosmogenic effects (such as gamma rays and neutrons that escape from planetary surfaces). To stimulate discussion one participant wondered, if production rates could be predicted to within a few percent, what meteoriticists would do with them. However, the many problems mentioned during the workshop, some presented in the next few paragraphs, make it clear that there is much that could be done with improved production rates, especially high-quality ones.

High among the general problem areas mentioned at the workshop was the need for better shielding corrections that can account for the size and shape of the target object and for the sample's location in that object. There is a need to identify the strengths and weaknesses of the presently used shielding corrections and to determine where their applications are limited, such as low $^{22}\text{Ne}/^{21}\text{Ne}$ ratios. New shielding indicators are needed for a few cases, such as $^{78}\text{Kr}/^{83}\text{Kr}$ for some achondrites. Additional methods to acquire exposure ages that are independent of shielding effects (such as possibly $^{10}\text{Be}/^{21}\text{Ne}$ ratios) are needed. Several participants wondered if commonly accepted approaches, such as $^{81}\text{Kr}/\text{Kr}$ ages, are more limited than generally accepted.

The quality of some of the data used in cosmogenic-nuclide studies was questioned. For example, it is realized that cross sections measured decades ago could be wrong, either because of experimental deficiencies or poor cross sections for the reactions used to monitor the incident beam. The incorrect atmospheric neon composition used prior to 1965 needs to be considered in using older neon measurements. Other participants mentioned doubts about the quality of older measurements of cosmogenic nuclides. Another question involving experimental measurements is whether weathering has affected the concentrations of certain cosmogenic nuclides in meteorite finds. Some participants felt that only fresh falls should be considered for problems requiring high-quality measurements of meteorites.

Some specific problem areas still persist in the field of cosmogenic nuclides. For example, it has not been resolved why there are high production rates inferred

using the ^{26}Al activities in meteorites with short exposure ages. Work is needed on unfolding the results for meteorites with short exposure ages. Another old question concerns variations in the fluxes of galactic-cosmic-ray (GCR) particles in the past, including changes during the last few million years, during the last $\sim 10^8$ - 10^9 years, and ~ 4.6 Ga ago. An important problem is determining the fraction of stony meteorites with complex exposure histories, which is important in determining their origins.

A few new problems have arisen. One that created some discussion but no resolution during the workshop is whether the matrix of a meteorite (e.g., stone vs. iron) affects the flux and spectral distribution of secondary cosmic-ray particles, especially neutrons. Some results implied large matrix effects; others indicated small or no effects. More measurements and some theoretical calculations (such as with Monte Carlo codes) are needed before this question can be well answered.

EXPERIMENTAL DATA ON COSMOGENIC NUCLIDES

Several presentations described the state of knowledge about the measured data for stable and radioactive cosmogenic nuclides in meteorites and lunar surface samples. There now exists a large body of data that is easily accessible thanks to two recent compilations for meteoritic measurements of the radionuclides ^{10}Be , ^{26}Al , ^{36}Cl , and ^{53}Mn by K. Nishiizumi (*Nucl. Tracks Radiat. Meas.*, 13, 209-273, 1987) and the light noble gases (He, Ne, and Ar) by L. Schultz and H. Kruse (*Meteoritics*, 24, 155-172, 1989). It would be very good to continue these collections and to publish updates in order to keep track of new measurements.

For the cosmogenic-nuclide data there exist differences in quality or scientific value. For many meteorites and lunar samples there now exist detailed depth profiles, which are valuable experimental descriptions of the depth and size dependence of production rates. However, a few of these "test" cases are poor ones, such as using the core measurements from St. Severin to test models that assume spherical geometries. Work is being done now on detailed studies of small meteorites (such as Salem). Several workshop participants noted the need for good depth-vs.-concentration profiles in meteorites with large preatmospheric sizes (i.e., radii greater than 50 cm).

Many "same sample measurements," which allow for good comparisons of production ratios, are now available for cosmogenic nuclides. Accelerator mass spectrometry has made it easy to perform measurements of many long-lived radionuclides in small

aliquots. Some new cosmogenic nuclides are being measured, such as ^{129}I and ^{41}Ca , that have half-lives or production mechanisms different from those of the nuclides typically measured. As many cosmogenic nuclides as possible should be measured on several samples. There is also an increasing number of measurements for rare meteorite classes, often due to their availability from the Antarctic meteorite collections. These analyses will improve our knowledge about the influence of the target chemistry on the production rates. For many samples there is a need to measure the abundances of the target elements, especially for minor and more variable elements (such as those from which Kr isotopes are made).

Recent measurements have enlarged the number of cosmogenic nuclides for which solar-cosmic-ray (SCR) effects have been established in lunar samples or have improved the quality of such measurements. The existence of SCR-produced nuclides in small meteorites is now well established. A lack of cross sections, which often hampers the interpretation of these SCR effects, should soon be overcome. The SCR isotopes will then allow us to study more long-term fluxes and spectral distributions of SCR particles and to resolve still existing discrepancies.

We now realize that "mean production rates" are often of limited value when interpreting cosmogenic-nuclide data, because they mix depth- and size-effects in a manner that is biased by the random collection of meteoritic debris. However, such results, especially those with some simple shielding corrections like the noble-gas results recently reported by O. Eugster (*Geochim. Cosmochim. Acta*, 52, 1649-1662, 1988), are good starting points. The empirical data and semi-empirical models have not provided criteria to sufficiently unravel shielding and chemistry effects on cosmic-ray production rates. We need effective solutions to the following critical problems: (1) how to derive precise exposure ages for normal meteorites (i.e., those those with simple exposure histories); (2) how to distinguish "normal" from "interesting" meteorites (such as those with complex exposure histories); and (3) how to determine the exposure geometries and times for the different stages in meteorites with complex histories.

CROSS SECTIONS

Reliable thin-target excitation functions for the relevant nuclear reactions are a *sine qua non* for any physical model of the production of cosmogenic nuclides. As far as primary cosmic-ray particles are concerned, protons and ^4He nuclei have to be considered, while neutrons are the dominating secondary particles. Reactions of other particles, such as pions,

may contribute, but from the present state of the art in modeling the production of cosmogenic nuclides they are usually neglected. Even for proton-, neutron-, and ^4He -induced reactions the existing experimental databases are neither comprehensive nor reliable. While many cross sections exist for proton-induced reactions, cross sections for reactions induced by ^4He and by high-energy ($E > 14$ MeV) neutrons are scarce. Moreover, most of the existing cross sections are not for relevant cosmogenic nuclides.

In several workshop contributions, the present unsatisfactory status for the desired cross sections was described, and the more urgent needs for data were outlined. Reports were given about experimental studies and theoretical predictions by which the situation might be improved in the future. It was estimated that several hundred excitation functions are needed for reactions producing cosmogenic nuclides. As the range of incident particles and their energies and of product nuclei is large, several teams should do the measurements. Occasional overlap of measurements would serve as a check of the quality of the measured cross sections. In reporting measured cross sections, the cross sections used to monitor the irradiation should be given. There is a serious need for strong, well-characterized sources of energetic neutrons. A compilation of existing cross sections, especially for cosmogenic nuclides, would be very useful.

SIMULATION EXPERIMENTS

Surveys were given on recent simulation experiments, including irradiations of both stationary and moving thick targets. Stationary targets are useful to study the interactions of GCR particles with planetary surfaces, provided that the targets are large enough to keep secondaries inside. In this case they can give valuable information about the production of secondary particles, cosmogenic nuclides, and gamma rays. The latter will be of interest for the Mars Observer mission.

Stationary thick-target experiments poorly simulate the GCR irradiation of meteoroids, especially small ones. This problem can be overcome by bombardments of moving targets by which the isotropic GCR irradiation is well simulated. The particle leakage in these isotropically-irradiated artificial "meteoroids" matches that under cosmic irradiation conditions. Such experiments have been performed during the last few years. They demonstrated the importance of secondary neutrons for the production of cosmogenic nuclides, especially in relatively small objects.

Considerable progress has been made by simulation experiments. However, a complete simulation cannot be achieved because irradiation experiments with a

continuous spectrum of bombarding particles that matches that of primary GCR particles are not possible. The multiplicities for secondary particle production strongly depends on the energies of the primary particles. Consequently the production rates measured in simulation experiments clearly cannot be directly compared with those observed in extraterrestrial matter. Simulation experiments provide excellent benchmarks with which to test calculational models because irradiation conditions are fully controlled.

Thick-target irradiations are elaborate undertakings, and there is a need to carefully select the irradiating conditions and the products measured. Several research teams should be involved to maximize the return from such irradiations. The secondary particle fields in such targets, especially fast and slow neutrons, should be measured. Eventually simulations could be done by deploying and later retrieving a synthetic meteoroid in space.

MODEL CALCULATIONS

For SCR interactions a number of models exist that adequately describe the production of cosmogenic nuclides in cosmic dust, meteoroids, and on the lunar surface. These models are based on physically straightforward calculations of the depth-dependent spectra of solar protons and alpha particles and on the evaluation of the response integrals using thin-target excitation functions. The quality and reliability of these model calculations depend very much on the availability of thin-target excitation functions for energies up to ~ 200 MeV/nucleon.

For the interaction of GCR particles with matter, the situation is much more complicated. Due to the higher energies of GCR particles, secondary particle fields become important in all but the very smallest targets. The spectral distributions and intensities of these particles depend strongly on the size of and depth inside the irradiated object and on its chemical composition. Spectral variations in the primary radiation could also influence the secondary particle fields.

The existing models describing GCR interactions with extraterrestrial matter can be categorized as semi-empirical, parametric, or physical ones. In semi-empirical models, production rates are calculated by folding empirically derived depth- and size-dependent "GCR nucleon spectra" with thin-target excitation functions. A feature of these models is that the depth and size dependences of GCR nucleon fluxes are usually described by only a few depth- and size-dependent parameters, such as a normalization constant and a spectral hardness parameter. These models usually do not explicitly distinguish among different particle types.

Some semi-empirical models are poor for small meteoroids because there is not a smooth transition of the "nucleon" spectra to the free-space GCR spectra.

In another type of semi-empirical model, production rates are derived by empirical formulas based on spallation systematics, taking the mass difference between target material and product nuclide as the key characterizing quantity. Production rates are calculated using two parameters, one normalizing the production rates to a "reference production rate" and the other a shielding factor, which, however, is not yet related quantitatively to the physical depth of a sample in or to the size of the irradiated body.

In the parametric models, the depth and size dependence of production rates are derived by assuming attenuation lengths for the various reacting nuclear fields and by fitting the proposed functions to observed depth profiles afterward. These models are capable of reproducing the shapes of measured production depth profiles in meteorites. However, the parameters used cannot be interpreted physically, and extrapolations to very different meteoroid sizes should be used with caution.

Physical models are those approaches that try to calculate production rates by basic physical principles and from nuclear quantities. In such models the complex phenomena in the intra- and internuclear cascades are calculated, in particular production and transport of secondary particles. The production rates of cosmogenic nuclides are derived either directly by Monte Carlo calculations or indirectly by integrating over energy the product of the calculated depth- and size-dependent fluxes of the different nuclear active particles and thin-target cross sections of the contributing nuclear reactions.

The direct calculation of residual-nuclide distributions by intranuclear-cascade-evaporation (INCE) models has some disadvantages, however. It is extremely time consuming and practically impossible to calculate a large number of cosmogenic nuclides in one Monte Carlo run. Even worse, the accuracy of this method is not adequate because these codes at present only consider an initial phase of fast interactions dominated by nucleon-nucleon interactions and a second evaporation phase modeled with a statistical model of nuclear reactions, thereby neglecting both pre-equilibrium reactions and other formation processes such as fragmentation. Such direct calculations of residual nuclei are often very poor for isomers, such as 0.7-Ma ^{26}Al .

A more promising application of INCE models and Monte Carlo techniques for the modeling of cosmogenic nuclides in extraterrestrial matter is to calculate the depth- and size-dependent spectra of primary and secondary GCR particles and then to combine them

with thin-target cross sections of the respective nuclear reactions. This method has been successfully used to describe the production rates observed in terrestrial simulation experiments and is now being applied to production-rate calculations for lunar and meteoroidal irradiation conditions. Calculations presented for lunar surface conditions demonstrated that the high-energy Monte Carlo calculations are extendible to low-energy neutron fields and that the results describe well the measurements made in the Lunar Neutron Probe Experiment.

Another physical approach makes use of INCE calculations with respect to the emission spectra of secondary neutrons and protons from the target nuclei. Depth- and size-dependent spectra of primary and secondary GCR particles are then calculated by solving numerically the transport equation, starting from primary GCR proton spectra and the emission spectra of secondary particles. This method up to now has only been applied to high-energy products in iron meteorites but presently is being extended to stony meteoroids and low-energy products.

More of the model calculations should be tested with the depth-vs.-concentration profiles measured in meteorites such as Knyahinya. How well the calculations reproduce the general trends reported in systematic studies of many meteorites should also be examined. Extending the range of meteorite sizes used in such comparisons is needed, especially for very small and very large objects.

PLANETARY GAMMA RAYS

The same physical processes produce both gamma rays and cosmogenic nuclides. Production rates of gamma rays are needed for the interpretation of spectra from remote-sensing missions such as the planned Mars Observer and Lunar Observer missions. The description of gamma-ray production rates also needs a good modeling of the interaction of cosmic rays with planetary or asteroidal surfaces. As with cosmogenic-nuclide production, both model calculations and simulation experiments are needed. Two contributions presented the current status and first results of model calculations.

PANEL DISCUSSION AND CONCLUSION

The panel discussion helped to bring all aspects of work on cosmogenic nuclide production rates into focus. There were some disagreements, reflecting the widespread interests of the participants and the diversity of open problems, as well as the different opinions

about the most promising ways to obtain improved production rates. General agreement existed on the importance of the quality (accuracy and precision) of the experimental data (especially of cross sections and extraterrestrial sample measurements), on the necessity of having same sample measurements for as many cosmogenic nuclides as possible, and on the need to derive reliable models for the description of the depth, size, and composition dependence of production rates. Consortia studies can help to achieve the first two needs, in particular if good methods of interlaboratory comparisons and exchanges of standard materials are practiced. Large integrated experiments with many research teams working together will speed the achievement of these goals.

On the subject of model improvements, opinions ranged from requests for further and more sophisticated thick-target simulation experiments to large research programs to measure needed thin-target cross sections. Intense discussion made it clear that the best improvements of modeling can only be achieved if both aspects are considered. There is a need for further simulation

experiments because they provide the only means to test calculational methods under controlled conditions, while measured cross sections provide the physical basis for many models.

Arguments from a more practical point of view called for simple relationships to describe the complex processes of cosmogenic-nuclide production. Some doubted whether such simple concepts can successfully describe the various and complex dependencies of production rates. Consensus was found in stating that models should be "user friendly" and flexible so that an experimentalist can work with them in interpreting his cosmogenic nuclide measurements. The main purpose of modeling is to extract from the experimental data the answers to the major questions in extraterrestrial studies: the history of the cosmic radiation and the exposure histories of irradiated solar-system bodies. More systematic measurements, improved simulation experiments, cross-section measurements, and advanced model calculations should soon give us a better understanding of cosmogenic nuclide production rates for use in such studies.

ABSTRACTS

51-90
321019
P-5

**ISOTOPE PRODUCTION BY SOLAR AND GALACTIC COSMIC RAYS:
EXPERIMENTAL DEPTH PROFILES AND MODEL CALCULATIONS; N.Bhandari,
Physical Research Laboratory, Navrangpura, Ahmedabad, India.**

The production rates of cosmogenic nuclides in lunar samples and meteorites are directly related to the energy spectra of solar (SCR) and galactic (GCR) cosmic rays. Induced activity of radionuclides of different half lives have been used to monitor their fluxes in the past. However, due to complicated exposure history and fragmentation of lunar rocks and meteorites and the difficulty in calculating the production profiles in rocks of different shape and size, there has been considerable debate about the fluxes of SCR and GCR and their variation with time. Here we describe the results of our study on some lunar samples and meteorites made to obtain their fluxes and production functions of different nuclides.

1. Solar Cosmic Rays: It has been shown from measurements of track density profiles, $\rho(x)$, that micrometeorite erosion is an important process on the lunar surface and fragmentation of rocks occur over time periods of a few million years. For determining SCR fluxes we have, therefore, selected rocks having simple exposure history determined by a plateau in $\rho(x)/\rho(x)$ and counted only surface areas having well preserved microcraters (1,2). Determination of exposure age, right on the surface of the moon, is vital for estimating the degree of saturation of radionuclides and for this purpose we have used the *sun-tan* or *plateau ages* based on track density profiles. The rare gas ages usually include burial exposure, thus being too high to be used for exposure to solar flares, and lead to erroneous results. The surface radioactivity of ^{26}Al in six Apollo 16 and 17 lunar rocks so selected was measured by a non destructive $\beta^+ - \gamma$ coincidence counting technique which enables measurement in a thin surface layer (90 mg/cm^2) without resorting to its mechanical separation. In rock 61016, a detailed depth profile was also obtained by radiochemical separation of aluminium from different depths and counting ^{26}Al on a low background $\beta - \gamma$ coincidence detector. The observed ^{26}Al profile is shown in fig.1 (1-3).

Calculation of isotope profile due to SCR is straight forward because of negligible secondary nucleon production. After taking correct erosion rate (ϵ) and the zenith angle (θ) of exposure, as indicated in Fig. 1, it was found that the profile of ^{26}Al in rock 61016 matches SCR spectrum with $J_s (>10 \text{ MeV}) = 125 \text{ p/cm}^2 \text{ sec.}$ and rigidity $R_0 = 125 \text{ MV.}$ Slightly different combinations of

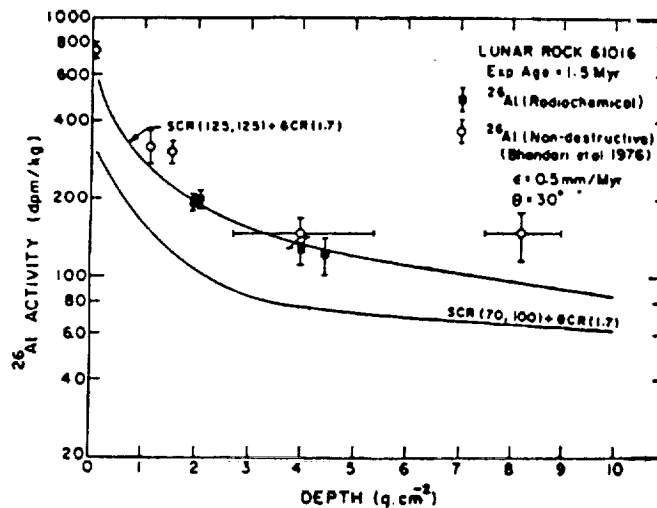


Fig. 1. The measured ^{26}Al activity in rock 61016 as a function of depth (1-3). The thick curves show production profiles expected for SCR and GCR parameters as indicated. A good fit is obtained with SCR ($J_s=125, R_0=125$). The observed activity is higher than that calculated from SCR parameters given by Kohl et al. (4), lower curve.

SCR FLUX AND GCR PRODUCTION RATES : N. Bhandari

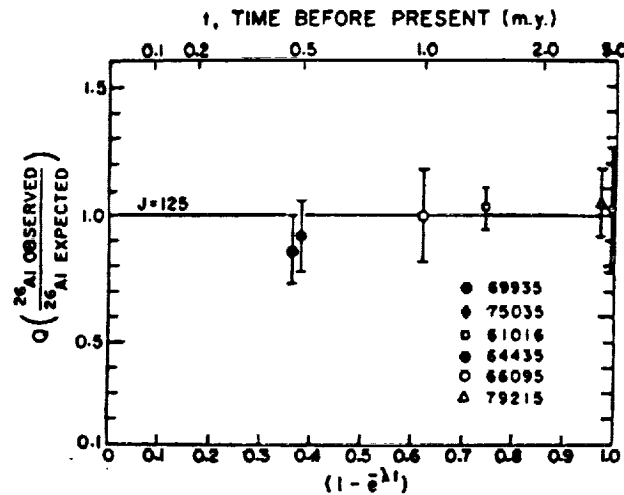


Fig. 2. Ratio $Q(t)$ of the observed ^{26}Al activity in various lunar rock surfaces to that expected from the SCR parameters ($J_s, R_o = 125, 125$), as a function of time. The deviation of Q from unity is small which rules out significant changes in the solar flare fluxes in the past few million years.

J_s and R_o would also fit the data. The activity near the surface ($<1\text{cm}$) indicated slightly higher J_s (10%). The observed activity in the six rocks having surface exposure ages ranging between 0.5 and 5 Ma are compared with the calculated activity with this flux in Fig. 2. It appears that the *average* solar flare proton flux has been constant. This conclusion (1) based on the study of a single radioisotope (^{26}Al), in the very surface regions of the rocks, has certain advantages since uncertainties in absolute values of flux, spectral shape, excitation function or sampling thickness are eliminated. There is a tendency in Fig. 2 for a small decrease in flux towards the present but more measurements are required on short exposure age rocks or shorter lived radionuclides to confirm this trend.

There has been a considerable debate over SCR fluxes over the past 10^6 - 10^7 years. Estimates as low as $J_s = 70 \text{ p/cm}^2 \text{ sec.}$ have been obtained (4) but these have now been revised to $145 \text{ p/cm}^2 \text{ sec.}$ (5,6), in close agreement with the flux value given by us earlier (2,3). However, there is still some discussion of the value of R_o , whose estimates range between 85-125 MV. It is possible that this can be resolved by use of proper exposure ages and excitation functions.

From our measurements it has been concluded that the *average* flux of SCR has been $125 \text{ p/cm}^2 \text{ sec.}$ and this has been nearly constant over the past few million years (1).

2. Galactic Cosmic rays: Calculation of production rates of nuclides by GCR is complicated because of secondary nucleon production which depends on the size of the meteoroid and depth within it. It has been shown (7) that the production rate of some spallation products varies by nearly a factor of 2 in chondrites of different size and with depth. Reasonably precise measurements of radionuclides are being made now using high resolution gamma ray counting and accelerator mass spectrometry but there remains large uncertainty in predicting the production rates. Since deviation of the observed activity from the expected levels, based on the present GCR flux, could give information on (i) time variation in GCR flux (ii) spatial variation of GCR intensity in the orbital space of the meteoroid (iii) modulation of GCR by sun spot and other solar activity cycles or (iv) complex exposure and fragmentation history of the meteoroid, it is important to predict the production profiles of different cosmogenic isotopes in meteorites.

To obtain production rates we have used an experimental approach that the observed profile in a meteorite with simple (single stage) exposure history gives the production profile (1,7). We,

SCR FLUX AND GCR PRODUCTION RATES : N. Bhandari

therefore, first select chondrites, on the basis of a combined study of track density profiles and neon isotopes, which have simple exposure history and determine their preatmospheric size, shape and the exposure age T_x . The observed activity profiles of some chosen radioisotope in such meteorites, together with its excitation function can yield "effective" energy spectra of nucleons as a function of depth in meteoroid of a given size, as is done in the Reedy-Arnold model for the moon (8). This spectra, together with the excitation function for any isotope, can define its production function. Such an approach has some limitations but, as we shall see, can make reasonably good predictions in case of some isotopes and isotope pairs.

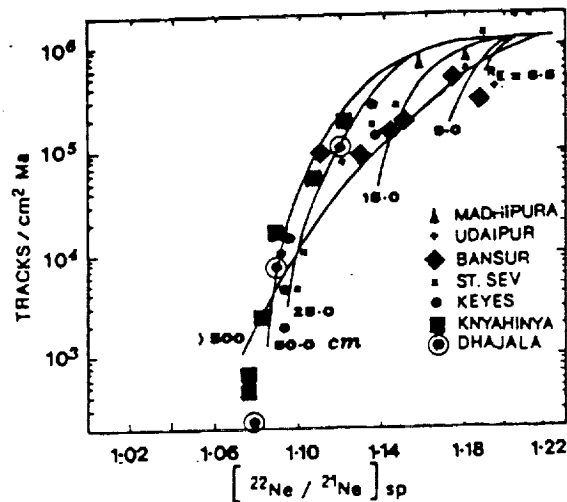


Fig.3 Track production rate vs NeR correlation diagram for meteoroids with different radii, following (13). Experimental data points for the seven meteorites discussed in the text are shown (7,9-11 and references their in).

Two criteria have been developed to identify chondrites with simple exposure history (9). The first one is based on the correspondence between track production profile ($TPM = \rho(x)/T_x$) and spallation $^{22}\text{Ne}/^{21}\text{Ne}$ (NeR), both of which have been extensively used as shielding parameters. Since the VH nuclei, which give rise to tracks, and protons, which are responsible for production of neon isotopes, have widely different attenuation lengths, a good correlation between them ensures constant geometry of exposure and exists only for meteorites with simple exposure history. In Fig. 3 the calculated correlation for TPM and NeR is shown for meteoroids of different radii (9). It can be seen that for the selected seven meteorites: Madhipura (L), Udaipur(H), Bansur (L5), St. Severin (LL), Keyes(L6), Knyahinya (L5) and Dhajala (H3/4), there is a good agreement between the observations (7,9-11) and calculations. The track production rate (ρ) in surface samples allowed their ablation and hence the *effective* pre-atmospheric radii (R_E) to be determined to be 6.5, 9, 15, 20, 30, 45, and about 50 cm respectively. Small deviations in the slope of the profile may be due to non-spherical shape of the meteoroid assumed in the calculations. The other criterion is based on concordance of ^{26}Al - ^{21}Ne exposure age with ^{53}Mn - ^{21}Ne exposure age. Instead of calculating the exposure age from each pair of isotopes, which requires prior knowledge of their absolute production rates, we prefer to present this correlation between $^{21}\text{Ne}/^{26}\text{Al}$ and $^{21}\text{Ne}/^{53}\text{Mn}$ in conventional units of measurement (^{21}Ne in 10^{-8} cc STP/g., ^{26}Al in dpm/kg meteorite and ^{53}Mn in dpm/kg Fe). Three curves have been calculated (Fig. 4) using production ratio of $^{21}\text{Ne} : ^{26}\text{Al} : ^{53}\text{Mn} = 0.31 : 60 : 415$ (^{21}Ne in 10^{-8} cc STP/g.Ma, ^{26}Al in atoms/min.kg meteorite and ^{53}Mn in atoms/min.kg Fe) in L chondrites. Curve 1 is for constant GCR flux ($J_G = 1.7 \text{ p/cm}^2 \cdot \text{sec} \cdot 4\pi \text{ sterad.}$); curve 2 assumes that the flux during the past 2 Ma has been 2 times the previous flux and curve 3 assumes that the flux during the past 2 Ma has been half of the previous flux. Meteorites with complex exposure history lie off curve 1, generally in the region below it, because the net consequence of fragmentation is to increase the secondary nucleon flux within the meteoroid

SCR FLUX AND GCR PRODUCTION RATES : N. Bhandari

(9). The data points from the seven meteorites, inferred to have simple exposure history from Fig 3, fall close to curve 1, confirming their single stage exposure to GCR and ruling out any variation in GCR flux during the past 1-10 Ma as has been proposed sometimes (12).

Depth profiles of ^{26}Al or ^{53}Mn have been measured in these seven meteorites (7,9-11 and references there in), which provide a simple way of understanding depth and size dependence of the production function. Some systematics emerge from these profiles:

- (i) The isotope depth profiles in small ($R_E < 15$ cm) meteorites is nearly flat.
- (ii) The isotope production rate increases with depth for meteorites ($15 < R_E < 30$ cm).
- (iii) The production rate near the centre of the meteorite increases with size for chondrites ($6 < R_E < 30$ cm) as shown in Fig. 5.
- (iv) For larger meteorites ($R_E > 30$ cm), the production rate slowly decreases with size and depth of > 20 cm.

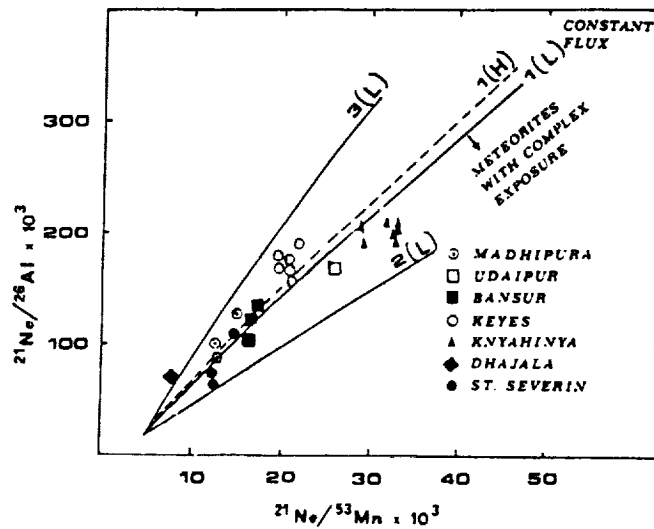


Fig. 4. $^{21}\text{Ne}/^{26}\text{Al}$ vs $^{21}\text{Ne}/^{53}\text{Mn}$ correlation diagram for L chondrites. Curve 1 is for constant GCR flux and curves 2 and 3 for a change in GCR intensity during the past 2 Ma by a factor of 2 and 0.5 respectively (9). The data points for the seven meteorites (7,9-11) discussed in the text are shown which agree with constant GCR flux. The units used are described in the text. Curve 1 for H chondrites is also shown for illustrating the extent of dependence on target element composition.

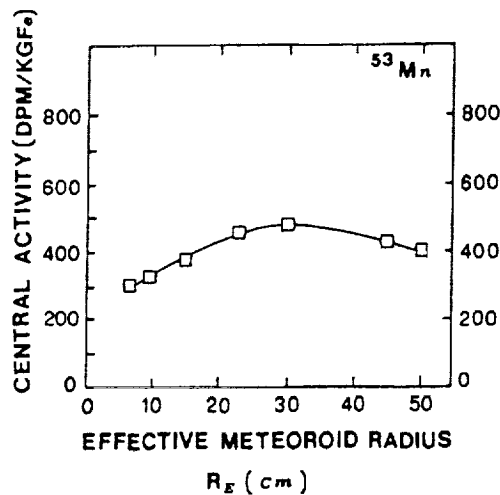


Fig 5. Activity of ^{53}Mn near the center of meteoroids of different radii (R_E) based on the experimental data (7,9-11).

SCR FLUX AND GCR PRODUCTION RATES : N. Bhandari

We use the depth profile of ^{26}Al or ^{53}Mn in these meteorites with our model (1) to obtain the spectral shape parameter α of nucleons within meteoroids of different sizes. Better depth profiles from meteorites and excitation functions have enabled us to improve the estimation of α compared to the values given earlier (1,13), which are shown in Fig. 6. The prediction of this model agrees within 30% for all the 20 radioisotopes studied in Torino meteorite (14) and in many cases the agreement is better than 10%.

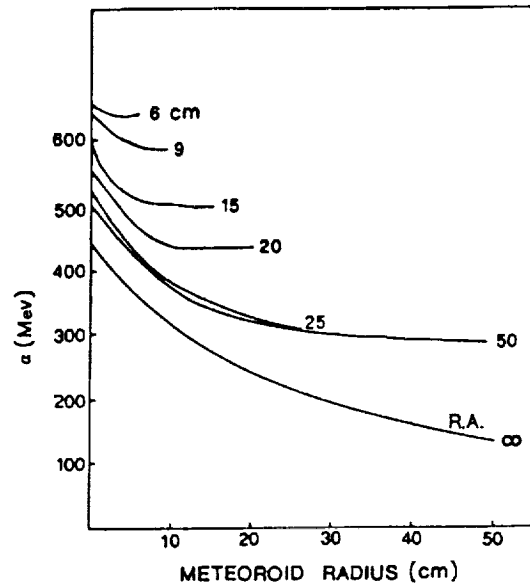


Fig 6. The depth profile of the spectral hardness parameter of nucleons, α , in meteoroids of different radii.

From the above discussion we conclude that the average GCR flux has remained nearly the same over the past 10 Ma and our approach of predicting isotope production rates in meteorites works well in case of several isotopes. Specifically it correctly predicts the observed NeR (Fig.3) and ratios of several isotope pairs (eg. Fig. 4). The disagreement in many cases eg. ^{52}Mn , ^{54}Mn , ^{48}V etc. is high (~30%) and requires better models, involving more rigorous approach (15).

We thank Mr M.S.Patel for help in computer programming and Mr K.M.Suthar for assistance. We are grateful to NASA for providing us the lunar samples for this study.

References:

1. Bhandari, N. (1981) *Proc. Ind. Acad. Sci.* 95, 359-382.
2. Bhandari, N. et al., (1976) *Proc. Lunar Sci. Conf 7th*, 513-523.
3. Shukla, P.N. et al., (1983) *Proc. Int. Conf Cosmic Rays*, Bangalore, OG7-15, 307.
4. Kohl C.P., et al., (1978) *Proc. Lunar Planet. Sci. Conf. 9th*, 2299.
5. Nishiizumi, K. et al., (1988) *Proc. Lunar and Planet. Sci. Conf. 18th*, 79.
6. Reedy, R.C. and Marti, K. (1989) in *Sun in Time*, preprint.
7. Bhattacharya, S.K. et al., (1980) *Earth Planet. Sci. Lett.* 51, 45-57.
8. Reedy, R.C. and Arnold, J.R. (1972) *J. Geophys. Res.* 77, 3519-3531.
9. Bhandari, N. (1986) *Proc. Ind. Acad. Sci.* 95, 183-191.
10. Graf, Th. et al., (1989) *Geochim. Cosmochim. Acta* (In press).
11. Potdar, M.B. et al., (1986) *Proc. Ind. Acad. Sci.* 95, 183-191.
12. Nishiizumi, K. et al., (1980) *Earth Planet. Sci. Lett.* 50, 156-170.
13. Bhandari, N. and Potdar, M.B. (1982) *Earth Planet. Sci. Lett.* 58, 116-128.
14. Bhandari, N. et al., (1989) *Meteoritics*, 24, 29-34.
15. Michel, R. and Stuck, R. (1984) *J. Geophys. Res. suppl. B*, 673-684.

52-91
321020

p-4

STUDIES OF THE COSMIC RAY INDUCED γ -EMISSION AT PLANETARY SURFACES USING MONTE-CARLO TECHNIQUES IN RESPECT OF THE MARS OBSERVER MISSION; G. Dagge, P. Cloth, P. Dragovitsch, D. Filges, KfA Jülich, Institut für Kernphysik, POB 1913, D-5170 Jülich, F. R. Germany, and J. Brückner, Max-Planck-Institut für Chemie, Abteilung Kosmochemie, Saarstraße 23, D-6500 Mainz, F. R. Germany

Introduction. Recent calculations on cosmogenic nuclide production in lunar or planetary surfaces were based on modeled fluxes of cosmic particles as a function of depth. The validity of these models, being dependent on the incident GCR spectrum and on the chemical composition of the surface, is not always obvious. A more general treatment is presented here. In particular, a method for calculating the γ -albedo of planetary surfaces is developed which is of special interest in regard to the Mars-Observer Mission. Before applying this method to Mars it was tested for a lunar surface, where comparisons with experimental data can be performed.

Calculational procedure. The HERMES code system (1) is the basis of the calculations. It consists of four modules HETC/KFA-2, NDEM, EGS4 and MORSE-CG along with several auxiliary codes for data analysis. The system is mainly applied for shower calculations of calorimeters and is described in detail by Ref. (2). The basic input data required for the presented method are differential particle-particle cross sections for HETC/KFA-2 and cross section libraries for the coupled n- γ transport calculations in MORSE-CG. Using analog Monte-Carlo methods, the primary and secondary particle fluxes as a function of depth and energy are calculated dependent on the source spectrum, material and geometry of the problem. These results can be folded with any available reaction cross section to obtain the production rates of interest.

The 2π -irradiation of an infinite disk gives a quite good simulation of the GCR-irradiated lunar surface for low orbiting heights and is an excellent approximation for Mars because of the attenuating effect of its atmosphere. The incident GCR spectrum used in the HETC-calculations was taken as the average energy distribution from solar minimum (1965) and solar maximum (1969) of GCR-protons between 1 MeV and 10 GeV. Neutrons below 15 MeV were passed over to MORSE-CG as input for a coupled n- γ transport calculation. For this application a special cross section library based on ENDF-B/IV data was evaluated for all elements of interest. This coupled n- γ library contains cross section data for 118 neutron groups (19 thermal groups) from 0.01 meV to 14.9 MeV and 21 γ -groups from 10 keV to 14 MeV. Additional narrow gamma groups were inserted to provide cross section data for the most important gamma ray lines. The production of prompt photons from residual nuclei or from inelastic neutron scattering by neutrons with $E > 15$ MeV was calculated by NDEM. This photon source was also passed over to MORSE-CG for a transport calculation, whereas the decay of π^0 particles and the subsequent γ -transport was performed by EGS4. Gammas from naturally occurring radionuclides may be included in future calculations.

Results for the lunar surface. For studies concerning the Moon, experimental data from Apollo missions are available. A comparison with the Lunar Neutron Probe Experiment

STUDIES OF THE COSMIC RAY INDUCED ..., G. Dagge et al.

(LNPE, Ref. 3-5) is presented, since the nuclear reactions involved here give access to the present day lunar neutron spectrum. An averaged lunar material composition listed in Table I was used to calculate the differential particle fluxes of protons and neutrons as a function of depth.

Table I: Chemical composition of lunar soil.

elem.	O	Mg	Al	Si	Ca	Ti	Fe	Gd
[g/g]	0.420	0.048	0.072	0.202	0.090	0.035	0.124	$30.0 \cdot 10^{-06}$

The total neutron density was calculated directly from the differential fluxes and can be compared with the results given by Woolum (3). The experimental results were obtained by measuring the reaction rate $^{10}\text{B}(n,\alpha)^7\text{Li}$, which is directly proportional to the neutron density. The agreement between theoretical calculations and the experimental data is excellent (see Fig. 1).

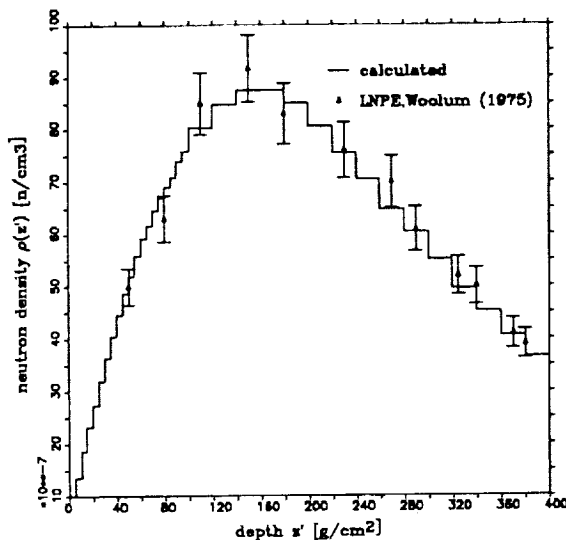


Fig. 1: Calculated depth profile of the neutron density in the lunar surface compared to experimental data (3) obtained via the $^{10}\text{B}(n,\alpha)^7\text{Li}$ reaction rate.

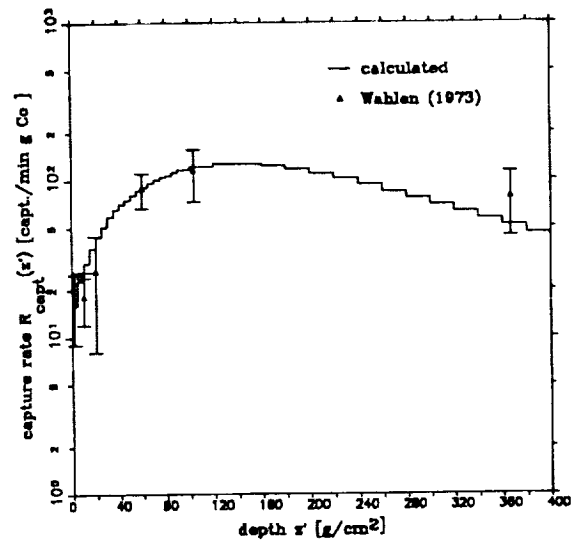


Fig. 2: Calculated capture rate from ^{59}Co as a function of depth in the lunar surface compared to experimental results from Ref. (5).

The fission rate for ^{235}U which is also roughly proportional to the neutron density could be reproduced as well (4). As a check for the neutron spectrum, the capture rate for ^{59}Co was calculated and compared with experimental data from Wahlen (5). The absorption cross section of this nucleus has a resonance at 132 eV. Calculated and experimental data for this reaction rate are in excellent agreement (Fig. 2). The experimental data from the LNPE experiment also include the Cd-ratio within the lunar surface. The results of the calculation and the corresponding data from Burnett (6) can be found in table II.

All these results validate that the method presented here is able to calculate the neutron flux as function of depth and energy properly, which is essential for a calculation of gamma

STUDIES OF THE COSMIC RAY INDUCED ..., G. Dagge et al.

ray fluxes. Fig. 3 shows the calculated gamma albedo from the lunar surface. A comparison of calculated line intensities with data from Reedy (7) shows a good overall agreement. However, the gamma line intensities have to be seen as preliminary data, since several photon production cross sections will be updated and statistical uncertainties above 20 % in each gamma group have to be taken into account.

Table II: Comparison of calculated and experimental Cd-ratios in a lunar surface.

depth z' [g/cm ²]	x_{Cd} exp. (Ref. 5)	x_{Cd} calc.
150.	1.1 ± 0.2	1.2 ± 0.1
370.	1.9 ± 0.3	1.3 ± 0.1

The Cd-ratio x_{Cd} is defined as

$$x_{Cd} = \frac{\rho_n(E < 0.5eV)}{\rho_n(E > 0.5eV)}$$

ρ_n : neutron density

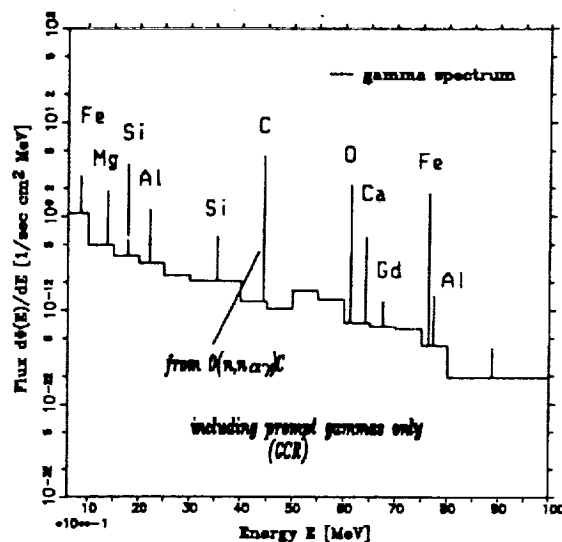


Fig. 3: Calculated gamma albedo of a lunar surface.

Table III: Chemical composition of Martian a) surface, b) atmosphere.

a)	elem.	O	Mg	Al	Si	Ca	Ti	Fe	
	[g/g]	0.466	0.037	0.041	0.215	0.044	0.004	0.135	
	elem.	H	C	Na	S	Cl	K	Cr	Mn
	[g/g]	0.001	0.006	0.008	0.030	0.007	0.001	0.002	0.003
	elem.	Co	Ni	Th	U				
	[ppm]	33.00	52.00	0.45	0.13				
b)	elem.	C	O	N					
	[g/g]	0.262	0.698	0.027					

Predictions for Mars. Minor changes in the setup for the lunar case allow a calculation of particle fluxes and gamma albedo of the Martian surface. Material compositions for the Martian atmosphere and for a "dry" Martian soil containing 0.1 % hydrogen (0.9 % water) can be found in Table II. The atmosphere was implemented as an upper material layer of 16 g/cm². Compared to the extremely dry lunar surface, the particle fluxes in the Martian soil show a flatter depth profile. The thermal part of the neutron spectrum is enhanced due

STUDIES OF THE COSMIC RAY INDUCED ..., G. Dagge et al.

to the water content of the Martian soil. These neutron fluxes were used to calculate gamma spectra at the Martian surface as well as above the atmospheric layer, the latter one is presented in Fig. 4. The gamma spectrum shows strong carbon lines caused by the atmosphere, whereas the low energy part of the spectrum is obviously influenced by attenuation effects. In this context it should be noticed again that the weak lines are afflicted with large statistical errors for the present calculations.

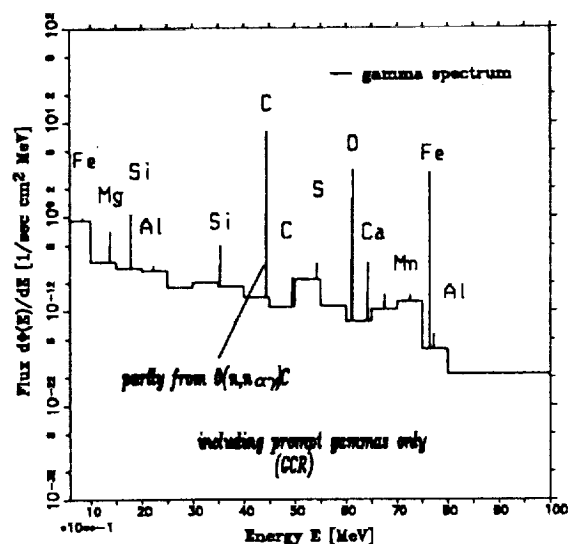


Fig. 4: Calculated gamma albedo above the Martian atmosphere for a dry soil composition.

Conclusions. The HERMES Code system has been used to calculate particle fluxes in the lunar surface. The results are in excellent agreement with available experimental data. On this base, a method for calculating the gamma albedo from arbitrary surfaces was developed. The flexibility of this code system also permits investigations about the gamma background at the detector site. Therefore, application of HERMES to the Mars Observer project is very promising.

Parameter studies on variations in chemical composition and layered surface structures can be performed. Other gamma ray sources like naturally occurring radionuclides will be taken into account in future.

References:

- (1) P. Cloth et al., HERMES User's Guide, Jül-2203, May 1988
- (2) P. Dragovitsch et al., (1989) Applications of the HERMES Code System in Meteoritics, this report.
- (3) D. S. Woolum et al. (1975) *The Moon* 12,p.321-250.
- (4) D. S. Woolum and D. S. Burnett (1974) *Earth and Planet. Sci. Lett.* 21,p.153-163.
- (5) D. S. Burnett and D. S. Woolum (1974) *Proc. of the 5th Lunar Conf. (Supplement 5, Geochimica et Cosmochimica Acta) Vol. 2,p.2061-2074.*
- (6) M. Wahlen et al. (1973) *Earth and Planet. Sci. Lett.* 19,p.315-320.
- (7) R. C. Reedy, (1978) *Proc. Lunar and Planet. Sci. Conf. 9th, p.2961-2984.*

33-90

321021

P-8

CROSS SECTIONS FOR LONG-LIVED RADIONUCLIDES FROM HIGH ENERGETIC CHARGED-PARTICLE-INDUCED REACTIONS

B. Dittrich, U. Herpers, Abteilung Nuklearchemie, Universität zu Köln, FRG; R. Bodemann, M. Lüpke, R. Michel, Zentraleinrichtung für Strahlenschutz, Universität Hannover, FRG; H.J.Hofmann, W. Wölfli, ETH Zürich, CH

During the last years our group did several irradiations to determine the cross sections of cosmogenically interesting nuclear reactions. These data are necessary to calculate and model depth-profiles of the production-rates of cosmogenic nuclides in extra-terrestrial matter (1,2,3). Also, on base of these data one can interpret the depth profiles in meteorites which can give important information on processes in solar system in the past.

The target materials (see Table 1) were chosen with regard to the composition of the stony and iron meteorites and of course to problems in nuclear physics.

Table 1: Target materials

Element	Form	Purity(%)
C	graphite	99.9
O	SiO ₂	suprasil
N	Si ₃ N ₄	99.9
Mg	metal	99.9
Al	metal	99.999
Si	metal	wafer
Ca	CaF ₂	p.a.
Ti	metal	99.6
V	metal	99.8
Mn	alloy	88 (12% Ni)
Fe	metal	99.99
Co	metal	99.99
Ni	metal	99.98
Cu	metal	99.99
Nb	metal	99.9
Rh	metal	99.9
Zr	metal	99.8
Au	metal	99.99
Ba	glas	p.a.

The energy-distribution of the galactic cosmic rays shows the maximum between 500 and 1000 MeV per nucleon, whereas the maximum of the energy range of the solar cosmic rays is found up to 200 MeV per nucleon. The irradiations were done at these energies with protons and alpha particles, which make up 87% and 12% of the cosmic rays respectively (4). Table 2 shows the irradiations realized during the last years. Irradiations indicated with a star were done by stacked-foil technique so that several energy points from only one irradiation were obtained.

CROSS SECTIONS OF LONG-LIVED RADIONUCLIDES, DITTRICH B. ET AL.

Table 2: Irradiations carried out

Particle	Energy (MeV)	Accelerator	Date	Flux ($10^{10} \text{ cm}^{-2} \text{ s}^{-1}$)	Time (s)
p	* 100	Gustaf-Werner-Institute (S)	24.03.88	20.5	15000
	600	CERN (CH)	22.11.84	1.97	45700
	800	LANL (USA)	22.07.88	8.67	20400
	1200	LNS (F)	17.12.87	6.99	39600
	2600	LNS (F)	15.03.88	2.33	43100
α	* 120	PSI (CH)	22.04.89	39.5	18000
	* 170	KFA (FRG)	07.07.89	22.5	10000

The fluxes are given as typical values. For each target element an individual flux of protons or alpha particles was determined. The flux determination based on the cross sections of the monitor reactions from Al-27 to Be-7, Na-22 and Na-24 (5). After gamma-spectrometric measurements the chemical separations were done to get samples for accelerator mass spectrometry (AMS) for all long-lived radionuclides from only one irradiated foil. The determination of Be-10 and Al-26 by AMS is already done and in preparation for Ca-41, Mn-53 and Ni-59. The target materials that are in work and the interesting radionuclides are given in table 3.

Table 3: Target materials investigated and radionuclides determined

Target material	Product nuclide
C, N, O	Be-10
Mg, Al, Si	Be-10, Al-26
Ti	Be-10, Al-26, (Ca-41)
Mn, Fe, Co	Be-10, Al-26, (Ca-41, Mn-53)
Ni	Be-10, Al-26, (Ca-41, Mn-53, Ni-59)
Ca	Al-26, (Ca-41)

In general, the chemistry is done by adding carriers and solving the target in a suitable acid. The separation itself is based on ion exchange, precipitation (especially for hydroxides) and extraction. The element fractions are cleaned by fuming with aqua regia, hydrofluoric acid and perchloric acid. The ammonia precipitate at the end of the separation is washed with bi-distilled water and glowd to a stable form. In figures 1 and 2 the separation schemes of the target elements aluminum and manganese are given as examples.

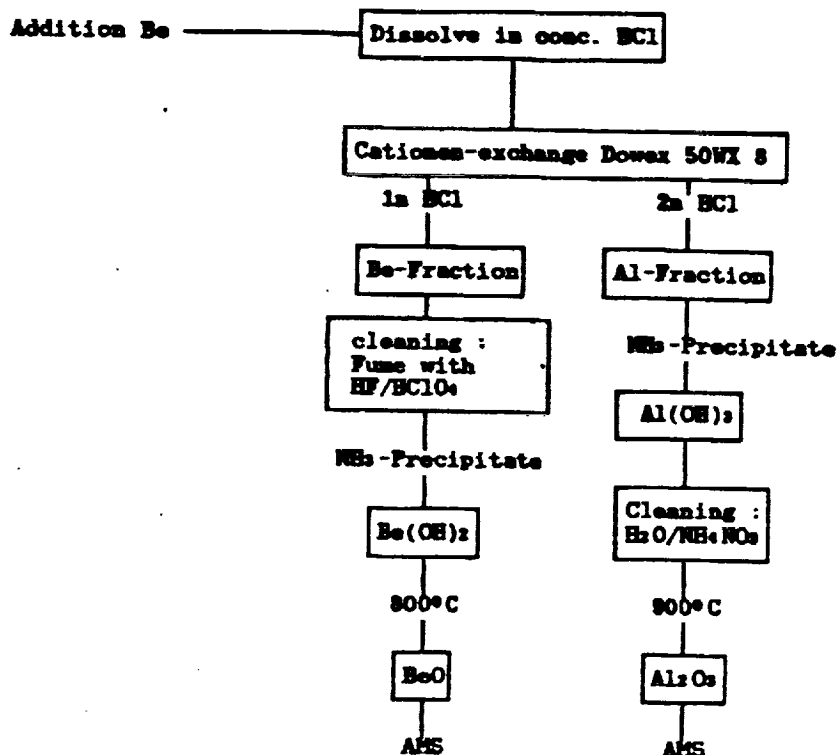


Figure 1: Separation scheme of the aluminum targets

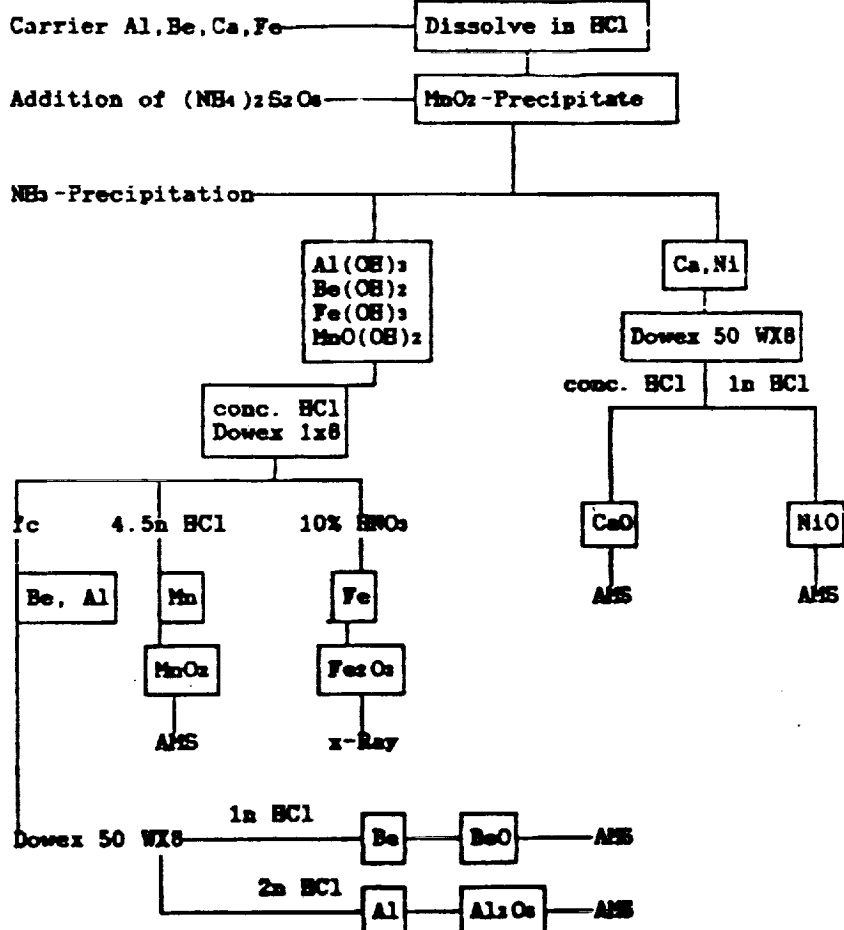


Figure 2: Separation scheme of the manganese targets

CROSS SECTIONS OF LONG-LIVED RADIONUCLIDES, DITTRICH B. ET AL.

The technique of AMS is described elsewhere (6). The production of Be-10 from oxygen, magnesium, aluminum, silicon and iron are shown in the figures 4-8 in comparison to other data.

Oxygen: Our data fit very well the data of literature (7,8,9). There seems to be a maximum in the region of 1000-1200 MeV for this proton-induced reaction. The threshold of the reaction $O(p,5pxn)Be-10$ is in the region of 50-60 MeV.

Magnesium: The values at 800, 1200 and 2600 MeV from this work might be in contradiction to the data at 600 MeV (7,9), whereas the measurement of Raisbeck (8) seems to be in better agreement. But more data are needed to determine the cross sections in the region of the threshold.

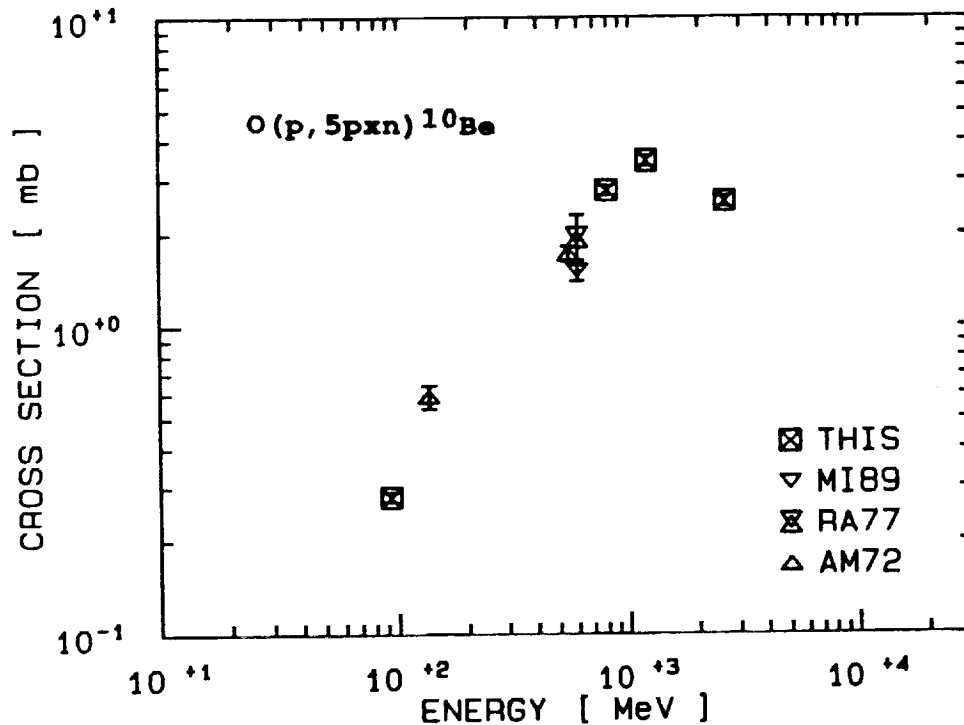


Figure 3: Cross sections for the reaction $O(p,5pxn)Be-10$

Aluminum: The data of the reaction $Al-27(p,10p8n)Be-10$ fit well to the value of Michel (9).

CROSS SECTIONS OF LONG-LIVED RADIONUCLIDES, DITTRICH B. ET AL.

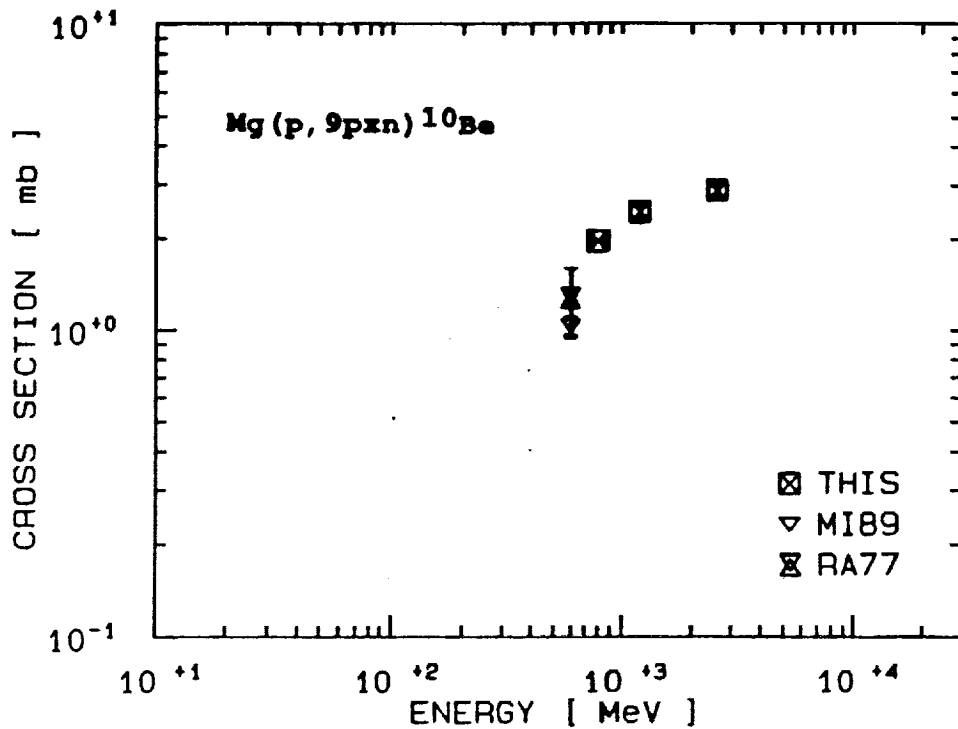


Figure 4: Cross sections for the reaction $\text{Mg}(p, 9pxn)\text{Be-10}$

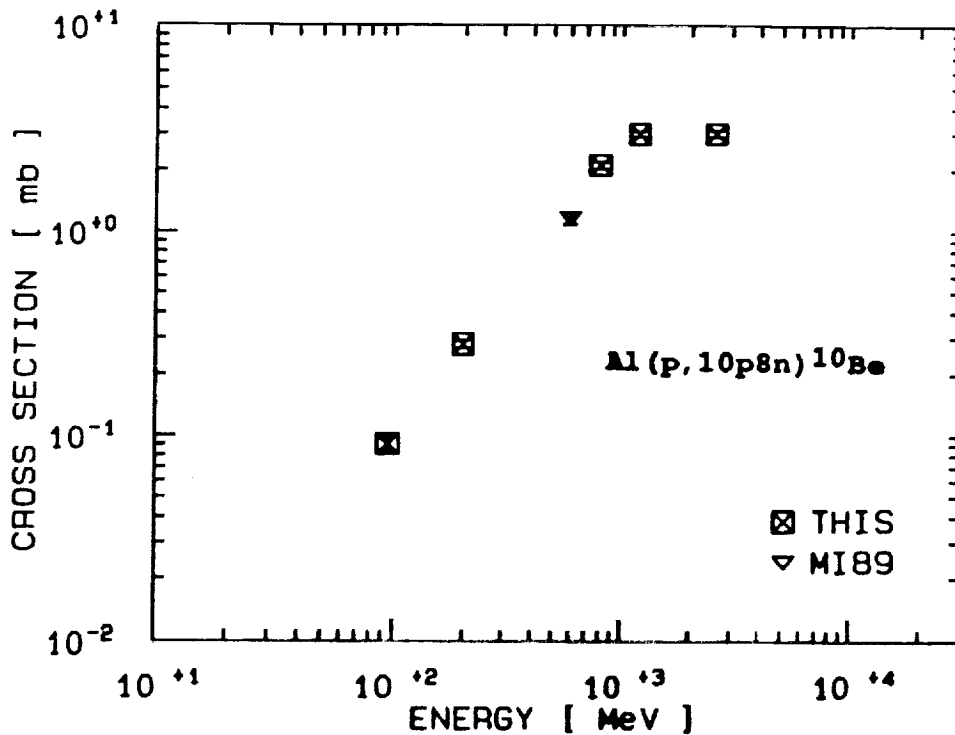
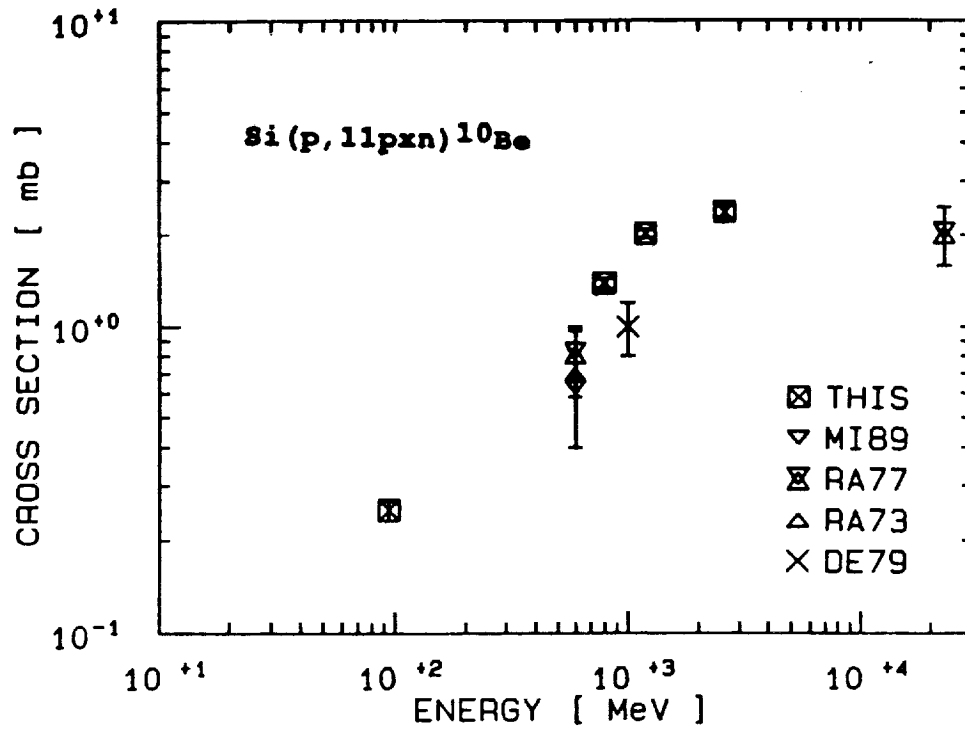
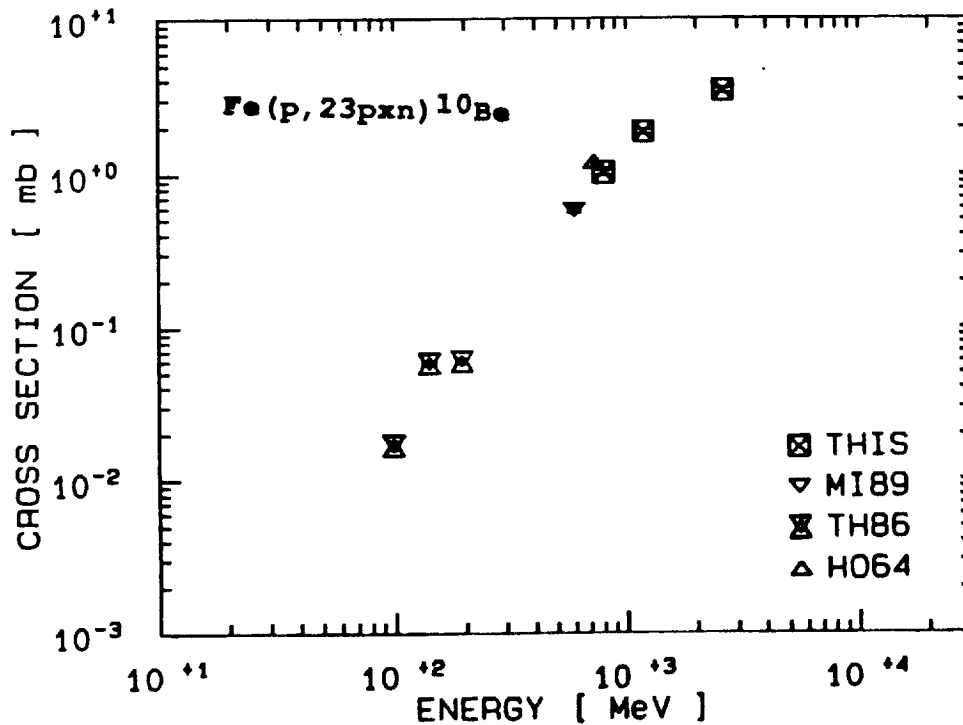


Figure 5: Cross sections for the reaction $\text{Al}(p, 10p8n)\text{Be-10}$

CROSS SECTIONS OF LONG-LIVED RADIONUCLIDES, DITTRICH B. ET AL.

Figure 6: Cross sections for the reaction $\text{Si}(p, 11\text{pxn})\text{Be-10}$ Figure 7: Cross sections for the reaction $\text{Fe}(p, 23\text{pxn})\text{Be-10}$

CROSS SECTIONS OF LONG-LIVED RADIONUCLIDES, DITTRICH B. ET AL.

Silicon: The measurements of this work are in good agreement to each other, and to the newer value of Raisbeck (8), whereas his older measurement (10), the data of Dedieu (11) and Michel et al. (9) are lower. These contradictions have to be clarified, as well as the measurements at lower energies near the threshold have to be done.

Iron: For the reaction $\text{Fe}(p,23\text{pxn})\text{Be-10}$ our data fit very well the value of Honda (12) in the high-energetic region. The point of interest in this case is in the region of lower energies, too, because the existing data are contradictory to each other (13).

The figures 8 and 9 give the dependence of the cross sections of the production of Be-7 and Be-10 versus the mass number of the target material for 600 and 2600 MeV protons. The part with the lower mass numbers of the targets shows at 600 MeV a decrease of the cross sections for the production of Be-7 which is typical for a spallation reaction, whereas for higher masses the typical plateau for fragmentation processes is found. The Be-10 production seems to be built up at this energy only by fragmentation processes. This is shown by the plateau of the cross sections. The same diagram, but for reactions induced by 2600 MeV protons, shows that the production of Be-7 and Be-10 bases only on the fragmentation process.

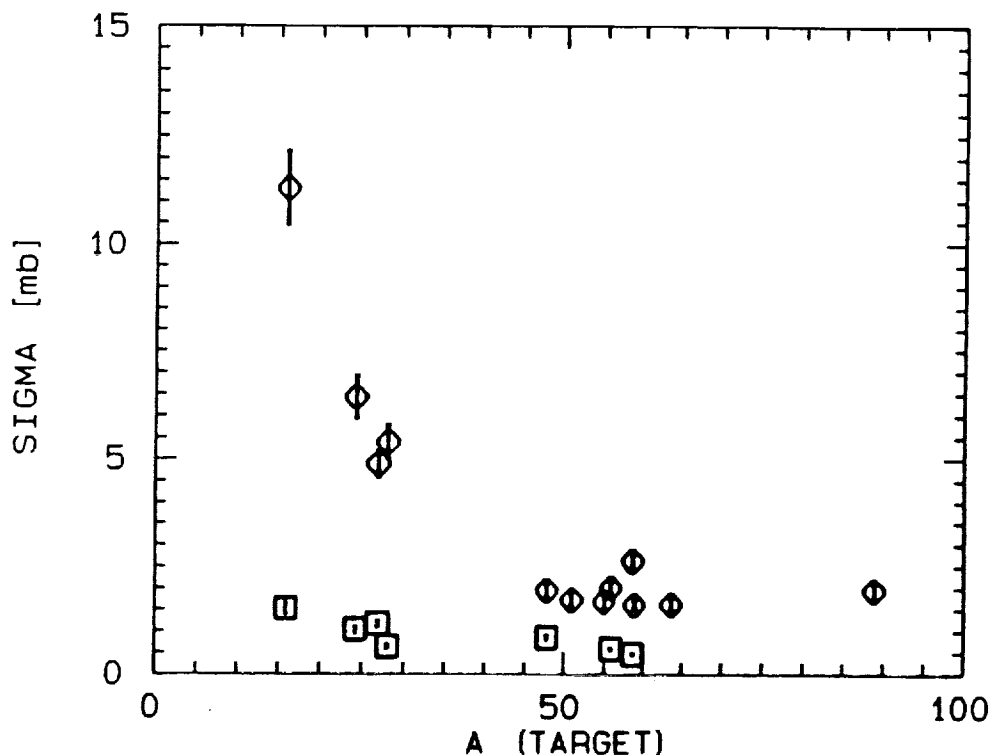


Figure 8: Cross sections of Be-7 (rhomboid) and Be-10 (square) in dependence of the mass number of the target material for 600 MeV protons

CROSS SECTIONS OF LONG-LIVED RADIONUCLIDES, DITTRICH B. ET AL.

The cross sections of the reactions producing these radionuclides vary in the region of a mean value with structures in the shape. These structures are significant and cannot be explained with a simple spallation or fragmentation model.

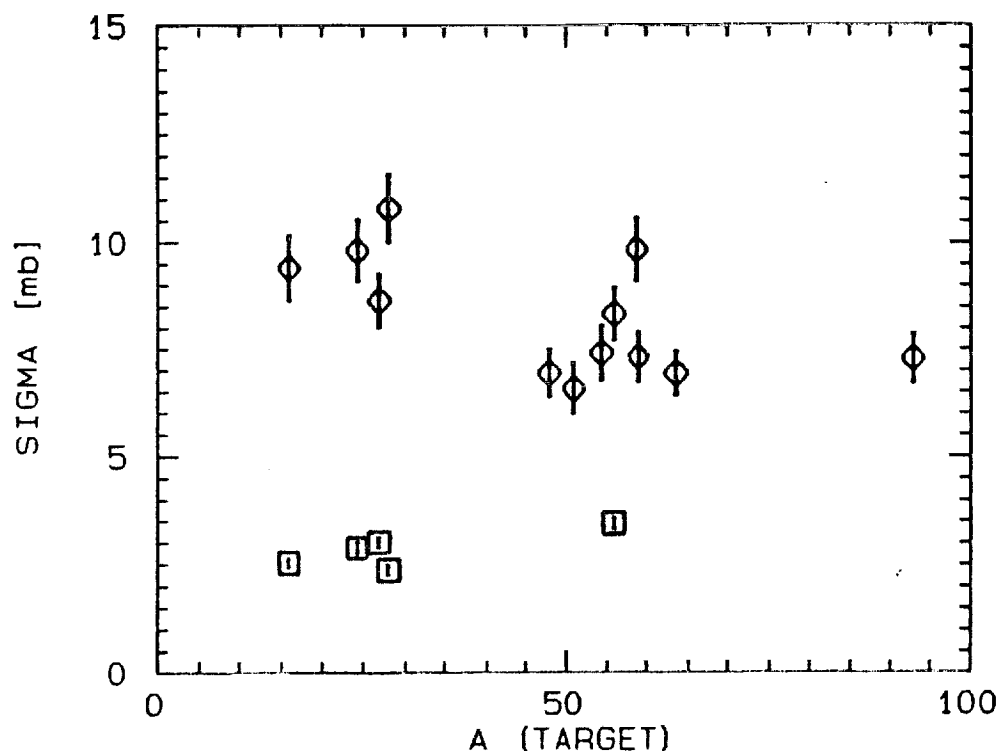


Figure 9: Cross sections of Be-7 (rhomboid) and Be-10 (square) in dependence of the mass number of the target material for 2600 MeV protons

References: (1) Michel R. (1989) On the production of cosmogenic nuclides in meteoroids by galactic protons, in: Proc. 20th LPSC Houston, submitted (2) Reedy R.C. (1985) Proc. 15th LPSC, in: J. Geophys. Res. 90, Supplement, C722-C728 (3) Signer P., Nier A.O. (1960) J. Geophys. Res. 65, 2947-2964 (4) Alsmiller et al., (1972) ORNL-RSIC-35 (5) Tobailem J., de Lassus St. Genies C.H. (1981) CEA-N1466 (6) Suter et al. (1984) Nucl. Instr. Meth. in Phys. Res. B5, 117-122 (7=AM72) Amin B.S. et al. (1972) Nucl. Phys. A195 311 (8=RA77) Raisbeck G.M. et al. (1977) 15th Int. Cosmic Ray Conf. Plovdiv-2 203 (9=MI89) Michel R. et al. (1989) Analyst 114 287-293 (10=RA73) Raisbeck G.M., Yiou F. (1973) 13th Int. Cosmic Ray Conf. Denver-1 494 (11=DE79) Dedieu J. (1979) Thesis, Bordeaux (12=HO64) Honda M., Lal D. (1964) Nucl. Phys. 51 363-368 (13=TH86) Theis St. (1986) Thesis, University of Cologne

Acknowledgement: This work was supported by the Deutsche Forschungsgemeinschaft. The authors wish to thank the Wacker Chemietronic, Burghausen, for placing the Silicon-wafers at our disposal.

54-90
321022
P 3

INC MODEL CALCULATION OF COSMOGENIC NUCLIDE PRODUCTION IN STONY METEORITES*

M. Divadeenam,¹ T. A. Gabriel,² O. W. Lazareth,¹ M. S. Spergel,³ and T. E. Ward¹

Intranuclear Cascade Model Monte Carlo calculations of ^{26}Al and ^{53}Mn production due to cosmogenic proton induced spallation of a model meteorite composition similar to L Chondrite were made. The calculated predictions are consistent with the observed decay rates in L Chondrite stony meteorites. The calculated ^{26}Al production rate in a 1 m diameter meteorite is within 1/2 S.D. of the mean taken from 100 bulk determinations in L Chondrite samples compiled by Nishiizumi. Similarly the calculated average value for ^{53}Mn is consistent within one S.D. of the mean in the widely scattered ^{53}Mn data. The production rates of ^{12}C , ^{13}C , and ^{14}C are also predicted.

In our calculations, use is made of Monte Carlo techniques for identifying nuclear collisions and specific nuclear reactions as well as establishing the transport of the incident nucleon and its generated nucleons. It is thus possible to use an integrated calculational approach in predicting the cosmogenic nuclide production rate and depth dependence. Previous calculational approaches have examined the production of nuclides by separating the collision into spallation, neutron capture and fragmentation processes. The calculations use a transport type mechanism for predicting the depth dependence of the cosmic ray induced nuclides (i.e. cosmogenic nuclides). One of the problems in predicting the production of cosmogenic nuclides, as a function of depth in meteorites, has been the need to determine the numerous nucleon-nuclear cross sections and then the subsequent nuclide excitation rates. In the case of neutron capture induced nuclides these difficulties have led many authors [e.g. (1-6)] to utilize the similarity in the shape to the production of ^3H for predicting the production of neutrons. These tritium rates were normalized to neutron production observations either for the Moon or for Chondrite meteorites.

In particular, the High Energy Intranuclear Cascade (INC) and Internuclear Cascade Transport Code, HETC [e.g. (7)] is used to calculate directly the nuclide production rate due to spallation. It is planned to link the neutron source results generated with HETC to the low energy neutron transport code, MORSE. The neutron induced cosmogenic nuclide production will be calculated without the resort to extrapolations of excitation functions.

The isotropic irradiation of a stony asteroid in space is modeled by utilizing the observed cosmic ray proton spectrum up to 200 GeV to select energy and frequency via Monte Carlo techniques. The composition of the bombarded asteroid is taken to be an L Chondrite like composition [e.g. (8)]. The HETC code follows the incident particle and its subsequent descendent light particles ($A < 5$) until they are absorbed, exit the meteorite (presently set at 1 m diameter) or drop below the low energy cut off. The neutrons generated in collisions which are below their 15 MeV cut off, are recorded at their site of production with their kinematic descriptors. These neutrons are stored in a file for subsequent neutron capture studies. The nuclei produced are also recorded at their collision sites with their production energy. The abundance and distribution of these nuclei, essentially the spallation induced nuclei, were analyzed in 5 shells of equal volume. The HETC calculations were performed for 48000 proton source particles sampled from an observed cosmic ray proton spectrum.

*Work performed under the auspices of the Department of Energy under contract nos. DE-AC02-76CH00016 (BNL) and DE-AC05-84OR21400 (ORNL).

¹Brookhaven National Laboratory, Upton, NY 11973

²Oak Ridge National Laboratory, Oak Ridge, TN 37831

³York College, CUNY, Jamaica, NY 11451

The analysis of the history events generated by HETC utilizes 4 outer shells down to a depth of 30 cm and the central sphere to yield the production rate of ^{26}Al at 3.1810×10^{-3} no. $\text{sec}^{-1} \text{cm}^{-3}$ which is equivalent to 54 dpm/kg for the decay rate predicted. The predicted ^{53}Mn production rate is 2.91×10^{-3} no. $\text{sec}^{-1} \text{cm}^{-3}$. Here the decay rate is calculated using the accepted Bogou standard: kg (Fe +1/3Ni), to give 223 dpm/kg for the ^{53}Mn decay rate.

Depth dependent neutron source spectra were calculated for a 1 m diameter meteorite in order to calculate the neutron capture contribution to nuclide production. Spallation and neutron induced production of cosmogenic nuclides both have to be examined in detail for measured radiogenic nuclides. It is expected that the spallation contribution will dominate near the surface while neutron induced contributions will dominate deep within the meteorite. Since cosmogenic nuclide ratios are less sensitive to incident flux normalization, selected isotopic ratios will be examined to give insight into inherent properties of the meteorite, such as pre-atmospheric-exposure size. In the present work only the spallation reaction product nuclei production rates are presented.

Monte Carlo calculations of ^{26}Al and ^{53}Mn production in model meteorite composition similar to L Chondrite has yielded predictions which are consistent with the observed decay rates in L Chondrite stony meteorites [e.g. (9)]. The calculated ^{26}Al production rate (54 dpm/kg) in a 1 m diameter meteorite as seen in fig. 1, is within 1/2 S.D. of the mean (49 ± 11 dpm/kg) taken from 100 bulk determinations in L Chondrite samples compiled by Nishiizumi. Similarly calculated average value for ^{53}Mn (223 dpm/kg) is consistent (cf fig. 2) with one S.D. off the mean in the widely scattered ^{53}Mn data (362 ± 113 dpm/kg) compiled by Nishiizumi.

An examination of the depth dependence of these nuclei are seen in figs. 3 and 4. According to the HETC predictions, there is a gradual rise in the rate of production for ^{26}Al up to a depth of about 8 cm, (or 25 g/cm^2) as seen in fig. 1 (bottom). The production rate as a function of depth shown for ^{53}Mn displays an "expected" behavior, rising as a function of depth shown in fig. 1 (top). In addition to the ^{26}Al and ^{53}Mn , spallation calculations have also been made for the cosmogenic nuclei ^{12}C , ^{13}C , and ^{14}C in the meteorite. Carbon isotope production is most unusual, since it is not expected in this L chondrite meteorite, yet it is produced at low levels by the spallation reactions as seen in fig. 4. However, the production rate indicates some statistical deviation from the mean as a function of depth.

In conclusion, considering the success of the HETC calculations in general and the level of statistical confidence presently generated, it is felt that the calculations must be performed with larger number of cascade particles. It may well be that the physical requirement to sample the large range of energies (40 MeV to 200 GeV) seen in the galactic cosmic ray spectrum demands more cascade particles.

1. Eberhardt, P., J. Geiss, and M. Lutz (1963) *Earth Science and Meteorites*, J. Geiss and E.D. Goldberg, eds., pp. 143-168.
2. Lingenfelter, R.E., and R. Ramaty, (1967) *High Energy Nuclear Reactions in Astrophysics*, ed., B.P. Shen, pp. 99-158.
3. Reedy, R.C. and J.R. Arnold (1972) *J. Geophys. Res.*, 77, 537-585.
4. Reedy, R.C., G.F. Herzog, and E.K. Jessberger (1979) *Earth Planet. Sci. Lett.*, 44, 341-348.
5. Reedy, R.C. (1985). *J. Geophys. Res.* 90, C722-728.
6. Spergel, M.S., R.C. Reedy, O.W. Lazareth, P.W. Levy, and L.A. Slates (1986) *J. Geophys. Res.*, 91, D483-520.
7. Armstrong, T.W., R.G. Alsmiller Jr., K.C. Chandler, and B.L. Bishop, (1972), *Nucl. Sci. and Eng.* 49, 82.
8. Mason, B. (1979) *Cosmochemistry; Part 1*, Sixth edition; 440-B-1.
9. Nishiizumi, K. (1987) *Nucl. Tracks Radiat. Meas.*, Vol. 13, No. 4, pp. 209-273.

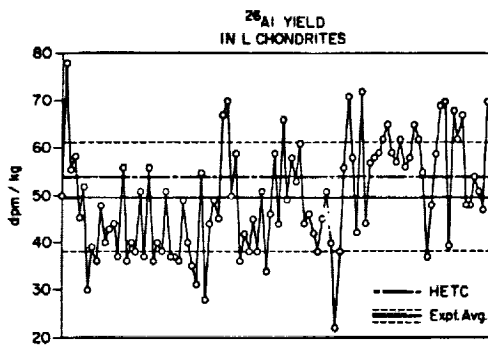


Fig. 1. ^{26}Al production rate: One hundred experimental data points taken from Nishiizumi's compilation are plotted to demonstrate the degree of fluctuation from the mean value (—). The HETC calculated mean value (—) over the meteorite volume is shown for comparison.

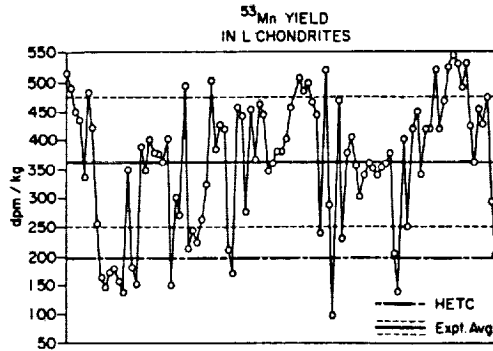


Fig. 2. ^{53}Mn production rate: One hundred experimental data points taken from Nishiizumi's compilation are plotted to demonstrate the degree of fluctuation from the mean value (—). The HETC calculated mean value (—) over the meteorite volume is shown for comparison.

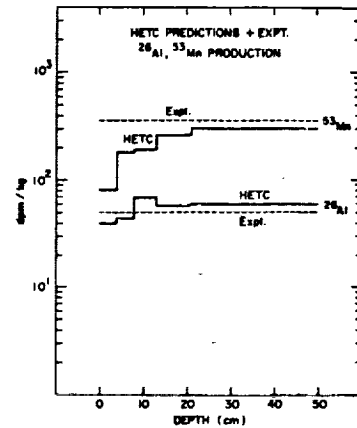


Fig. 3. Production rate of ^{26}Al (bottom) and ^{53}Mn (top) as a function of meteorite depth: Comparison of experimental mean value with HETC predicted averages over the meteorite volume. Conversion of production rate to dpm/kg units in the case of ^{53}Mn by making use of the Bogou standard.

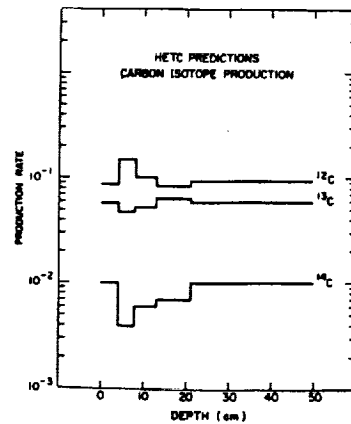


Fig. 4. HETC calculated spallation product production rates for carbon isotope ^{12}C , ^{13}C , and ^{14}C as a function of meteorite depth.

55-90
321023

p-5

APPLICATIONS OF THE HERMES CODE SYSTEM IN METEORITICS

P. Dragovitsch, P.Cloth, G.Dagge, D.Filges (Institut für Kernphysik KFA Jülich, POB 1913, D-5170 Jülich), R.Michel (ZfS Universität Hannover, Am kleinem Felde 30, D-3000 Hannover-1)

A promising way to understand the effects of galactic cosmic ray particle radiation (GCR) in extraterrestrial matter is to simulate the complex irradiation of the respective body by suitable computer codes. By this method beside the observation of integral quantities (e.g. production of cosmogenic nuclides in meteorites) also detailed studies of the mechanisms of particle transport, interaction and production can be done in a wide range of irradiation conditions. In this context the extensive capabilities of the newly developed HERMES (1) code system offer themselves for an application to meteoritical research.

HERMES (High Energy Radiation Monte Carlo Elaborate System) is a system of off-line coupled Monte Carlo Codes which are needed to treat the different physics to be considered in the computer simulation of radiation transport and interaction problems. Additional HERMES offers comprehensive capabilities of Monte Carlo analysis and to merge the intermediate outcomes of partial programs into final results. The easy interchange of input/output data between the different modules is realized by an interfacing system using standardized data structures (Fig. 1). For all codes identical terms of geometry description (Combinatorial Geometry, CG) are given, permitting the build up of particle cascades within very complex geometries and material configurations. The program modules of HERMES are able to simulate secondary particle histories induced by primary projectiles of any energy from thermal energies (e.g. neutrons) up to some 10 GeV. The particles being considered by the program are p, n, π^+ , π^0 , π^- , μ^+ , μ^- , e^+ , e^- , γ , and light-heavy ions to $A = 10$.

The main physics modules of HERMES are HETC/KFA-2, MORSE-CG and EGS4. Beside some minor physics programs they are surrounded by a framework of modules treating for example the Monte Carlo analysis, the geometric setup, the command language or the graphical reproduction of the results.

In general the transport of an incoming high energy projectile (except γ -rays) is performed by HETC/KFA-2. The code follows the history of the incident particle to its first collision with a nucleus and performs the production of secondary particles using the intranuclear cascade-evaporation model (INCE) (1, and refs. therein). The outgoing secondary particles of the respective nuclear reaction are stored on a temporary stack. Their history is followed one after the other until predefined cut-off energies are reached or the geometry is left. Those particles and particles which cannot be handled by the code, are written on a submission file and can be used as input for the other modules. Neutrons with energies below 15 MeV are submitted to MORSE which does a stochastic simulation of neutral particle (neutrons, γ 's) transport. The electromagnetic part of a shower is performed with EGS4 providing Monte Carlo simulation of the coupled transport of electrons and photons in the energy range between a few eV to some TeV.

The properties of HERMES discussed above show its excellent suitability to simulate cosmic ray interactions with extraterrestrial matter. In the past HERMES already was used to calculate the setups of accelerator-experiments simulating the 4π -isotropic GCR-irradiation of meteoroids (2,3,4) with monoenergetic protons. The equivalence between the experimental and the calculational approach (5) allows the extension of the computer simulations to realistic GCR-irradiations of extraterrestrial bodies in space.

A series of Monte-Carlo simulations of the isotropic and homogeneous irradiation of H- and L-Chondrites with GCR-protons was performed in the recent year. The meteoroids were assumed to be spherical with radii varying between 5 and 65 cm (tables 1,2). The differential energy-distribution of the incident GCR-protons was created from the average value of the GCR-fluxes of solar minimum 1965 and solar maximum 1969 to get a realistic source. Since the physical

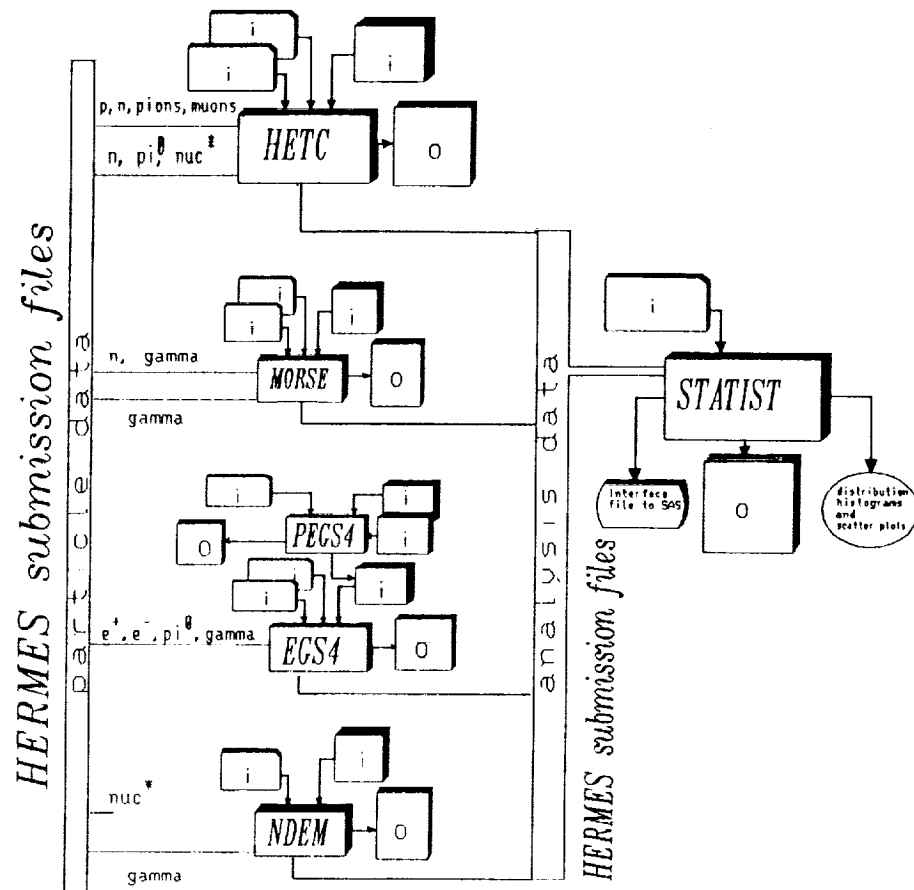


Fig.1: Organization scheme of the HERMES program system

Element	Diorite ($\rho = 3.0 \text{ g/cm}^2$)	L-chondrite ($\rho = 3.5 \text{ g/cm}^2$)	H-chondrite ($\rho = 3.5 \text{ g/cm}^2$)
O	49.5	40.0	35.7
Na	2.37	0.66	---
Mg	2.07	15.2	14.2
Al	7.89	1.1	1.01
Si	27.7	18.7	17.1
K	1.1	0.09	---
Ca	4.5	1.28	1.19
Cr	---	---	0.35
Fe	4.83	21.8	27.6
Ni	---	---	1.7

Tab. 1. : Material compositions of the meteoroids and meteoroid models calculated with HERMES

Composition	Radius (cm)	Depth Resolution (cm)
Diorite	5.	1.
	15.	1.
	25.	1.
L-chondrite	10.	1.
	25.	1.
	40.	4.
	65.	5.
H-chondrite	5.	0.5
	10.	1.
	25.	1.
	32.	3.2
	40.	4.
	65.	5.

Tab. 2. : Cases of meteoroids and meteoroid models calculated with HERMES using a realistic GCR source energy distribution

meaning of the residual nuclei distribution generated by transport codes in general is questionable, the analysis of the Monte Carlo events was done with respect to the fluxes of primary and secondary protons and neutrons. The fluxes of these particles were registered inside equidistant spherical shells of the meteoroids delivering depth dependent differential flux densities. Some results for the H-chondritic cases are shown in the figures 2-5. They manifest the sensitivity of primary and sec-

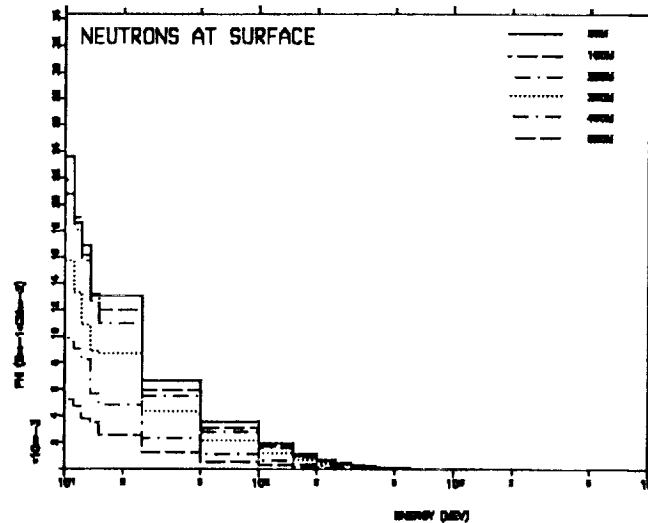


Fig. 2: Double differential flux densities of neutrons at the surface of H-chondrites induced by a realistic GCR proton spectrum

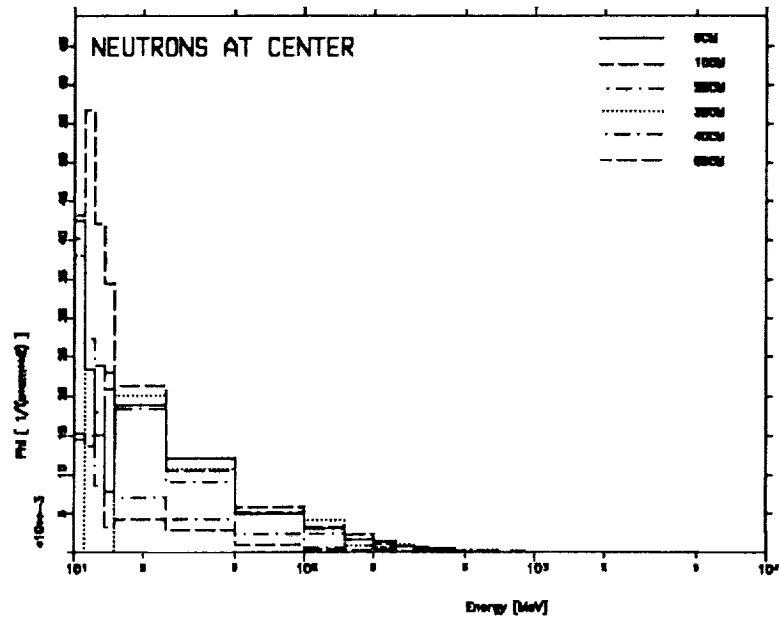


Fig. 3: Double differential flux densities of neutrons at the center of H-chondrites induced by a realistic GCR proton spectrum

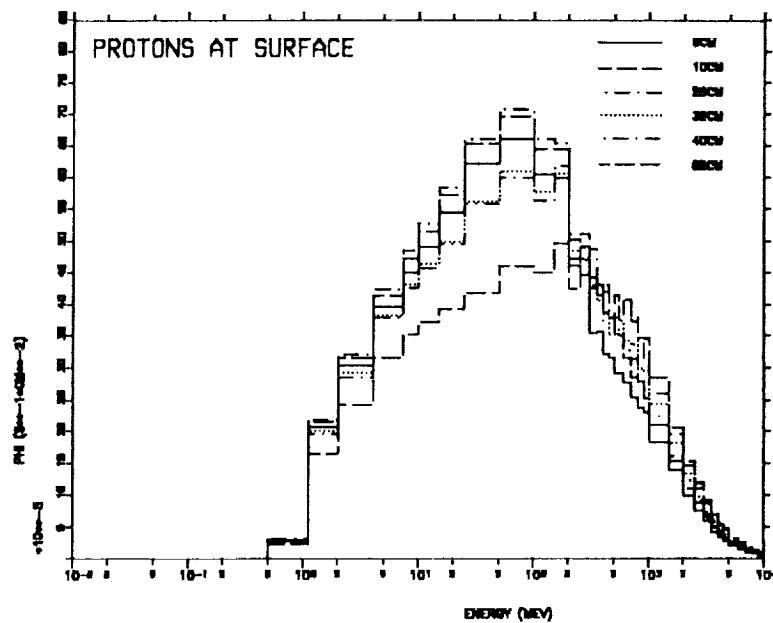


Fig. 4: Double differential flux densities of protons at the surface of H-chondrites induced by a realistic GCR proton spectrum

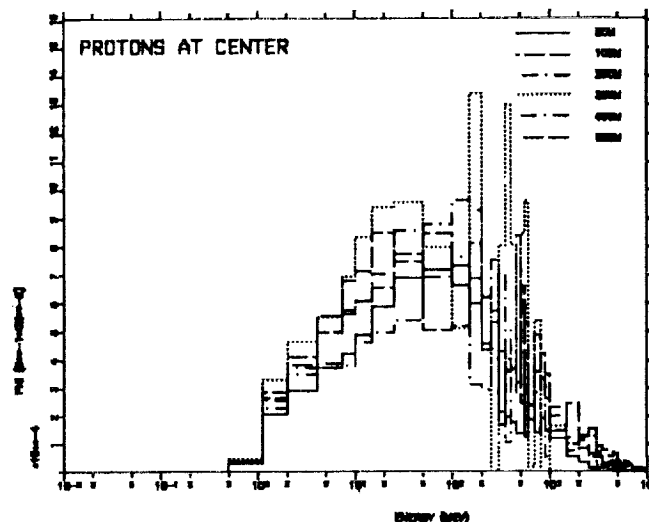


Fig. 5: Double differential flux densities of protons at the center of H-chondrites induced by a realistic GCR proton spectrum

ondary particles referring to the size of the respective meteoroid and the location inside. These changes can be seen in the total number as well as in the energy distribution of the particles. Hereby quite different systematics can be observed for protons and for neutrons.

The large data base of differential flux densities created by the HERMES calculations now allows to study the depth dependence of cosmogenic nuclide production in meteoroids with varying compositions and radii at realistic irradiation conditions. The integration of the presented results with reliable thin-target excitation functions leads (e.g. 2-5) to reproducible depth and size dependent production rates of cosmogenic nuclides. This way to calculate cosmogenic nuclide production - basing only on modern nuclear and medium-energy physics - allows a direct comparison with measurements of cosmogenic nuclides in meteorites (7). Without any other free parameter than the spectral distribution of the incident GCR particles it offers the chance to get concrete informations about the GCR-variations in time, intensity, energy-distribution and composition.

References:

- (1) P.Cloth et al. (1988) Jül-2203
- (2) Cologne Collaboration CERN SC96 Experiment (1987) Jül 2130
- (3) R.Michel et al. (1985) Nucl. Instr. Meth. Phys. Res. B16, 61-82.
- (4) R.Michel et al. (1989) Nucl. Instr. Meth. Phys. Res. B42, 76-100.
- (5) P.Dragovitsch et al. (1989) Simulation of the GCR Irradiation of Meteoroids: Unification of Experimental and Theoretical Approaches. This report.
- (6) R.Michel et al. (1989) Thin Target Cross Sections for the Production of Cosmogenic Nuclides in Extraterrestrial Matter by Galactic Cosmic Ray Particles. This report.
- (7) R.Michel et al. (1989) Monte Carlo Modelling of the Production of Cosmogenic Nuclides in Extraterrestrial Matter by Galactic Cosmic Ray Particles. This report.

56-90
321024
p.3

SIMULATION OF THE GCR IRRADIATION OF METEORIODS: UNIFICATION OF EXPERIMENTAL AND THEORETICAL APPROACHES P. Dragovitsch (Institut für Kernphysik KFA Jülich, POB 1913, D-5170 Jülich) and the Cologne Collaboration (1)

By the interaction of galactic cosmic ray particles (GCR) a large variety of stable and radioactive nuclides is produced in meteoroids. The observed abundances of these cosmogenic nuclides in meteorites provide a multitude of information on the irradiated matter as well as on the cosmic radiation itself. The interpretation of cosmogenic nuclides in terms of the irradiation history or of the temporal and spatial behavior of the GCR itself requires a precise and accurate modelling of the depth and size dependence of *all* nuclear interactions leading to the respective nuclide production. The approaches made in the past to uncover these mechanisms were not satisfactory, due to the lack of physical foundation of most calculational models and due to systematic experimental problems for nearly all simulation experiments. Therefore a collaboration (1) was initiated in 1983 to improve this situation. Two independent approaches - an experimental and a calculational - were made to study the transport and interaction phenomena of GCR in meteoroids.

A series of thick target irradiations of spherical meteoroid models with radii of 5, 15 and 25 cm with 600 MeV protons was performed at the CERN-synchrocyclotron. The artificial meteoroids were made out of diorite ($R = 5$ cm) and gabbro ($R = 15$ and 25 cm) with a density of 3 g cm^{-3} approximating a chondritic composition.

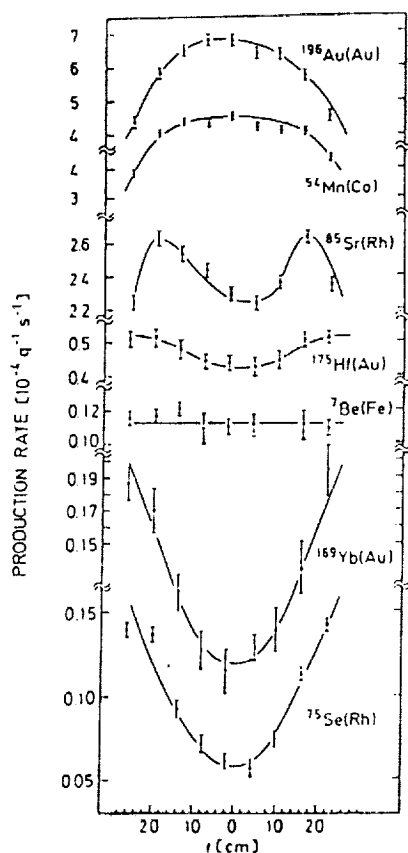


Fig. 1: Some depth profiles in meteoroid models after a 4π irradiation with 600 MeV protons

A homogeneous 4π irradiation of the models was achieved by complete mechanical integration of the accelerator beam using a sophisticated irradiation machine. The depth dependent production of a wide range of radionuclides from target elements O, Mg, Al, Si, Ti, Fe, Co, Ni, Cu, Ba, Lu, and Au was measured. Furthermore, the production of He and Ne isotopes from Al, Mg, Si and from degassed meteoritic material was determined. Including data derived from thin target experiments the size dependence of nuclide production for radii from 0 to 75 g cm^{-2} was investigated. For a detailed description see references (3) and (4) and the references therein.

The theoretical approach was to calculate the spectra of primary protons and of secondary protons and neutrons in the artificial meteoroids by computer simulation of the experimental setups. For this the HERMES code system (5) was engaged. HERMES is a system of Monte Carlo computer codes solving the physical problems of radiation transport and interactions within matter. A detailed description of the codes and the performance of the calculations is given in references (5) and (6).

SIMULATION OF THE GCR IRRADIATION OF METEOROIDS ... P.Dragovitsch et al.

Already the experimental depth profiles of nuclide production showed a wide variety of shapes depending both on the sizes of the meteoroid models and on the individual reaction channels possible for the respective nuclide. The strongest size dependence was observed for ^{60}Co from Co with center production rates increasing by a factor of 100 for radii between 5 cm and 25 cm. For other low energy products an increase up to a factor of 3.5 was typically observed. For products requiring extremely high incident energies a decrease of center production was seen up to a factor of 10. In between shapes having pronounced maxima (low energy products) and minima (high energy products), respectively, all transitional shapes could be observed (Fig. 1).

The calculated fluxes of the secondary protons and neutrons depended strongly on depth and size of the meteoroid models. The differences between proton and neutron spectra were considerable both in their shape and in their magnitude. For a detailed discussion see references (1) and (2). On the basis of thin-target excitation functions (1,2,3,4) these resulting spectra can be integrated to theoretical production rates:

$$P_i(R,r) = \sum_j \sum_k \int_E N_j \sigma_{ijk}(E_k) \Phi(E_k, R, r, t) dE$$

with

j	target element
k	projectile (p,n,...)
E_k	energy of the projectile
N_j	number of target atoms
σ_{ijk}	cross section of the reaction j(k,x)i (calculated or experimental, see eg. refs (7,8))
Φ	local differential particle flux density at r (calculated with HERMES)
R	radius of the meteoroid

The depth profiles calculated in this way allow to distinguish the different contributions of primary and secondary protons and of neutrons and to unravel the individual production modes of cosmogenic nuclides in meteoroids. The agreement between theoretical and experimental depth profiles (1,2) was a convincing validation of the suitability of the used computer codes in cosmic ray applications. So the HERMES calculations make it possible to model the production of residual nuclei in real meteoroids, provided that reliable excitation functions are given.

As a first extension of the theoretical approach the irradiation of meteoroid models in space with GCR-protons was simulated, using again a dioritic composition of the matrix. For this the energy distribution of the incident protons was assumed to be the average value of the GCR-fluxes of solar minimum 1965 and solar maximum 1969. So the differences between a monoenergetic and a spectral irradiation could be observed without changing any other parameter.

The comparison of the resulting particle fluxes with those of the monoenergetic 600MeV case showed significant differences by an increase both of secondary proton and neutron fluxes by simulating the "GCR" irradiation (2). The shapes of the particle spectra were quite different, too. The resulting depth dependent production rates (e.g. Fig.2) already showed a better approximation to those measured in meteorites than those of the monoenergetic cases (2,4) but the matrix dependent differences as well in their absolute values and as in their ratios were almost large. This indicated the necessity to study the effect of the meteoroid matrix by changing the chemical composition from diorite to H- and L-chondritic ones. These calculations were done in the recent year (6) for several meteoroid sizes. The resulting depth and size dependent production rates of cosmogenic nuclides now can be compared with real meteorites directly (9) showing an excellent agreement. So for the first time a parameterfree model is developed and validated which is able to predict cosmogenic nuclide production rates in meteoroids. More than this the model offers the capabilities to study

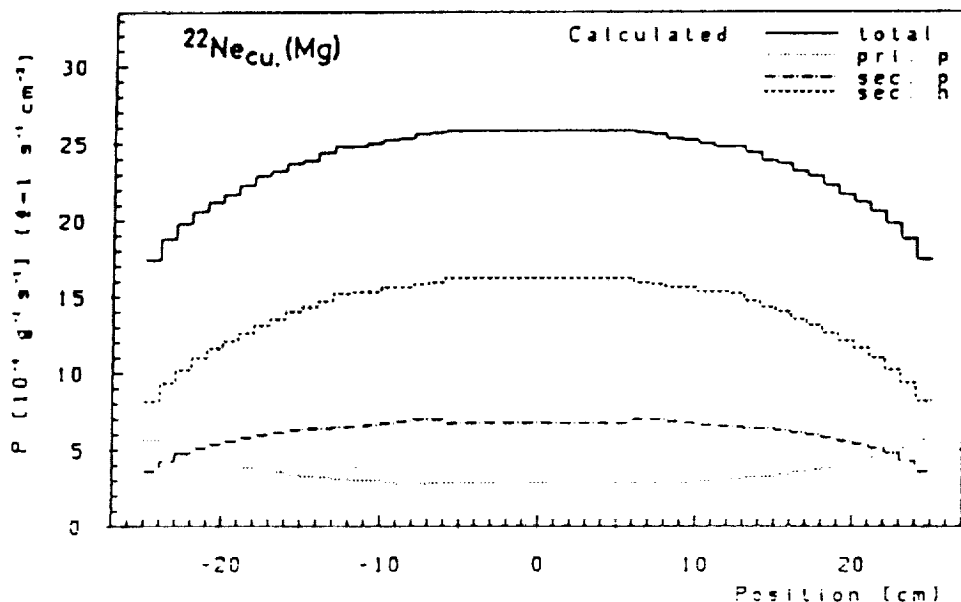


Fig. 2: Depth profile of the cumulative ^{22}Ne production from Mg inside a meteoroid with dioritic composition in the case of a 4 irradiation with a representative GCR-proton spectrum. Data are normalized to $\Phi_{\text{GCR}} = 1 \text{ proton s}^{-1} \text{ cm}^{-2}$.

the influence of the spectral distributions of GCR protons as well as the influence of GCR- α -particles. The connection of fluxes calculated by HERMES with reliable production cross sections promise to find out both the GCR-intensity and GCR-energy distribution in history as an unequivocal function of time.

References:

- (1) Cologne Collaboration CERN SC96 Experiment (1987): D.Alymer, F.Begemann, P.Cloth, P.Dragovitsch, P.Englert, D.Filges, U.Herpens, G.F.Herzog, A.Jermaikan, J.Klein, T.H.Kruse, R.Michel, R.K.Moniot, R.Middleton, F.Peiffer, P.Signer, R.Stück, S.Theis, C.Tuniz, S.Vadja, H.Weber and R.Wieler (1987) Jül 2130
- (2) P.Dragovitsch (1987) Thesis, University of Cologne.
- (3) R.Michel et al. (1985) Nucl. Instr. Meth. Phys. Res. B16, 61-82.
- (4) R.Michel et al. (1989) Nucl. Instr. Meth. Phys. Res. B42, 76-100.
- (5) P.Cloth et al. (1988) Jül-2203
- (6) P.Dragovitsch et al. (1989) Applications of the HERMES Code System in Meteoritics This report.
- (7) R.Michel and H.Lange (1989) Prediction of Thin-Target Cross Sections of Neutron-Induced Reactions up to 200 MeV. This report.
- (8) R.Michel et al. Thin-Target Cross Sections for the Production of Cosmogenic Nuclides by Charged-Particle-Induced Reactions. This report.
- (9) R.Michel et al. (1989) Monte Carlo Modelling of the Production of Cosmogenic Nuclides in Extraterrestrial Matter by Galactic Cosmic Ray Particles. This report.

SIMULATION EXPERIMENTS FOR COSMOGENIC NUCLIDE PRODUCTION RATES;
Peter A.J. Englert, Department of Chemistry, San Jose State University, San Jose, CA 95192

The major problems of accurate prediction of cosmogenic nuclide production rates depend on the way how the complex physical processes that lead to their production are understood and incorporated into models. Cosmogenic nuclide production cross sections, especially for neutron induced nuclear reactions are not known for all incident particle energies. This is a significant problem, as secondary neutrons form the major cosmogenic nuclide producing component of the secondary particle cascade within a meteorite or a planetary surface exposed to cosmic radiation [e.g. 1]. Furthermore, the secondary particle cascade itself is a function of the primary cosmic ray particle flux, the energy and charge of the entering particles, the depth within the meteorite and planetary surface, and the composition of the target. The flux, composition and energy of the primary cosmic radiation is well known and understood. Consequently, the two areas of major concern are nuclear interaction cross sections in particular for neutrons, and the development of the secondary particle cascade as a function of shielding and chemical composition of the meteorite or planetary surface.

Though, a priori, the determination of numerous reaction cross sections for residual nuclei, nature, energy and angular distribution of exit particles, would seem to be the best way to solve all problems, it is immediately obvious that this is a long-term ambitious task. For proton and alpha-particle cross-section extensive tables have been established since about 1978 by Michel et al. [e.g. 2].

Simulation experiments are not equivalent to cross section experiments. In general, a few parameters are precisely known or controlled. A few, but by far not all effects of a controlled parameter change on the complex system are observed, in order to allow conclusions on the unobserved multitude of parameters. The result of a simulation experiment is therefore not a new physical parameter, but rather a step towards a better physical understanding of the phenomenon of interest or indication for changes of a model. The use of simulation experiments will therefore serve two aspects, the improvement and extension of our physical understanding of the complex phenomena as well as the validation of existing semiempirical models.

The different approaches of simulation experiments obtain their justification from the fact that no charged particle accelerator is able to produce particle beams with energy spectra even partially similar to that of the solar or galactic cosmic radiation. In addition, only one charged species can be produced at a time. In order to simulate the interaction of cosmic radiation with matter several experimental runs with different particle types and different energies would have to be made to approach the problem. On the other hand, complex neutron spectra, as they occur upon interaction of the galactic cosmic radiation inside matter are not too difficult to produce with monoenergetic charged particles from accelerators, but to determine their energy spectra and fluxes at a certain location within the irradiated matter is everything else but trivial; it is frequently not possible.

The first approach is based on the bombardment of thick targets: High energy charged particles bombard a target of defined dimensions to develop secondary particle fluxes as they may occur in reality. Elements or simple chemical compounds are exposed to different particle fields inside the target and subsequently analyzed for nuclear reaction products. A second approach consists in the generation of complex neutron beams of reasonably well known

or measured energy spectra and flux. These spectra may represent those occurring under certain conditions in planetary surfaces or meteorites, and cosmogenic nuclide production rates can be determined for those conditions.

Research in the past was concerned with the production of residual stable and radioactive nuclides, many of which were short-lived and only partially useful in cosmogenic nuclide studies. A compilation of Thick Target experiments performed until 1984 can be found in [3]. Much progress has been made with thick target bombardments for cosmogenic nuclide studies in meteorites recently, i.e. after 1984. Two contributions of this workshop will discuss the CERN meteorite model irradiations series, model validation and application of the results to meteorites [4].

Only one additional thick target experiment has been performed and results relevant to cosmogenic nuclide research were obtained recently. This experiment was the exposure of a very thick rock target to 2.1 GeV protons and 800 MeV/nucleon alpha particles, in order to simulate the interaction of galactic cosmic radiation with matter. The effect of the projectile type on the build up of the low energy neutron component of the secondary cascade was analyzed [5]. It was shown that in case of alpha-particle impact the low energy neutron flux maximum occurred at shallower depths than in the case of the proton experiment. A ^{14}C depth profile along the beam axis was determined in the target rock material [6], and a ^{10}Be and ^{26}Al profile in aliquots of the same samples are in progress. The ^{14}C -contents follow the secondary cascade development as a function of depth as modeled for undisturbed lunar surface cores. The dependence of ^{14}C -production on the low energy component suggests strongly detailed studies of the depth dependent production of the isotope in meteorites and meteorite model irradiations. No extensive model calculations were done in this case.

Complex neutron spectra are obtained around beam stops of accelerators. If facilities are available to irradiate samples in these beam stop areas, simulation experiments with thin targets in these neutron fields are possible. The difficulty that arises immediately is the determination of the neutron spectra and fluxes. Under cosmogenic nuclide production conditions only threshold monitor reactions are applicable, and, consequently, energy spectra and to some extent also fluxes have a high degree of uncertainty.

Beam stop exposure experiments were continued and focussed especially neutron produced ^{10}Be , ^{14}C , and ^{26}Al in silicon dioxide as it is important for terrestrial applications [7,8]. Though absolute production rates cannot be determined in such experiments, production rate ratios obtained contain useful information.

Thick target bombardments have proven to be very successful simulation experiments useful for cosmogenic nuclide production rate studies. The difficulties of determining neutron fluxes and energy spectra in beam stop environments make experiments there less somewhat less useful.

REFERENCES: [1] R.C. Reedy and J.R. Arnold, *J Geophys. Res.* 77 (1972) 537. [2] R. Michel, G. Brinkmann, and R. Stueck, *Earth Planet Sci. Lett.* 59 (1982) 33. [3] R.C. Reedy and P. Englert (1986) LPI Tech. Rpt. 86-06. [4] R. Michel et al., accepted for publication in: *Nucl. Instr. Meth. B.* (1988) [5] P. Englert, R.C. Reedy, and J.R. Arnold, *Instr. Meth.* A262 (1987) 496. [6] P.A.J. Englert, A.J.T. Jull, D.J. Donahue, and R.C. Reedy, *Lunar Planet. Sci. Conf. XIX, Abstr.* (1988) 303. [7] Reedy, R.C., D. Lal, K. Nishiizumi, J.R. Arnold, D. Elmore, P. Kubik, J. Klein, R. Middleton, and P. Englert, *Progress at LAMPF, IA-11339-PR*, (1987) 148 [8] A.J.T. Jull, P.A.J. Englert, D.J. Donahue, R.C. Reedy, and D.Lal, *Lunar Planet. Sci. Conf. XX, Abstr.* (1989) 490.

58-90
321026 p-9
49

A MODEL FOR THE PRODUCTION OF COSMOGENIC NUCLIDES IN CHONDRITES

Th. Graf*, H. Baur, P. Signer. ETH-Zürich, Switzerland. *Pres. address: Univ. of California, San Diego.

The production rates of cosmic-ray produced nuclides depend on the chemical composition of a meteoroid, its size and shape and the location of the samples within it. In turn, the accuracy of exposure age estimates depends on the knowledge of the production rates. We developed a model to calculate the production rates of the stable nuclides He, Ne, and Ar as well as of the radionuclides ^{10}Be , ^{26}Al , and ^{53}Mn in chondrites of any shape and size. This model is based on the production rate equation used by Signer and Nier [1] to model the distribution of the light noble gases in iron meteorites. The equation contains 2 free parameters for each nuclide which were fitted to our new data from the cross section of the L5 chondrite Knyahinya [2,3]. The validity of the model was then tested by comparing the predictions with experimental data on Keyes [4], St. Severin [5], and ALHA78084 [6]:

Fig. 1 shows predicted and measured $^{22}\text{Ne}/^{21}\text{Ne}$ ratios in the three test meteorites and in Knyahinya. The predictions are in excellent agreement with the experimental data. In fact, the deviations from the calculated depth profiles are comparable to the experimental uncertainties. To obtain agreement of the model predictions with $^{22}\text{Ne}/^{21}\text{Ne}$ ratios observed in St. Severin, the assumption of a nonspherical shape for this meteorite is required. We use an ellipsoidal shape with semi-axes of 40 cm, 25 cm, and 20 cm, which is consistent with the shape derived from track densities [7]. For ALHA78084, Keyes, and Knyahinya we adopt preatmospheric radii of 15 cm, 31 cm, and 45 cm, respectively. Exposure ages based on the production rates of ^{21}Ne and ^{38}Ar agree within 5% for each of the meteorites. Furthermore, the model reproduces the shape of the measured depth profiles of ^{10}Be , ^{21}Ne , ^{22}Ne , ^{38}Ar , and ^{53}Mn within error limits, which unfortunately are still large compared to those of the $^{22}\text{Ne}/^{21}\text{Ne}$ ratios. Differences between ^3He ages and ^{21}Ne ages are up to 10% and a comparison of measured and predicted $^3\text{He}/^{21}\text{Ne}$ ratios yields similar differences. This indicates a shortcoming of our model which predicts a size and shape independent linear correlation between the ratios $^3\text{He}/^{21}\text{Ne}$ and $^{22}\text{Ne}/^{21}\text{Ne}$. In distinction, the correlation lines of all three test meteorites are considerably flatter than the one of Knyahinya.

Fig. 2 shows calculated production rates of ^{21}Ne versus $^{22}\text{Ne}/^{21}\text{Ne}$ ratios for spherical meteoroids of various radii. The $^{22}\text{Ne}/^{21}\text{Ne}$ ratio is widely used to calculate shielding corrected exposure ages. The dashed line in Fig. 2 shows the empirically determined shielding dependence of $P(^{21}\text{Ne})$ proposed by Eugster [8]. Because most meteorites have preatmospheric radii between 10-50 cm and the shielding depth of most samples exceed several centimeters, the relation between $P(^{21}\text{Ne})$ and $^{22}\text{Ne}/^{21}\text{Ne}$ ratios is an approximation that allows in some cases the determination of exposure ages with an uncertainty of 10-20%. However, Fig. 2 shows clearly, that the $^{22}\text{Ne}/^{21}\text{Ne}$ ratio does not uniquely quantify the shielding conditions of a sample. It is expected that the shielding dependence of production rate ratios is in general smaller than that of production rates. For many years, ratios of stable and radioactive nuclides were used to determine exposure ages. Thereby the production rate ratio of the two nuclides has to be known. Our model predicts that 3-isotope correlations which use the same reference isotope are linear [9]. This might be an oversimplification, especially for the correlations of $^3\text{He}/^{21}\text{Ne}$ and $P(^{26}\text{Al})/P(^{21}\text{Ne})$ ratios with

$^{22}\text{Ne}/^{21}\text{Ne}$ [3]. However, within error limits such a correlation exists for the $P(^{10}\text{Be})/P(^{21}\text{Ne})$ ratios of Knyahinya, Keyes, St. Severin, and ALHA7808. It can be used to compute size and shielding corrected exposure ages in chondrites:

$$\frac{t}{1 - \exp(-4.6 \times 10^{-7} \times t)} = \frac{P(^{10}\text{Be})/P(^{21}\text{Ne})_{(1.11)} + (0.053 \pm 0.03) \times (^{22}\text{Ne}/^{21}\text{Ne} - 1.11)}{(^{10}\text{Be}/^{21}\text{Ne})_{(m)}}$$

The production rate ratio $P(^{10}\text{Be})/P(^{21}\text{Ne})_{(1.11)}$ is given in atoms/atom and for a $^{22}\text{Ne}/^{21}\text{Ne}$ ratio of 1.11. The index m denotes the measured values. Adopting an exposure age for Knyahinya of 40.5 Ma [2], we determine $P(^{10}\text{Be})/P(^{21}\text{Ne})_{(1.11)} = 0.141 \pm 0.002$. Exposure ages of St. Severin and ALHA78084 derived by this method agree within 5% with those based on noble gas profiles. Note, that the slope of the correlation line may be 0 within 2σ error limits, indicating that the production of ^{10}Be by lower energy particles is about as important as for ^{21}Ne .

References: 1) Signer P. and Nier A.O. (1960) *J. Geophys. Res.* 65, 2947-2964. 2) Graf Th. et al. (1989) submitted to *Geochim. Cosmochim. Acta*. 3) Graf Th., Baur H., and Signer P. (1989) submitted to *Geochim. Cosmochim. Acta*. 4) Cressy P. J. (1975) *J. Geophys. Res.* 80, 1551-1554, and ref. therein. 5) Tuniz et al. (1984) *Geochim. Cosmochim. Acta* 48, 1867-1872, and ref. therein. 6) Sarafin R. et al. (1985) *Earth Planet. Sci. Lett.* 72, 171-182. 7) Cantelaube et al. (1969) in: *Meteorite Research*, ed: P.M. Millman, D. Reidel Publishing Company, Dordrecht, Holland, 705-713. 8) Eugster O. (1988) *Geochim. Cosmochim. Acta* 52, 1649-1662. 9) Voshage H. (1984) *Earth Planet. Sci. Lett.* 71, 181-194.

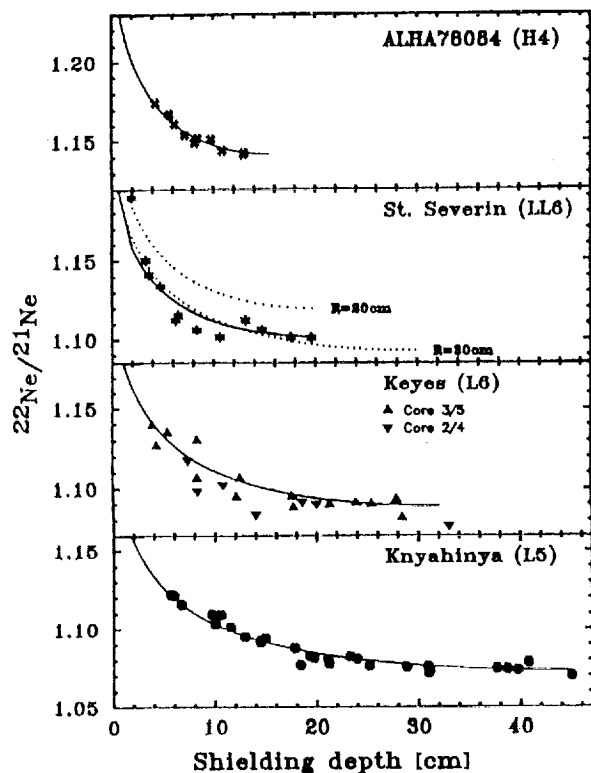


Fig. 1: Comparison of experimental $^{22}\text{Ne}/^{21}\text{Ne}$ ratios with predictions of our model. The dotted lines indicate model lines for a spherical shape and preatmospheric radii of 20 cm and 30 cm.

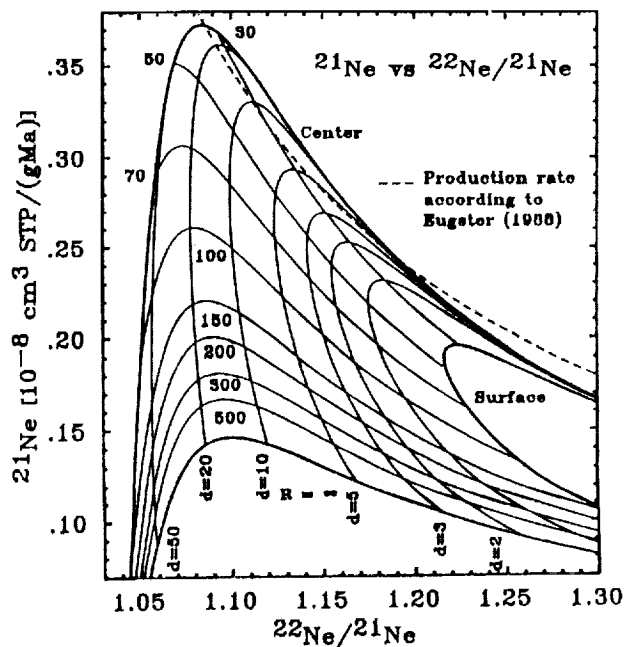


Fig. 2: Correlation between $P(^{21}\text{Ne})$ and the $^{22}\text{Ne}/^{21}\text{Ne}$ ratios at different positions in L-chondrites of various sizes. Numbers indicate radius and depth in cm. The dashed line indicates the shielding correction of the ^{21}Ne production rate proposed by Eugster [8].

COMPOSITION DEPENDENCE OF COSMOGENIC NUCLIDE PRODUCTION RATES;
G.F. Herzog, Dept. Chemistry, Rutgers Univ., New Brunswick, NJ 08904.

The rate P_i at which cosmic rays produce a cosmogenic nuclide i in a meteoroid or a planet depends in part on the composition of the irradiated body (Equation 1):

$$(1) \quad P_i = \sum_j N_j \sum_k \int_0^{\infty} \sigma_{i,j,k}(E) \phi_k(E) dE$$

Here N_j represents the absolute elemental abundances, the index k runs over all types of nuclear-active particles (principally p , α , n), ϕ refers to the various particle fluxes and σ gives the cross sections for the formation of the nuclide as a function of the bombarding energy E . To the extent that ϕ_k is independent of composition and other factors, one can approximate P_i as a linear combination of terms, $P_i = \sum_j N_j P_{ij}$, where P_{ij} may be regarded as an elemental production rate. A set of numerical values for P_{ij} has practical utility: With such a set, one may normalize the concentrations of cosmogenic nuclides measured in bodies with different compositions to those expected in some compositional standard. Two related methods for estimating P_{ij} directly from measurements of cosmogenic nuclides were first applied to the cosmogenic noble gases.

Stauffer [1] analyzed the He, Ne and Ar contents of an assortment of meteorites with known and markedly different compositions. By using regression analysis, he obtained production coefficients for the ratios $^{21}\text{Ne}/^3\text{He}$ and $^{38}\text{Ar}/^3\text{He}$. With the assumption that P_3 is constant, the expressions he derived become estimates of the relative elemental production rates of ^{21}Ne and ^{38}Ar . Hintenberger et al. [2] modified the approach by analyzing minerals separated chemically from a single specimen of the L6 chondrite Holbrook. The restriction to one sample removes from the regression analysis noise due to shielding differences at the possible cost of some loss of generality. Bogard and Cressy [3] applied this method to minerals separated magnetically and by density from Bruderheim (L6) and reviewed earlier work for light noble gases. Table 1 presents a partial summary of results for GCR production of selected cosmogenic nuclides. To facilitate comparisons we have normalized production rates to those expected for the principal target element.

Model calculations and simulation experiments usually provide information about the composition dependence of production rates in tabular or graphical rather than equation form (e.g., [4,5]). Hohenberg et al. [6] and Regnier et al. [7] give elemental production rates for the cosmogenic noble gases in the moon. Table 1 includes an approximation of Reedy's calculations of P_{10} in St. Severin. It also includes some average values of P_{ij} for P_{21} and P_{26} from simulation experiments [8].

The assumption that $\phi_k(E)$ is independent of composition (and hence the inference $P_i = \sum_j P_{ij} N_j$) fails under certain conditions. **A)** If a nuclide is produced to a significant degree by thermal neutrons (e.g., ^{36}Cl [9], ^{80}Kr and ^{82}Kr [10], and ^{129}I [11]), then P_i will not equal $\sum_j N_j P_{ij}$ when the matrices to be compared contain different concentrations either of hydrogen (because H moderates the neutron spectrum effectively) or of elements with high cross sections for reactions with neutrons [12]. **B)** Begemann and Schultz [13] argue that the assumption of composition-independent $\phi_k(E)$ breaks down for the products of interactions at somewhat higher energies, e.g., ^{38}Ar from Ca. They suggest that the rate of secondary production should vary with the average atomic number of the matrix. **C)** The assumption of constant ϕ_k may fail for reasons not directly related to the composition of the body (temporal and spatial variation of the primary flux or the occasional influence of solar cosmic rays). In practice, these effects are treated separately and indeed, may be identified by the failure of the conventional composition- and shielding-dependent equations to reproduce measured values [14].

References: 1. Stauffer H. (1962) *J. Geophys. Res.* 67, 2023-2028. 2. Hintenberger H. et al. (1964) *Z. Naturforsch.* 19a, 88-92. 3. Bogard D.D. and Cressy P.J. (1973) *Geochim. Cosmochim. Acta* 37, 527-546. 4. Reedy R.C. (1985) *Proc. Lunar Planet. Sci. Conf.* 15th,

COMPOSITION DEPENDENCE OF PRODUCTION RATES: Herzog G.F.

J. Geophys. Res. 90, C722-C728. Reedy R.C. (1987) *Nucl. Inst. Meth.* B29, 251. 5. Michel R. et al. (1986) *Nucl. Inst. Meth.* B16, 61-82. Michel R. et al. (1989) *Lunar Planet. Sci.* 20, 693-694. 6. Hohenberg C.M. et al. (1978) *Proc. Lunar Planet. Sci. Conf. 9th*, 2311-2344. 7. Regnier S. et al. (1979) *Proc. Lunar Planet. Sci. Conf. 10th*, 1565-1586. 8. Aylmer D. et al. (1987) *Ber. Kernforschungsanlage Julich Nr.* 2130, pp. 1-261. 9. Eberhardt P., Geiss J. and Lutz H. (1963) In: *Earth Science and Meteoritics*. North-Holland, Amsterdam, pp. 143-168. 10. Marti K., Eberhardt P. and Geiss J. (1966) *Z. Naturforsch.* 21a, 398-413. 11. Nishiizumi K. et al. (1986) *Geochim. Cosmochim. Acta* 50, 1017-1021. 12. Evans L.G. and Squyres S.W. (1987) *J. Geophys. Res.* 92, 9153-9167. Lapidés J.R. (1981) Ph.D. thesis, Univ. of Maryland, 115 pp.. Spergel M.S. et al. (1986) *Proc. 16th Lunar Planet. Sci. Conf., part 2, J. Geophys. Res.* 91, D483-D494. 13. Begemann F. and Schultz L. (1988) *Lunar Planet. Sci.* 19, 51-52. 14. Begemann F. and Wanke H. (1969) In: *Meteorite Research*. D. Reidel, Holland, pp. 363-371. Cressy P.J. and Rancitelli L.A. (1974) *Earth Planet. Sci. Lett.* 22, 275-283. Evans J.C. and Reeves J.H. (1987) *Proc. Lunar Planet. Sci. Conf.* 18, 271-272. Nishiizumi K. et al. (1983) *Nature* 305, 611-612. 15. Moniot R.K. et al. (1988) *Geochim. Cosmochim. Acta* 52, 499-504. 16. Tuniz C. et al. (1984) *Geochim. Cosmochim. Acta* 48, 1867-1872. 17. Bochsler P. et al. (1969) In: *Meteorite Research*. D. Reidel, Holland, pp. 857-874. 18. Hampel W. et al. (1980) *Geochim. Cosmochim. Acta* 44, 539-547. 19. Fuse K. and Anders E. (1969) *Geochim. Cosmochim. Acta* 33, 653-670. 20. Cressy P.J. (1971) *Geochim. Cosmochim. Acta* 35, 1283-1296. 21. Keith J.E. and Clark R.S. (1974) *Proc. 5th Lunar Conf.*, 2105-2119. 22. Begemann F. et al. (1976) *Geochim. Cosmochim. Acta* 40, 353-368. 23. Nishiizumi K. (1978) *Earth Planet. Sci. Lett.* 41, 91-100.

Table 1. Relative production rates for selected isotopes.

Isotope	P_{ij}							Ref.
	<u>Q</u>	<u>Mg</u>	<u>Al</u>	<u>Si</u>	<u>S</u>	<u>Ca</u>	<u>Fe</u>	
¹⁰ Be	1.0	0.94	≅1.1Mg	≅0.5Mg	≅0.5	≅0.3	≅0.16	15
	1.0	0.36		0.21			0.11	16
	1.0	0.32	0.28	0.17				8
	<u>Mg</u>	<u>Al</u>	<u>Si</u>	<u>S</u>	<u>Ca</u>	<u>Fe</u>	<u>Ni</u>	
²¹ Ne	1.0	≅1.35Si	0.15					1
	1.0		0.55	0.16		0.01		2
	1.0	≅1.35Si	0.19		≅~3Fe	0.006	≅Fe	17
	1.0		0.19	0.13	0.04	0.01	≅Fe	3
	1.0	0.36	≅0.19	≅0.13	≅0.04	≅0.01	≅Fe	18
	1.0	0.42	0.38					8
²⁶ Al	≅0	1.0	0.65	0.08	≅0.0157	≅0.005		19
	0.02	1.0	0.22	0.12	≅0.02	≅0.002	≅Fe	20
	0.09	1.0	0.56	≅0.27	≅0.05	≅0.006		18
	0.65	1.0	0.24					21*
		<u>K</u>	<u>Ca</u>	<u>Ti-Mn</u>	<u>Fe</u>	<u>Ni</u>		
³⁸ Ar				1.0		0.06		1
			7.0	1.0	0.22	0.056	≅Fe	3
				1.0		0.030		22
⁵³ Mn						1.00	0.33	23

*for lunar sample with mass = 1 kg.

510-90
321028
P 2

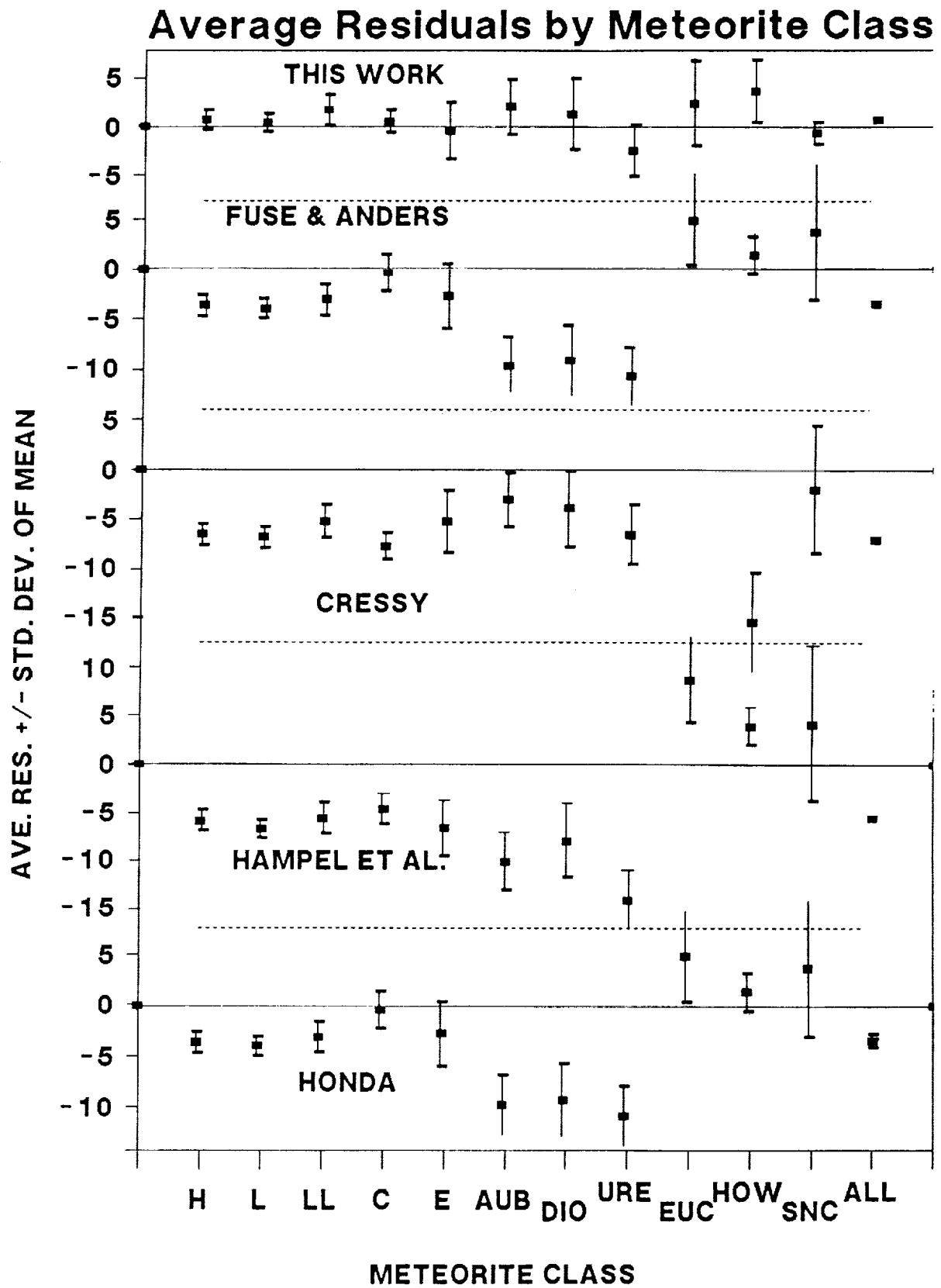
SATURATED ²⁶AL IN STONY METEORITES; J. E. Keith¹, H. R. Heydegger² and K. E. Kavana² 1. Johnson Space Center, Houston, TX. 2. Purdue University Calumet, Hammond, IN.

We have assembled from the literature a data base in which over 300 meteorites appear and which contains information on the bulk chemical analyses of these meteorites and their ²⁶Al content. Most numerical information in the data base is the average of several measurements.

We have regressed the ²⁶Al values on the chemical contents using the standard linear model with the pure constant set to zero. We have used an iterative algorithm which systematically eliminates under- and super-saturated ²⁶Al values, by forcing the residuals to be normally distributed. As a result, we obtain three sets of observations: 10 supersaturated, 128 saturated and 50 undersaturated, and an expression for the saturated ²⁶Al content as a function of the chemical composition. In the figure we compare the residuals predicted by our expression to those predicted by the expressions of other workers (1,2,3,4), class by meteorite class. The ideal result is zero, which is not forced, since in no case is the pure constant set to zero. As an examination of the figure will show, there is no bias in our prediction of saturated ²⁶Al content as a function of meteorite class, but there are biases in all previous predictive expressions.

We have explored the question of whether the regression coefficients will approach simple functions of the nuclear reaction cross sections, given increasing sample size. We show that this is not to be expected unless the mathematical model is correct, or the set of additional observations happens to be orthogonal to those comprising the assumed model. We demonstrate the consequences of attempting multiparameter regressions with nearly collinear data sets such as these without examining both the correlation structure of the X matrix and the residuals. We also examine the effects of increasing collinearity and decreasing sample size.

REFERENCES: 1) Fuse, K. and Anders, E. (1969) Geochim. et Cosmochim. Acta 33 653 - 670. 2) Cressy, P. J. Jr. (1971) Geochim. et Cosmochim. Acta 35 1283 - 1296. 3) Hampel, W. et al. (1980) Geochim. et Cosmochim. Acta 44 539 - 547. 4) Honda, M. (1988) Meteoritics 23 3 - 12.



COSMOGENIC NUCLIDE PRODUCTION IN EXTRATERRESTRIAL OBJECTS; D. Lal, Scripps
Institution of Oceanography, GRD, A-020, La Jolla, CA 92093, U.S.A.

P-3

The field of cosmogenic nuclides in extraterrestrial and terrestrial samples has come of age. It is beginning to make important contributions in the study of the evolutionary history of extraterrestrial and terrestrial samples (1,2,3,4,5). This is a result of (i) advancement in our capability of making sensitive measurements of nuclides in small samples, and (ii) better estimates of the production rates of nuclides. Besides delineating the evolutionary history of matter, an important aim of the cosmogenic studies is to evaluate how cosmic ray flux, energy spectrum and chemical composition changed in the geologic period (6). A prerequisite in these studies is an exact knowledge of the rates of production of cosmogenic nuclides in different targets for different irradiation geometries. Furthermore, the studies involve a fairly detailed knowledge of the geological history of samples (the term geological is being used here to convey the sense of time for extraterrestrial samples also). Any uncertainties can lead to erroneous interpretations of the cosmogenic data. The success of an experiment in this field depends crucially on these two factors.

The analytical functions describing the nuclide production rates can be written down fairly exactly for any irradiation geometry; however, two of the functions, the nuclide excitation functions, $\sigma(E)$, and the nucleon energy spectra $f(E)$, are generally not known well enough. In the case of the former, one often has to use the proton excitation functions, even in situations where most of the nuclide production occurs due to neutrons.

Experimental data on the nucleon energy spectra are virtually non-existent for the case of thick targets exposed in space. They have to be inferred from observations of nuclear disintegrations in cosmic ray experiments and studies of nuclide production in the atmosphere (7), or from simulation studies by irradiating of thick targets with high energy protons (8,9). In spite of the heroic efforts to simulate 4π irradiation geometry, and to include a large number of nuclides in these studies, these efforts have not yet reached a satisfactory conclusion, partly because high energy ($E \geq 1$ BeV) irradiations are lacking. These studies have triggered the development of sophisticated transport codes for the development of cascade nucleons in the thick targets (10,11).

The present situation on prediction of production rates of nuclides in the atmosphere, as well as in condensed materials (rocks, tree rings, ice, etc.) seems to be quite satisfactory (5,7,12). This is a consequence of the fact that basic cosmic ray data, e.g. the flux and energy spectra of low and high energy neutrons at all latitudes and altitudes, temporal variations in the neutron fluxes in the lower atmosphere, rates of nuclear disintegrations in the atmosphere, etc. are available for the atmosphere. The vertical thickness of the atmosphere corresponds to more than 12 interaction mean free paths for nucleons. Therefore, any

IN EXTRATERRESTRIAL OBJECTS: La1

calculations based on nucleonic cascade theories can lead to appreciable errors, in particular for the lower atmosphere, due to any uncertainties in the free parameters. For this reason, in their calculations, Lal and Peters (7) relied as far as possible on the experimental cosmic ray data, and subsequently, in favorable cases, normalized nuclide production rates obtained by measuring exposing various targets in the atmosphere. Recent studies of fall-out of the long-lived radionuclide, ^{10}Be , *in situ* production rates of long lived nuclides in geologically documented rocks, etc., all provide evidence for the accuracy in the prediction of nuclide production rates in the atmosphere (12,13).

In the case of extraterrestrial objects, one of course makes the fullest use of the atmospheric cosmic ray data, but the situation is not comparable. Large differences arise in the development of the cascade of unstable nuclear active particles π^\pm mesons and nucleons. In the atmosphere, most of the fast π^\pm mesons, of energies < 10 GeV decay. In condensed targets (e.g. the meteorites), all fast π^\pm mesons ($E > 100$ MeV) interact and produce fast nucleons and π^\pm mesons. In Fig. 1, is plotted the production spectrum of nuclear active particles in the upper atmosphere, based on observations of nuclear disintegrations in nuclear emulsions by Camerini *et al.* (see Ref. 14). For kinetic energies above 500 MeV, the shapes of the energy spectra at production for pions and nucleons are similar, but the pion intensity is about $3\times$ that of nucleons.

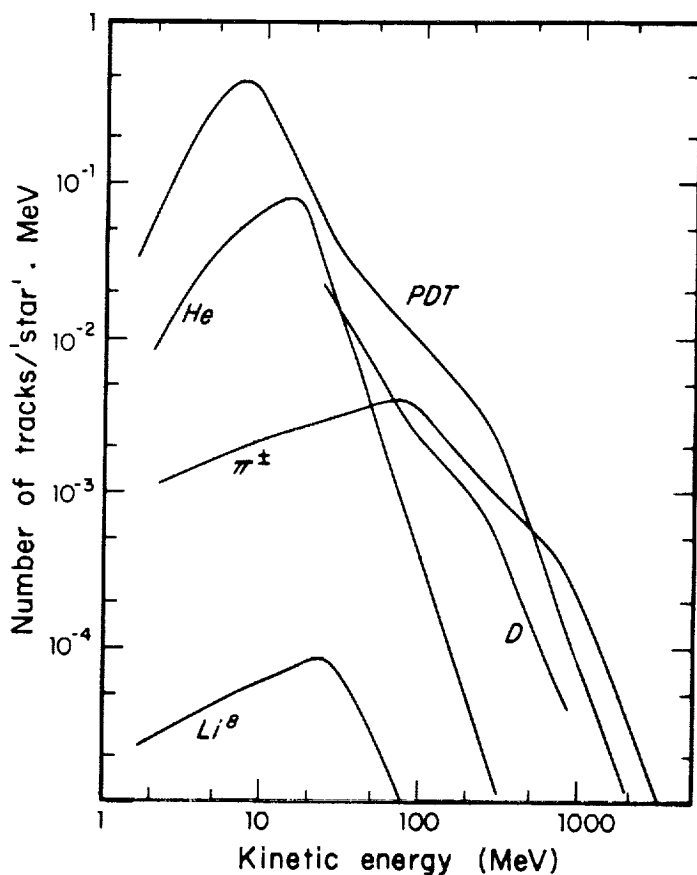


Fig. 1 Kinetic energy spectra of particles emitted in cosmic ray produced nuclear disintegrations in "nuclear emulsions" exposed at high altitude (Ref. 14). The curve labeled PDT refers to combined spectra of protons, deuterons and tritons.

IN EXTRATERRESTRIAL OBJECTS: Lal

The first estimates of nuclide production in meteorites were made by Signer and Nier (15), for ^3He in iron meteorites. They made use of the cosmic ray data, but in the final analysis, their method is based on an empirical approach, equating production rate to a function with two exponential terms to account for the nucleonic cascade. Subsequently, quantitative nuclide production rates were estimated, again for iron meteorites, by Arnold, Honda and Lal (16) who used the cosmic ray data to estimate fluxes of nuclear active particles within the meteorite. They took into account the characteristics of nuclear interactions, in particular the facts that (i) the incident nucleon emerged with an appreciable energy in the laboratory system, corresponding to an inelasticity of ~ 0.5 , and (ii) that the spectrum at production of nucleons and pions was known (Fig. 1). Several attempts were made subsequently to improve on the production estimates, in particular by Reedy and Arnold (17) and Reedy (18), who used the basic approach in Ref. 16, with modifications to include propagation of nucleons within larger bodies. At present the Reedy-Arnold model serves as the "standard model" for cosmogenic production in extraterrestrial samples.

The GCR model however needs considerable modifications to include the diversity of the size of the objects irradiated, and the nature of the problem studied. In particular, in small size objects (radius < 5 cms), the production becomes very sensitive to the shape of the GCR spectrum. The problem has been addressed by Reedy (18). In larger meteorites (of radii 20-45 cms), the recently measured depth profiles of several cosmogenic nuclides in several meteorites have warranted revisions of theoretical production rates (19,20). The work of Michel, Englert and their collaborators on simulated artificial irradiation of objects of radii 10-25 cm has produced an invaluable data set for improving on our production rate modeling capabilities (9,10).

At present, the largest uncertainties in the prediction of production rates must be ascribed to uncertainties in galactic cosmic ray fluxes and nuclide excitation functions for neutrons of energy 0.01-10 GeV. The principal improvements in recent years in the prediction of nuclide production rates has come about by comparing theoretical predictions with observations of a suite of nuclides in meteorites of different sizes. An interesting example of this is the detailed studies of Bhandari, Graf, Vogt and others who have included in their survey a wide range of meteorite sizes (19-22). This has led to gross revisions in the semi-empirical relations for production rates. These investigations are being incorporated in the theoretical framework (e.g. Refs. 16, 17) used for an objective prediction of nuclide production rates.

The production of nuclides by solar cosmic rays (SCR) is in contrast to the case of production by galactic cosmic rays (GCR), a much simpler problem. The first calculations of SCR nuclide production were made by Armstrong and Alsmiller (23) who made Monte Carlo calculations of the intra-nuclear cascade due to SCR particles. A more reliable and straight forward method, however, is to consider only the ionization losses of the SCR charged particles (protons or α -particles), and consider their interaction products alone, since the secondary particles produced do not play any significant role. This method was

developed independently by Reedy and Arnold (17) and Lal (24,25). The limitations at present for SCR predictions for any specified SCR energy spectrum are largely due to uncertainties in the nuclide excitation functions. The information on proton excitation function is growing rapidly at present (see papers presented at this meeting).

Future improvements in theoretical estimates of nuclear production in extraterrestrial samples.

As discussed earlier, an interactive process involving comparing observations with predictions would help achieving the goal. However, there are several pitfalls in this approach. Firstly, nature is always not kind enough to provide us with ideal extraterrestrial samples for this task. In the case of meteorites, their shapes are often very irregular, as a rule rather than the exception which makes modeler's task very hard. And in the case of both meteorites and lunar samples, irradiation history is often very complex.

Finally, and probably more importantly, efforts of this kind may lead to smoothening out of important anomalies/subtle deviations in extraterrestrial data set, and thereby escaping from discovering important milestones in the history of extraterrestrial samples. The purpose of the studies of cosmogenic nuclides can thus be partly negated.

I have therefore looked at the problem afresh, trying to improve our predictive capability relying largely on basic cosmic ray data. In doing this I have discovered an omission in our early work (16). In that paper, we considered the nucleon transport equations, and the production spectrum of pions, but forgot to consider the pion transport equations. Since there are no pions in the primary cosmic radiation, the flux of energetic pions ($E > 100$ MeV), which produce nuclides efficiently, undergoes a transition with depth in a target exposed to cosmic radiation. This leads to a more rapid growth of nuclear active particles in the first $100 \text{ gm} \cdot \text{cm}^{-2}$ depth in the target. The consequences of this would obviously be most significant in the interpretation of the data on nuclides produced both by GCR and SCR particles (26,27). Interestingly enough, the inclusion of the pion transport code also solves a long standing problem in some cosmic ray observations (cf. 28).

We will present detailed calculations of the nucleon and pion transport calculations elsewhere (29).

REFERENCES:

1. Reedy, R. C., Arnold, J. R. and Lal, D., 1983. Science **219**,127-135.
2. Vogt, S., Herzog, G. F. and Reedy, R. C., 1989. Rev. of Geophys. (in press).
3. Raisbeck, G. M. and Yiou, F., 1984. Accelerator Mass Spectrometry, AMS '84. Proc. Int. Symp. 3rd, Zurich, 1984. Nucl. Instrum. Methods Phys. Res. **233**, B5, 91-99.
4. Broecker, W. S. *et al.*, 1988. Paleoceanography, **3**, 659-669.

IN EXTRATERRESTRIAL OBJECTS: Lal

5. Lal, D., 1988. Ann. Rev. Earth Planet. Sci. **16**, 355-88.
6. Lal, D., 1974. Trans. Royal Soc. Lond. **277**, 395-411.
7. Lal, D. and Peters, B., 1967. In Handbuch der Physik **46/2**, Springer-Verlag, Berlin, 551-612.
8. Honda, M., 1962. J. Geophys. Res. **67**, 4847.
9. Michel, R. *et al.*, 1989. Nucl. Instrum. Methods Phys. Res. **B42**, 76-100.
10. Michel, R. *et al.*, 1989. Abstracts for the Workshop on Cosmogenic Nuclide Production Rates, Vienna, July 1989, 38-39.
11. Zanda, B., 1979. Abstracts for the Workshop on Cosmogenic Nuclide Production Rates, Vienna, July 1989, 56-57.
12. Somayajulu, B. L. K. *et al.*, 1984. Nucl. Instrum. Methods Phys. Res. **B5**, 398-403.
13. Nishiizumi *et al.*, 1989. J. Geophys. Res. (in press).
14. Powell, C. F., Fowler, P. H. and Perkins, D. H., 1959. The Study of Elementary Particles by the Photographic Method. Pergamon Press, New York/London, 669 pp.
15. Signer, P. and Nier, A. O., 1960. J. Geophys. Res. **65**, 2947-2964.
16. Arnold, J. R., Honda, M. and Lal, D., 1961. J. Geophys. Res., **66**, 3519-3531.
17. Reedy, R. C. and Arnold, J. R., 1972, J. Geophys. Res. **77**, 537-555.
18. Reedy, R. C., 1985. PLPSC, 15th J. Geophys. Res. **90**, Supplement, C722-C728.
19. Bhandari, N., 1988. Proc. Ind. Acad. Sci. (E.P.S.L.), **97**, 117-125.
20. Graf, T., Baur, H., and Signer, P., 1989. Abstracts for the Workshop on Cosmogenic Nuclide Production Rates, Vienna, July 1989, 17-18.
21. Vogt, S., 1989. Abstracts for the workshop on Cosmogenic Nuclide Production Rates, Vienna, July 1989, 54-55.
22. Bhandari, N., 1989. Abstracts for the Workshop on Cosmogenic Nuclide Production Rates, Vienna, July 1989, 1-3.
23. Armstrong, T. W. and Alsmiller, R. G. Jr., 1971. PLSC 2nd, MIT Press, Cambridge, 1729.
24. Lal, D., 1972. Space Sci. Rev. **14**, 3-102.
25. Bhattacharya, S. K. *et al.*, 1973. The Moon, **8**, 253-86.
26. Nishiizumi, K. *et al.*, 1984. Earth Planet. Sci. Lett., **70**, 157-163.
27. Nishiizumi, K. *et al.*, 1984. Earth Planet. Sci. Lett. **70**, 164-168.
28. Shapiro, M. M. *et al.*, 1951. Phys. Rev. **83**, 155-156.
29. Lal, D., Reedy, R. C. and Arnold, J. R., 1989. (to be published).

512-90
321030
60

R5

STATUS OF CHARGED PARTICLES AND NEUTRONS INDUCED NUCLEAR REACTIONS LEADING TO STABLE AND RADIOACTIVE ISOTOPES :

B. Lavielle

Centre d'Etudes Nucléaires de Bordeaux-Gradignan, Université de Bordeaux I
33170 GRADIGNAN (FRANCE)

Cosmogenic nuclides are produced in meteorites and lunar samples by nuclear reactions induced by solar or galactic cosmic-ray irradiation. They are formed either by the primary cosmic-ray particles or by induced cascade of secondary particles including protons and neutrons and covering the whole energy range.

The understanding of this complex interaction between extraterrestrial samples and cosmic-ray particles requires a good knowledge of the production rates of the stable and radioactive isotopes of which concentrations are measurable using different methods such as γ and X spectrometry, AMS or noble gas analysis. An evaluation of these production rates is possible if reliable excitation functions of all the involved nuclear reactions are available in literature.

So the purpose of this report is to give the status of charged particles and neutrons induced nuclear reactions leading to stable and radioactive isotopes indicating what excitation functions are correctly known and what cross section measurements are still to do.

The table 1 lists cosmogenic nuclides of interest in this type of study. The main target elements from which most production of the isotopes occurs are also reported.

Table 1: cosmogenic nuclides of interest in meteorite study

Cosmogenic nuclides	Half life (year)	Targets
124,126,128-132,134,136 Xe	stable	Te,I,Ba,La,Ce
129I	$1.6 \cdot 10^7$	Te,Ba,La,Ce
78,80,82,83,84,86 Kr	stable	Br,Rb,Sr,Y,Zr
81Kr	$2.1 \cdot 10^5$	Rb,Sr,Y,Zr
60Co	5.27	Ni
60Fe	$1.5 \cdot 10^6$	Fe,Ni
59Ni	$7.6 \cdot 10^4$	Fe,Ni
56Co	79 days	Fe,Ni
55Fe	2.7	Fe,Ni
54Mn	312 days	Mn,Fe,Ni
53Mn	$3.7 \cdot 10^6$	Mn,Fe,Ni
48V	16 days	Ti,Fe,Ni
46Sc	84 days	Ti,Fe,Ni
44Ti	47.3	Ca,Ti,Fe,Ni
41Ca	$1.0 \cdot 10^5$	Ca,Ti,Fe,Ni

Table 1 (continue)

^{39,41} K	stable	K,Ca,Ti,Fe,Ni
⁴⁰ K	1.3 10 ⁹	K,Ca,Ti,Fe,Ni
³⁹ Ar	269	K,Ca,Ti,Fe,Ni
³⁷ Ar	35 days	Cl,K,Ca,Ti,Fe,Ni
^{36,38} Ar	stable	Cl,K,Ca,Ti,Fe,Ni
³⁶ Cl	3.0 10 ⁵	Cl,K,Ca,Ti,Fe,Ni
²⁶ Al	7.1 10 ⁵	Mg,Al,Si,S,Ca,Ti,Fe,Ni
²² Na	2.6	Na,Mg,Al,Si,S,Ca,Ti,Fe,Ni
^{20,21,22} Ne	stable	Na,Mg,Al,Si,S,Ca,Ti,Fe,Ni
¹⁴ C	5730	C,O,Mg,Al,Si,S,Ca,Fe,Ni
¹⁰ Be	1.6 10 ⁶	C,O,Mg,Al,Si,S,Ca,Fe,Ni
⁷ Be	53 days	C,O,Mg,Al,Si,S,Ca,Fe,Ni
³ He, ⁴ He	stable	C,O,Mg,Al,Si,S,Ca,Fe,Ni
³ H	12.3	C,O,Mg,Al,Si,S,Ca,Fe,Ni

Over the last 25 years, production cross sections of numerous isotopes have been measured by many laboratories in thin-target irradiations.

Such measurements require a calibration of proton or neutron integrated fluxes obtained during the irradiations. This calibration can be determined using a monitor nuclear reaction of which the excitation function is well known.

However, corrections are sometimes necessary if the monitor cross section values have changed since the time of the measurement. So, all the data shown or discussed in this report are corrected according the latest published data from the compilations given in references [1,2,3,4].

A - Protons induced nuclear reactions

For every target and product, three distinct energy ranges are considered and respectively symbolized by :

- L for low energy range (0 - 100 Mev)
- M for medium energy range (100 Mev - 800 Mev)
- H for high energy range (> 800 Mev)

The letter then indicates in which energy range additional measurements are needed. Two letters may be used if two energy ranges must be considered. If the whole energy range has to be covered, it is indicated by a dash "-".

On the contrary, a full square "◻" means that the excitation function is quite well documented. An empty square "◻" indicates that the excitation function is also known but needs to be confirmed.

No symbol means that the isotope cannot be produced in the considered target element or that the resulting production yield is negligible relatively to the other ones leading to the same isotope.

Using this notation, the tables 2 and 3 show the present status of the

Status of charged particles and neutrons induced nuclear reactions ... ; B. Lavielle

knowledge of the excitation functions concerning the production in extraterrestrial samples of the cosmogenic isotopes mentioned in the table 1.

	Targets														
	C	O	Na	Mg	Al	Si	P	S	Cl	K	Ca	Ti	Mn	Fe	Ni
^3H	LM	L		-	□	LM		-	-					□	LM
^3He	L	LM		MH	M	M		-			-			□	M
^4He	LM	-		M	M	M		-			-			L	M
^7Be	■	M		■	■	■		MH				□		■	■
^{10}Be	□	-		-	-	H		-				H		H	H
^{14}C		-		-	-	-		-						-	-
^{20}Ne				□	■	□	-	-			□			□	-
^{21}Ne				□	■	□	-	-			□			□	-
^{22}Ne				□	■	□	-	-			□			□	-
^{22}Na			■	■	■	■	H	□	H		■	■		■	-
^{26}Al				□	MH	M	-	-			MH			H	-
^{36}Cl									-	-	-	-	-	□	-
^{37}Ar									MH	-	-	-	-	□	H
^{36}Ar									-	-	□	H	-	H	H
^{38}Ar									-	-	□	H	-	H	H
^{39}Ar									-	-	H	H	-	■	H
^{39}K										-	-	-	-	-	-
^{40}K										-	-	-	-	-	-
^{41}K										-	-	-	-	-	-
^{41}Ca										-	-	-	MH	H	H
^{41}Ti												-	-	-	-
^{46}Sc												H	MH	■	■
^{48}v												■	H	■	■
^{53}Mn												-	-	-	-
^{54}Mn												-	H	■	■
^{55}Fe													-	LM	-
^{56}Co														■	-
^{59}Ni														-	-

Table 2: recommended additional cross section measurements of production of some cosmogenic isotopes regarding different proton energy ranges.

This table suggests some remarks. Excitation functions of some long-lived radioactive isotopes like ^{10}Be , ^{14}C , ^{26}Al or ^{36}Cl are poorly known in most target elements possibly because the difficulty to measure induced activities by classical

Status of charged particles and neutrons induced nuclear reactions ... ; B. Lavielle

counting technics. Development of AMS, as it was for example already started for ^{41}Ca [5], should rapidly improve this situation [6].

Production of K isotopes, important cosmogenic nuclides in iron meteorites, is also not measured for similar reason. Production of light noble gases is more (Ne) or less (He,Ar) well-known and some experiments are still to do. Others isotopes like ^{44}Tl or ^{59}Ni which are not extensively studied in meteorites, are also badly documented.

	Targets								
	Rb	Sr	Y	Zr	Te	I	Ba	La	Ce
^{78}Kr	-	-	M	M					
^{80}Kr	-	-	M	M					
^{81}Kr	-	-	M	M					
^{82}Kr	-	-	M	M					
^{83}Kr	-	-	M	M					
^{84}Kr	-	-	M	M					
^{86}Kr	-	-	M	M					
^{129}I					-	-	H	-	-
^{124}Xe					-	-	H	-	-
^{126}Xe					-	-	H	-	-
^{128}Xe					-	-	H	-	-
^{129}Xe					-	-	H	-	-
^{130}Xe					-	-	H	-	-
^{131}Xe					-	-	H	-	-
^{132}Xe					-	-	H	-	-
^{134}Xe					-	-	H	-	-
^{136}Xe					-	-	H	-	-

Table 3: recommended additional cross section measurements of production of some Kr, I and Xe isotopes regarding different proton energy ranges.

Kr production is completely unknown in Rb and Sr, important target elements in meteorites. In Y and Zr, the situation is rather good but could be still improve by new cross section determinations at 600-800 Mev which corresponds to the region of the maximum of the excitation functions.

Xenon data are only available in Ba but new irradiations in progress should fill this lack of cross section determinations for xenon as well as for many other isotopes [7].

B - Neutrons induced nuclear reactions

In spite of the large contribution of the neutron induced nuclear reactions to

Status of charged particules and neutrons induced nuclear reactions ... ; B. Lavielle

cosmogenic nuclide production in meteorites and lunar samples, most of the excitation functions useful in this type of study are not known. The main reason certainly comes from the experimental difficulty to obtain simultaneously monoenergetic neutrons and high flux intensity.

So available data concern neutrons of energy between 14 and 15 Mev, energy range in which neutron production is quite possible with high flux intensity. More rarely, excitation functions have been measured from threshold to 25 or 30 Mev, but only a few are useful in cosmogenic nuclide study.

The table 4 summarizes available data of interest in this field (for details see for example reference [8]).

	Targets									
	Ne	Mg	K	Ca	Mn	Fe	Rb	Cs	Ba	
^{20}Ne	*	*								
^{21}Ne	□	*								
^{22}Ne	□	*								
^{22}Na	*									
^{36}Cl			*							
$^{36,37,39}\text{Ar}$				□						
^{54}Mn					□					
^{55}Fe						□				
^{82}Kr							□			
$^{129,131,134}\text{Xe}$										□
$^{130,132}\text{Xe}$								□		□

* data available in the energy range 0-20 Mev; □ data available only around 14.5 Mev

Table 4: available cross section measurements of production of some cosmogenic isotopes produced by neutrons.

It appears that production of ^{26}Al in Al, Ar in K, Kr in Rb, Sr, Zr and Xe in La suffer of a lack of experimental data. That could suggest further work in a near future because these nuclear reactions probably give measurable cross sections at energy and specially around 14.5 Mev.

References:

- [1] CEA-N-1466(1)1971, TOBAILEM et al
- [2] CEA-N-1466(3)1975, J. TOBAILEM and C.H de LASSUS St-GENIES
- [3] CEA-N-1466(4)1977, J. TOBAILEM and C.H de LASSUS St-GENIES
- [4] CEA-N-1466(5)1981, J. TOBAILEM
- [5] FINK et al, Nucl. Inst Meth. In Phys. Res. B29(1987)275
- [6] DITTRICH et al "Cross-Sections for Long-Lived Radionuclides from..."(this workshop)
- [7] MICHEL et al "Thin-Target Cross Sections for the Production of ..." (this workshop)
- [8] MANOKHIN et al, in IAEA, Handbook of Nuclear Activation Data, Technical Reports Series No 273, IAEA, Vienna(1985)305

513-90
321031
p-5 65

CROSS SECTIONS OF NEON AND KRYPTON ISOTOPES PRODUCED BY NEUTRONS :

B. Lavielle, H. Sauvageon and P. Bertin.

Centre d'Etudes Nucléaires de Bordeaux-Gradignan, Université de Bordeaux I

33170 GRADIGNAN (FRANCE)

The interaction of cosmic rays with meteoroids in space produces numerous species of stable and radioactive isotopes. Concentration of the cosmogenic production of rare gas may allow determination of the exposure age. But, a good knowledge of the excitation functions of the implied nuclear reactions is required in order to take into account parameters like the cosmic-ray flux, the shielding depth of the sample, the size and shape of the meteoroid and its chemical composition.

The evaluation of the production of nuclides induced by energetic secondary neutrons in meteorites suffers from a notable lack of experimental cross sections. So, two different types of irradiation by neutrons were performed in order to improve this situation.

1. Irradiation of natural Mg target by neutrons of 5,7,16 and 19 Mev

Targets of Mg were irradiated by neutrons induced by the 4 Mev Van de Graaff accelerator at the Centre d'Etudes Nucléaires at Bruyères-Le-Châtel (France) in collaboration with G. Hauat. Integrated fluxes of $5.1-8.4 \cdot 10^{12}$ particles of 5,7 and 16,19 Mev neutrons were respectively produced by the nuclear reactions $D(d,n)^3\text{He}$ and $T(d,n)^4\text{He}$.

Measured neon cross sections in Mg are shown on the figure 1 as well as available data in literature between 14 and 15 Mev from Reedy et al, 1979 [1] and Leich et al, 1986 [2]. The cross sections are corrected for atmospheric blank as well as for water, CO_2 and doubly charged ^{40}Ar ions contributions.

Below 20 Mev, ^{22}Ne can also be produced in natural Mg by the nuclear reaction $^{24}\text{Mg}(n,t)^{22}\text{Na}$. The threshold of these reaction being 16.3 Mev, a correction for ^{22}Na decay is only required at 19 Mev. Because the activity of ^{22}Na was too low to be measured, we adopted a cross section value of 4.5 ± 2.0 mb as estimated by Baros, 1984 [3] for ^{22}Na production in natural Mg.

The new measured cross sections agree very well with previous data and so well complete the knowledge of the excitation functions of neon isotopes produced by neutrons below 20 Mev.

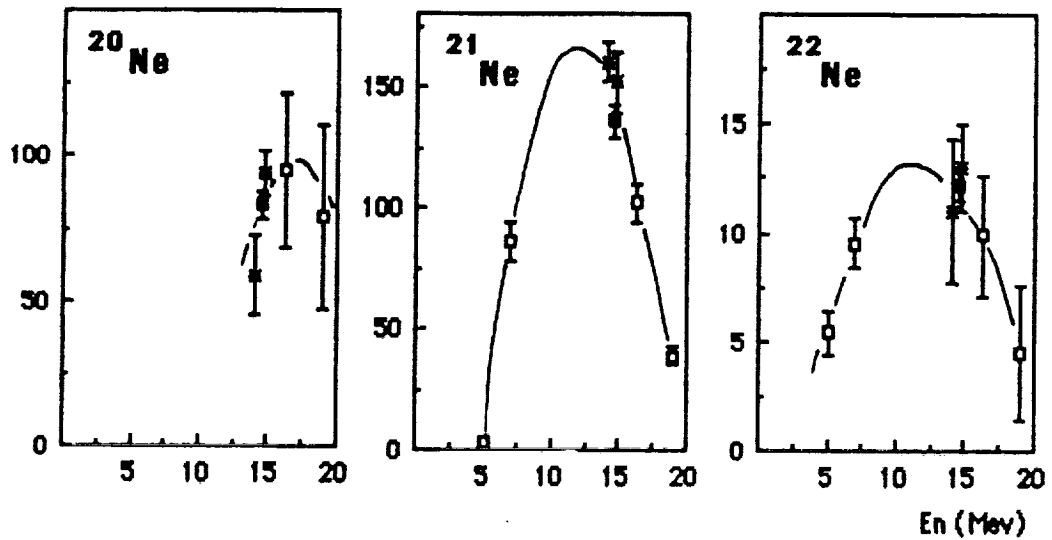


Figure 1 : Neon cross sections induced by neutrons in natural Mg. \square symbols are from this work, * from reference [1] and \square from reference [2]. ^{22}Ne values are corrected for contribution from the ^{22}Na decay.

2° Irradiation by neutrons in the energy range 0-180 Mev

Targets of Al, Mg, Rb_2SO_4 , SrF_2 and Y were irradiated with the Medium Energy Intense Neutron facility (MEIN) at the Brookhaven 200 Mev LINAC in collaboration with S. Katcoff and Y. Y. Chu. Characteristics of the neutron energy flux were previously described by collaborators [4]. It appears to be almost flat between 25 Mev and 180 Mev according to the calculations by Alsmiller et al, (1975) [5].

The figure 2 shows the expected shape of neutrons energy distribution for the

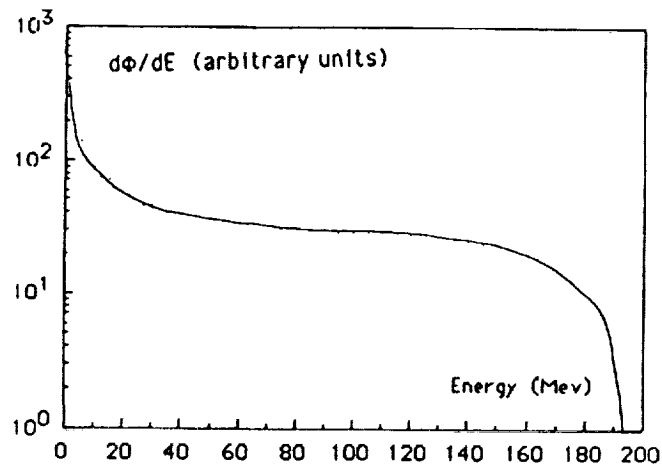


Figure 2 : Expected shape of neutron energy distribution in the irradiation with the Medium Energy Intense Neutron facility (MEIN) at the Brookhaven 200 Mev LINAC

Cross sections of neon and krypton isotopes produced by neutrons ; B. Lavielle et al

irradiations, deduced from reference [4] and [5] and calibrated at lower energy after the mesured activity of ^{88}Rb produced by the nuclear reaction $^{87}\text{Rb}(n,\gamma)^{88}\text{Rb}$.

An irradiation time of 2 hours provided us a neutron fluence of about $5 \cdot 10^{14}$ particles.

The measured production ratios of $^{20,21,22}\text{Ne}$ in Al, Mg and $^{78,80-86}\text{Kr}$ in Rb, Sr, Y which represent the first experimental data obtained in the energy range 0-180 Mev, are respectively given in the tables 1 and 2.

isotope	Mg	Al
^{21}Ne (atomes/g)	$3.31 \cdot 10^{11}$ 17	$1.09 \cdot 10^{11}$ 6
$^{20}\text{Ne}/^{21}\text{Ne}$	0.965 19	0.578 29
$^{22}\text{Ne}/^{21}\text{Ne}$	0.556* 17	1.066* 21
$^{22}\text{Ne}/^{21}\text{Ne}$	1.21† 10	2.46† 20

* ^{22}Ne corrected for contribution from ^{22}Na decay

† including contribution from ^{22}Na decay

Table 1 : Production ratios of $^{20,22}\text{Ne}/^{21}\text{Ne}$ in Mg and Al by the irradiation with the Medium Energy Intense Neutron facility (MEIN) at the Brookhaven 200 Mev LINAC

The ratios of $^{22}\text{Ne}/^{21}\text{Ne}$ (including ^{22}Na decay) in Mg and especially in Al are higher than those currently observed in meteorites. This result indicates the influence of the Mg and Al concentrations on neon production ratios in meteorite samples from shielded locations, where neutron flux can be developed.

Krypton data suggest some remarks. The ratio $^{78}\text{Kr}/^{83}\text{Kr}$ is significantly lower in Rb than in Sr or Y targets, implying a chemical effect on the ^{78}Kr production in Rb rich or poor meteorites relatively to Sr and Y abundances. The ratios $^{80}\text{Kr}/^{83}\text{Kr}$ and $^{82}\text{Kr}/^{83}\text{Kr}$ do not show any target dependence, probably due to the entire (^{83}Kr) or almost entire ($^{80}\text{Kr}, ^{82}\text{Kr}$) cumulative production yield of these isotopes. That gives a nearly constant $^{81}\text{Kr}/^{83}\text{Kr}$ production ratio of about 38.5 when calculated using the method suggested by Marti, 1967 [6] where

Cross sections of neon and krypton isotopes produced by neutrons ; B. Lavielle et al

$$P_{81} = 0.95 \cdot 0.5 \cdot [^{80}\text{Kr}/^{83}\text{Kr} + ^{82}\text{Kr}/^{83}\text{Kr}].$$

However, the measured ratios $^{81}\text{Kr}/^{83}\text{Kr}$ give much lower values and vary by about 15% showing a clear dependence with the target elements. These variations only concern a limited range of neutron energy and should be less important if the total production yield is considered. But, some little chemistry effects could be induced in shielded locations of meteorites.

isotope	Rb	Sr	Y
^{83}Kr (atomes/g)	$8.75 \cdot 10^{11}$ 44	$2.73 \cdot 10^{11}$ 14	$1.46 \cdot 10^{11}$ 7
$^{78}\text{Kr} / ^{83}\text{Kr}$	2.01 6	2.79 2	2.87 6
$^{80}\text{Kr} / ^{83}\text{Kr}$	21.42 41	21.36 12	21.89 16
$^{81}\text{Kr} / ^{83}\text{Kr}$	31.62 45	32.14 23	35.81 19
$^{82}\text{Kr} / ^{83}\text{Kr}$	59.97 40	58.87 33	59.73 31
^{83}Kr	100	100	100
$^{84}\text{Kr} / ^{83}\text{Kr}$	129.53 47	70.9 2.2	47.39 26
$^{85}\text{Kr} / ^{83}\text{Kr}$	6.61 4	4.92 7	.60 3
$^{86}\text{Kr} / ^{83}\text{Kr}$	5.48 18	2.1 8	.20 2

Table 2 : Production ratios of krypton in Rb, Sr and Y targets by the irradiation with the Medium Energy Intense Neutron facility (MEIN) at the Brookhaven 200 Mev LINAC

Compared with Kr production induced by protons in Y [7], the ^{84}Kr and ^{86}Kr data seem to confirm expected trends according to systematics of nuclear reaction channels induced by neutrons. The productions appear to be higher by incident

Cross sections of neon and krypton isotopes produced by neutrons ; B. Lavielle et al
 neutrons than by incident protons. These discrepancies can mainly be attributed to the nuclear reactions: $^{89}\text{Y}(n,\alpha 2n)^{84}\text{Kr}$, $^{89}\text{Y}(n,3pn)^{86}\text{Kr}$ which have no equivalent channels by incident protons in the same target.

References :

- [1] Reedy R. C., Herzog G. F. and Jessberger E. K. (1979) Earth and Planetary Science Letters, 44, pp 341-348
- [2] Leich D. A., Borg R. J. and Lanier V. B. (1986) In Workshop on Cosmogenic Nuclides (R. C. Reedy and P. Englert, eds) pp46-48. LPI Tech Rpt 86-06. Lunar and Planetary Institute, Houston.
- [3] Baros F. (1984), thesis, University of Bordeaux I
- [4] Katcoff S., J. B. Cumming, J. Godel, V. J. Buchanan, H. Susskind and C. J. Hsu (1975) Nuclear Instruments and Methods, 129, pp 473-485
- [5] Alsmiller R. G., R. T. Santoro and J. Barish (1975) Particle accelerators, 7, pp 1-7
- [6] Marti K. (1975) Physical Review Letters, 18, pp 264-266
- [7] Regnier S., B. Lavielle, M. Simmonoff and G. N. Simonoff (1982) Physical Review. C, 26, pp 931-943

P-1

EXPOSURE AGES AND LONG-TERM VARIATIONS OF THE COSMIC RAY FLUX: K. Marti, Chem. Dept., B-017, Univ. of Calif., San Diego, La Jolla, CA., 92093.

The flux of cosmic rays in the inner solar system changes with time. At least some of these variations are known to be due to solar modulation. While the recent cosmic ray flux has been studied by satellites and terrestrial radionuclide production rates (e.g. atmospheric ^{14}C), cosmic-ray-produced stable and radioactive nuclides in meteorites are widely used to study past variations of the cosmic ray flux. Galactic cosmic rays (GCR) dominate the average intensity of energetic particles above about 200 MeV. Therefore, long term variations, as observed in meteoritic ^{38}Ar versus ^{40}K - ^{41}K production rates, may also reflect changes in the interstellar medium (1,2). It is expected that solar modulation would mainly affect low energy particles and change the energy spectrum of GCR, while changes in the interstellar medium may affect the flux at all energies. The depth dependence of the production rates in meteorites is, at the present time, not sufficiently well known to decide between these possibilities.

Timescale 10^7 - 10^9 a: The radionuclide ^{40}K (1.3×10^9 a) relative to stable ^{41}K measured in iron meteorites indicates that the intensity of the cosmic ray flux on a 1Ga time scale was smaller than the present one (3,2). It was suggested that this increase may have taken place less than 200 Ma ago (2). The long half-life of ^{40}K renders the ^{40}K - ^{41}K method inappropriate for tests of flux changes on this time scale. A new method (4) involving ^{129}I (1.6×10^7 a) and stable ^{129}Xe in troilite inclusions of iron meteorites is now being developed to constrain the time of change. This method is self-correcting for the shielding dependence of the production rates. The reactions ^{128}Te (n, γ, β^-) ^{129}I and ^{130}Te ($n, 2n, \beta^-$) ^{129}I are both important and are especially suitable when low-energy secondary particles are predominant. For complex exposure histories, the assumed self-correction for shielding is violated, and the method may prove useful in identifying complex exposure histories. The nuclide ^{146}Sm (1.03×10^8 a) would present another most useful GCR flux monitor.

Timescale 10^5 - 10^7 a: A decade ago, a systematic calibration of the ^{21}Ne production rate in chondrites was carried out to test for possible variations of the cosmic ray flux during the past few million years (5). Three of the calibrations, using radioisotopes of different half-lives (^{22}Na , ^{81}Kr , ^{53}Mn), were in very good agreement, indicating that the cosmic ray flux was constant over 10^5 - 10^6 a time scales. These calibrations were extended to ^{10}Be (6) and confirmed more recently for ^{81}Kr (7). On the other hand, production rates, based on ^{26}Al (7.2×10^5 a), did not agree with this result. However, these ^{26}Al -based on production rates, are based on chondrites of very short exposure ages, and such exposure ages were recently found to indicate complexities in their exposure histories (6). If confirmed, this objection to a constant cosmic ray flux during the last 10^7 a would be removed.

References: (1) Jokipii J. R. and Marti K. (1986) IN THE GALAXY AND THE SOLAR SYSTEM; R. Smoluchowski, J. N. Bahcall, M. S. Matthews, Eds., Univ. of Ariz. Press, Tucson, 116-128, (2) Marti K., Lavielle B. and Regnier S. (1984) Lunar and Planet. Science XV, Lunar and Planet. Inst., Houston, 511-512, (3) Voshage H. (1984) Earth Planet. Sci. Lett. 71, 181-194, (4) Marti K. (1986) Workshop on Cosmogenic Nuclides, LPI Tech. Rpt., 86-06, Lunar and Planet. Inst., Houston, 49-51, (5) Nishiizumi K., Regnier S. and Marti K. (1980) Earth Planet. Sci. Lett. 50, 156-170, (6) Moniot R. K. et al. (1983) Geochim. Cosmochim. Acta 4, 1887-95, (7) Eugster O. (1988) Geochim. Cosmochim. Acta 52, 1649-1662, (8) Graf Thomas and Marti Kurt (1989) Chondrites: Exposure Ages and Thermal Events on Parent Bodies, Meteoritics, Abstracts, 52nd Met. Soc., Vienna (in press).

Galactic cosmic ray (GCR) can cause changes in extraterrestrial objects like meteorites, lunar samples and cosmic dust in different way. Those that are quantitatively important include the development of a secondary flux of particles under GCR bombardment, the slowing of charged particles by ionization energy losses, the moderation of neutrons, and the reaction of primary and secondary particles with nuclei of the solid body, which lead to a production of wide variety of stable and radioactive cosmogenic nuclides. Which process dominates depends on the type and the energy of the incoming particle and on the nature of the object exposed to this radiation i.e. its size, chemical composition etc. [1]. The goal of the theoretical model developed here is to calculate, with precision adequate for comparison with experiment the expected yield of daughter nuclides and the depth and size dependence of their concentration. By comparing the measured activities of nuclides with half-lives ranging from a few years to 10^8 years with calculated production rates it is possible to determine the average cosmic ray intensity over different periods of time.

Our method of calculating production rates of cosmogenic nuclides is based on the following expression

$$Q_n = \int dE N(E) \sum_k \int_0^E dE' \frac{\sigma_k^x(E')}{\sigma_k^{\text{inel}}(E')} \int_{V_n} d^3r \Psi_k(\vec{r}, E'; E) \quad (1)$$

where Q_n is the production rate in a chosen region of space V_n , $\sigma_k^x(E')$ is the cross section for the production of x-type nuclide by k-type incident particle with the energy E' , $N(E)$ is the energetic spectrum of primary particles, $\sigma_k^{\text{inel}}(E')$ is the inelastic collision cross section of k-type particle with the energy E' , $\Psi(\vec{r}, E', E)$ is the inelastic collision density for the k-type particle with energy E' at the position \vec{r} . The basic problem, the solution of transport equation of hadron cascade using Monte Carlo (MC) method is in the final analysis reduced to the calculation of the quantity

$$\Psi_{ijk}(E) = \int_{\Gamma_{ij}} d^3r dE' \Psi_k(\vec{r}, E', E) \quad (2)$$

where $\Gamma_{ij} = (E_i, E_{i+1}) \times V_j$. The calculation of the functional Ψ_{ijk} using the MC method is based on the estimation of the average quantity estimator which is defined on the region Ω of all possible trajectories α of chosen Markovian process [2], which represents the process of the hadron cascade. Therefore we can write

$$E(Z) = \int_{\Omega} Z(\alpha) dP(\alpha) \quad (3)$$

where E is the average value, α is the random realization of Markovian process (trajectory), P is the probability distribution defined on Ω .

We have used within our calculations two expressions for the considered estimators. For the first the estimator is defined as

$$Z_{ijk}(\alpha) = N \quad (4)$$

where $N = 1, 2, 3, \dots$ is the number of inelastic collisions of cascade particles of k -type belonging to the cascade and represented by the tree α in region Γ_{ij} . The second type estimator is defined as

$$\Psi_{ijk}(\alpha) = \sum_{m=1}^M w_m^{(1)} \quad (5)$$

where M is the number of cascade particles belonging to the cascade represented by the tree α , which range crossed the region Γ_{ij} . $w_{ij}^{(1)}$ is the probability that m -th particle of type 1, which range crossed the region Γ_{ij} undergo an inelastic interaction in this region.

The simulation of Markovian process is started by choice of primary particle characteristics. The particle history is followed taking into account its multiple Coulomb scattering up to the moment of the inelastic interaction. The choice of a random angle for the primary particle direction which has undergone multiple scattering is realized using the Gaussian distribution with quadratic angle deviation given by the Rossi formula [3]. The characteristic feature of collisions at these energies is the origin of new hadrons. They have enough energy to undergo further inelastic collision and to produce next generation of secondary particles. The multiplicities of each type of secondary particles originating in hadron-nucleon collision have been calculated using the following equation

$$K_{ij} = \frac{1}{E_i} \int E_j \frac{d^2 N_j}{dp d\Omega} dp d\Omega \quad (6)$$

where E_i is the kinetic energy of an incident particle in the laboratory system, E_j is the kinetic (in the case of pion - total) energy of j -type secondary particle in the laboratory system. This quantity is further corrected for excitations of the target nucleus. We have used correction

$$K_{ij} = K_{ij}^C (1 - E_{ex}/E_i) \quad (7)$$

SIMULATION OF CGN PRODUCTION, Masarik J. and Povinec P.

where E_{ex} is the nucleus excitation energy. The successive choice of always a higher generation of secondary particles is performed up to the case when the generated particle has momentum less than $p_{ef} = 0.3 \text{ GeV/c}$ or its momentum is in the interaction place less than the threshold momentum for production of the next generation of secondary particles or the particle leaves the target region. Except for the last case the investigated particle is followed within the low energy simulation. High energy collisions and also collisions at lower energies transform the target nuclei mainly through spallation and evaporation processes to radioactive or stable nuclei. Amongst strongly interacting hadrons it is sufficient to consider only protons, neutrons and pions. Other hadrons and electromagnetic cascades play only minor role in the development of the hadronic cascade and therefore they are considered only from the point of view of energy conservation. The sampling of cascade process is stopped when all particles generated in interactions of the primary particle are realized.

In the development of hadronic cascade we consider the following processes: inelastic nuclear reactions, elastic scattering, ionization and excitation of target atoms, decay of particles. Because we do not know all exclusive distribution function for the description of the inelastic interaction, we have used for their modelling procedures which are in agreement only with kinematic corrections and which are realised by satisfying fundamental laws such as energy-momentum and charge conservation. In our calculations we have used experimentally obtained functions, too. For example functions which give the secondary particles distribution as a function of the longitudinal p_L and perpendicular p_T component of their momenta in the hadron-nucleon centre of mass system.

Having the inelastic collision density the depth dependence and the energy dependence of the production rates of cosmogenic nuclides with consideration of contribution from the evaporation processes are calculated as

$$P_j(E) = \sum_{k,1} \varphi_{ijk} \sigma_k^x(E_i) / \sigma_k^{inel}(E_i) \quad (8)$$

We have used experimental values of total inelastic cross sections for interaction of above mentioned hadrons with target nuclei. In the region above 10 GeV/c we have supposed that the total cross section is constant. The main drawback of the method is connected with the uncertainties in the cross sections. In the case of known chemical composition of the target effective values of cross sections have been used

$$\sigma_k^{ef} = \sum w_n \sigma_{kn} \quad (9)$$

where k is the type of the incident particle, w_n is the relative statistical weight of n -type of target nuclei which gives the probability of its occurrence, σ_{kn} is the inelastic interaction cross section for a k -type particle with an n -type nucleus. The elastic scattering cross sections have been calculated using the formula

$$\sigma_{el}(A) = 6.38 A^{1.06} [\text{mb}] \quad (10)$$

We assume an isotropic flux of cosmic ray protons. The form of the spectrum [4] used in our calculations takes into account the influence of solar activity on the galactic CR intensity through the modulation parameter Φ

$$J(T, \Phi) = A \frac{T(T+2E_0) (T+\Phi+m)^{-\gamma}}{(T+\Phi) (T+2E_0+\Phi)} \quad (11)$$

where T (MeV) is the proton kinetic energy, E_0 its rest energy, Φ is the modulation parameter (MeV), $A=9.9 \times 10^8$, $\gamma=2.65$, $m=780 \exp(-2.5 \times 10^{-4})$. The parameter Φ acquire the value 100 MeV for the unmodulated GCR flux, 300 MeV for the solar minimum and 650 MeV for the average GCR flux [4]. This spectrum was corrected for the non-proton contribution, which can be estimated to be as high as 35-40%.

The method was tested and calibrated on simulation of ^{22}Na production. ^{10}Be , ^{36}Cl , ^{53}Mn and ^{26}Al were used for investigation of the cosmic ray behaviour in the past. The calculations were done for a target having the form of an infinite layer of material in the case of lunar samples and the form of the sphere with radius corresponding to the one half of the maximum dimension of real sample in the case of meteorites. For the purpose of investigation of production rate profiles the targets were divided into sublayers with thickness of 20 g/cm^2 . The effective chemical composition was taken to be in conformity with that of real samples. A comparison of calculated and measured depth dependence of the production rates of ^{22}Na in Apollo 15 samples [5] has shown that the best agreement was found for the modulation parameter $\Phi=650$ MeV, which corresponds to an average GCR flux a few years before the sample collection [6].

A comparison of calculated and measured results for ^{10}Be and ^{53}Mn in deep core lunar samples has shown a disagreement which is not at present well understood [7]. The calculated curves follows the shape of the experimental dependence, but at small depth there is an overproduction. The best agreement has been found for the modulation parameter $\Phi=200$ MeV, which

SIMULATION OF CGN PRODUCTION, Masarik J. and Povinec P.

indicate that these nuclides were produced mostly by an unmodulated GCR flux.

Fig.1 shows result of calculations of production rates of ^{53}Mn in the ALHA meteorite. The profiles of the depth dependence are much flatter than that calculated for the Moon, that can be explained by the isotropic irradiation of the meteorite from all sides and the same value (in order) of interaction length of GCR and the size of the meteorite. But in spite of that the weak decrease of production rate in the direction to the surface is visible. This decrease is dependent on the radius of meteorite and the dependence has the same character as the dependence of central activity on the effective meteorite radius [8].

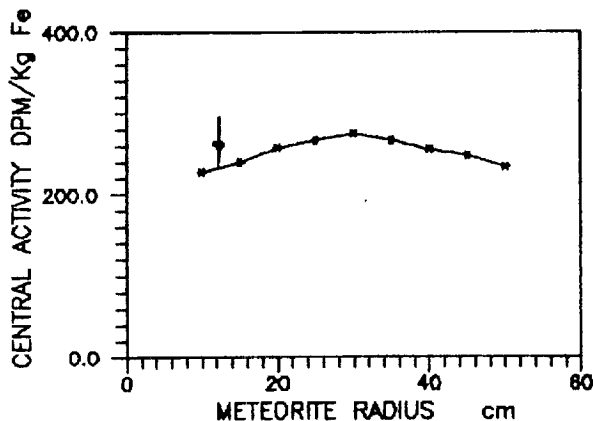


Fig.1. ^{53}Mn central activity as a function of meteorite's radius. Experimental data are taken from [9].

At present we are studying a possible application of the intranuclear cascade model and the uncertainties of the developed method for a better understanding of the discovered disagreement between the calculated and measured results.

References

1. Alsmiller R.G. (1967) Nucl.Sci.and Eng. 27, 158-172.
2. Spanier J. and Gelbard E.M. (1969) Monte Carlo Principles and Neutron Transport Problem, Eddison-Wesley pub. Comp. Massachusetts.
3. Rossi S. (1975) Kosmicheskiye luchi, Atomizdat, Moskva.
4. Bonino G., Castagnoli C. and Dardo M. Proc.16-th Int Conf. Cosmic Rays (IUPAP, Kyoto 1979) vol 12, 155-158.
5. Nishiizumi K., Klein J., Middleton R. and Arnold J.R. (1984) Earth and Planet. Sci. Lett. 70, 164-168.
6. Masarik J., Emrich P., Povinec P. and Tokar S. (1986) Nucl.Inst. Meth. B17, 483-489.
7. Masarik J. and Povinec P. Proc.20-th Int. Conf. Cosmic Rays (IUPAP, Moskva 1987) vol4. 315-318.
8. Masarik J. and Povinec P. Proc. 21-st Int Conf. Cosmic Rays (IUPAP, Adelaide 1990) SH 9.1-8 (in press).
9. Englert P., Herperts U., Herr W. and Sarafin R. Proc. 5-th Int. Conf. Geochron, Cosmochron. (Nikko 1982) 89-90.

516-90
321034
16

p-5

Prediction of Thin-Target Cross Sections of Neutron-Induced Reactions up to 200 MeV; R. Michel and H. Lange, Zentraleinrichtung für Strahlenschutz, Universität Hannover, F.R.G.

Nuclear reactions induced by secondary neutrons are the most important production modes of cosmogenic nuclides by galactic cosmic ray (GCR) particles in extraterrestrial matter. Only in cosmic dust and in very small meteoroids ($R < 10$ cm) the contributions of charged primary and secondary GCR particles exceed that of secondary neutrons. There are two important differences between neutrons and charged particle fields in meteoroids and planetary surfaces, e.g. [1]. First, the differential spectra are completely different, those of secondary neutrons decreasing monotonically with increasing energy, while those of charged particle show maxima around 100 MeV/A due to the action of electronic stopping at lower energies (fig. 1). This difference causes neutrons with energies below 100 MeV to outrange the protons by far. The second difference is with respect to depth and size dependences of particle fluxes. Secondary protons show a transition maximum around meteoroid radii of 30 cm, while secondary neutrons have not yet reached the maximum at a radius of 65 cm. Also the fluxes ($E > 10$ MeV) of secondary neutrons are higher than those of protons by up to a factor of 3 in L-chondrites with radii below 65 cm (fig. 2).

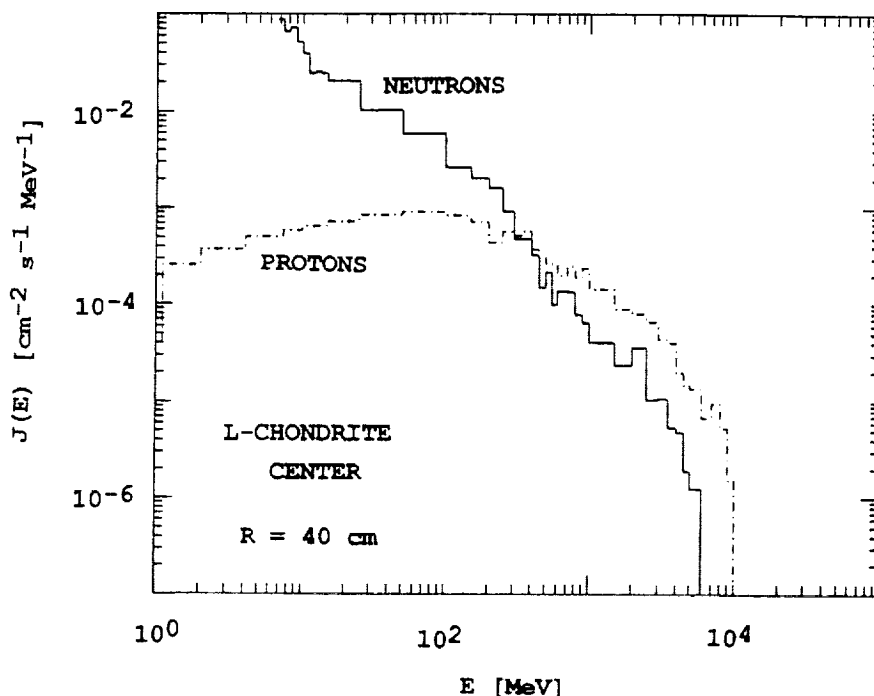


Fig. 1: Spectra of protons (primary + secondary) and secondary neutrons in the center of an L-chondrite with a radius of 40 cm irradiated with galactic protons. The data are normalized to an integral flux of primary protons of $1 \text{ cm}^{-2} \text{ s}^{-1}$.

PREDICTION OF THIN-TARGET CROSS SECTIONS...: Michel, R. and Lange, H.

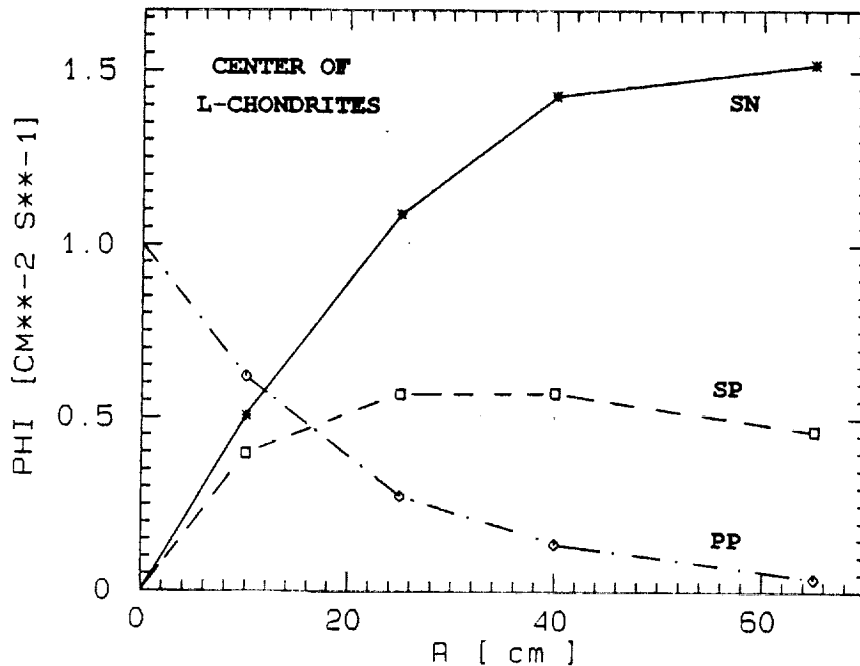


Fig. 2: Fluxes of primary and secondary protons and of secondary neutrons in the center of L-chondrites irradiated with GCR protons. The data are normalized to an integral flux of primary protons of $1 \text{ cm}^{-2} \text{ s}^{-1}$.

Consequently, neutron-induced reactions dominate the production of cosmogenic nuclides in normal-sized meteoroids and in planetary surfaces. Cross sections for n-induced reactions are most important for an accurate modeling of the production of cosmogenic nuclides in extraterrestrial matter. However, the available data base shows up with strongly differing quality depending on the neutron energy. At energies below 1 MeV, where besides some exceptional (n,p)- and (n,⁴He)-reactions only neutron capture is of importance, there exists a comprehensive and accurate data base, e.g. [2], intended to satisfy the needs of nuclear technology. For the target nuclides of interest for meteoritics as well as for lunar and planetary science, such as ¹⁴N, ³⁵Cl, ⁵⁹Co, ^{79,81}Br, ¹²⁸Te, ¹³¹Ba, ¹⁴⁹Sm, ¹⁵²Eu, ¹⁵⁷Gd, and ¹⁸⁶W, the required nuclear and cross section data exist and isotopic anomalies can be satisfactorily interpreted in the framework of existing models [3,4]. With these reactions we will not deal here further.

For neutron energies above 1 MeV the knowledge about production cross sections is completely insufficient. The existing data are nearly exclusively restricted to energies below 30 MeV using the T(d,n)⁴He or ⁷Li(p,n)⁷Be reactions as neutron sources. Moreover, most measurements are closely clustered around $E_n = 14.7 \text{ MeV}$ and only a few excitation functions have been measured over a larger energy range. A survey on compilations and evalua-

PREDICTION OF THIN-TARGET CROSS SECTIONS...: Michel, R. and Lange, H.

tions of the existing data may be found elsewhere [5]. At higher energies either deuteron break-up, (p,n)- or spallation reactions are used as neutron sources. For all these fast neutron irradiation facilities experimental problems arise from the fact that the neutron beams are either not monoenergetic or have too low intensities. Details on the related experimental techniques may be found elsewhere [6]. Though the number of fast neutron irradiation facilities is increasing it will take several years until the necessary experimental data will be available.

In order to overcome this problem we started a programme to predict thin-target excitation functions for neutron-induced reactions for neutron energies up to 200 MeV on the basis of the hybrid model of preequilibrium reactions [7]. The capability of this model to predict unknown excitation functions and to perform a priori calculations of nuclear reactions cross sections for a wide variety of reactions types is an outstanding feature of this theory. However, there are distinct differences in the quality of such calculations depending on the type of bombarding particle and on the excitation energies of the reacting systems. For p-induced reactions up to 200 MeV this model finally proved to be well capable to predict cross sections for the production of radionuclides from a wide range of target elements [8,9, and references therein].

A first set of excitation functions [10,11] was calculated using the hybrid model in the form of the code ALICE LIVERMORE 82 [12]. The calculated excitation functions were used successfully to interpret the experimental production rates measured in the course of the experiment CERN SC-96 [13,14]. Here, we report on a new data base, the excitation functions of which were calculated by the code ALICE LIVERMORE 87 [15], which is an extended version of the former one. This recent version of the hybrid model [15] of preequilibrium (PE) reactions has several advantages compared to the earlier versions. It contains some improvements which are essential for such calculations. First, it allows to use experimental nuclide masses as far as available. Secondly, it allows for the choice of broken exciton numbers, thus taking into account the statistical distribution of different possible initial exciton configurations. A detailed discussion of this feature was given by Blann and Vonach [16]. Thirdly, it takes into account multiple PE decay, allowing for both the emission of more than one nucleon from a single exciton configuration and for the PE emission of several nucleons in sequential exciton configurations.

The new data base "ZFS-NSIG-89" up to now contains thin-target excitation functions for the target elements Na, Mg, Al, Si, K, Ca, Ti, V, Mn, Fe, Co, Ni, Cu, Rb, Sr, Y, Zr, Ba, and La for neutron energies between 1 and 200 MeV. With regard to the product nuclides it covers all relevant cosmogenic radionuclides as well as stable rare gas isotopes with the exceptions stated below. For the long-lived and stable products the data are cumulative, i.e. they contain the contributions of shortlived progenitors. Exemplarily, in fig. 3 the excitation functions for the neutron-induced production of ^{53}Mn from Mn, Fe and Ni are shown.

PREDICTION OF THIN-TARGET CROSS SECTIONS...: Michel, R. and Lange, H.

There are no cross sections for the production of H- and He-isotopes and there still are some important target elements as e.g. O and C for which we do not have calculations. For the latter target elements the capabilities of the hybrid model are currently being tested for p-induced reactions.

The comparison of the calculated cross sections with experimental data in the low energy ($E_n < 30$ MeV) region shows the same good quality of the calculations as was earlier observed for proton-induced reactions for various target elements [9]. A comparison of excitation functions for the same target element/product combinations demonstrates that there can be strong differences between the cross sections of neutron- and proton-induced reactions and that the often made assumption of neutron cross sections being equal to those of proton-induced reactions is not justified (e.g. fig. 4).

The calculated neutron cross sections have been successfully used to calculate the depth and size dependent production rates measured in a number of 600 MeV simulation experiments [13,14] as well as for dosimetry purposes in radiation damage experiments in spallation neutron sources [17]. It has, however, to be stated that these neutron cross section just are first aid to satisfy our cross section needs for neutron-induced reactions. Measured data will easily replace them as soon they are available.

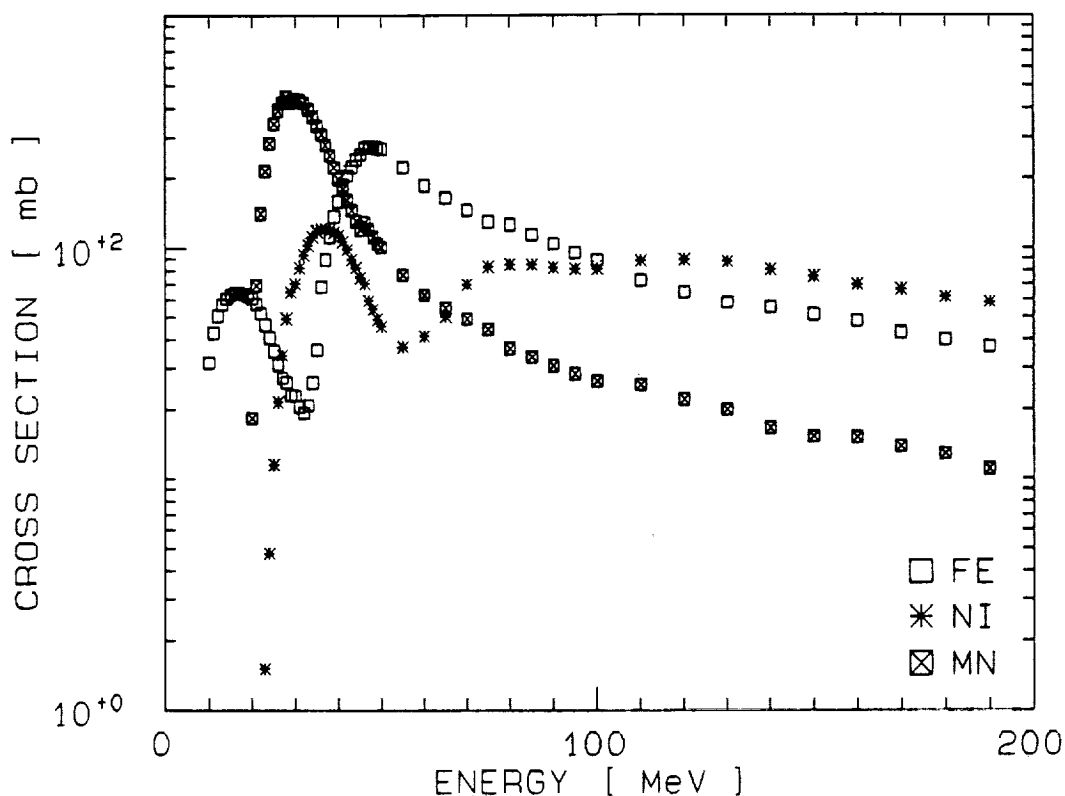


Fig. 3: Calculated excitation functions for the neutron-induced production of ^{53}Mn from Mn, Fe and Ni.

PREDICTION OF THIN-TARGET CROSS SECTIONS...: Michel, R. and Lange, H.

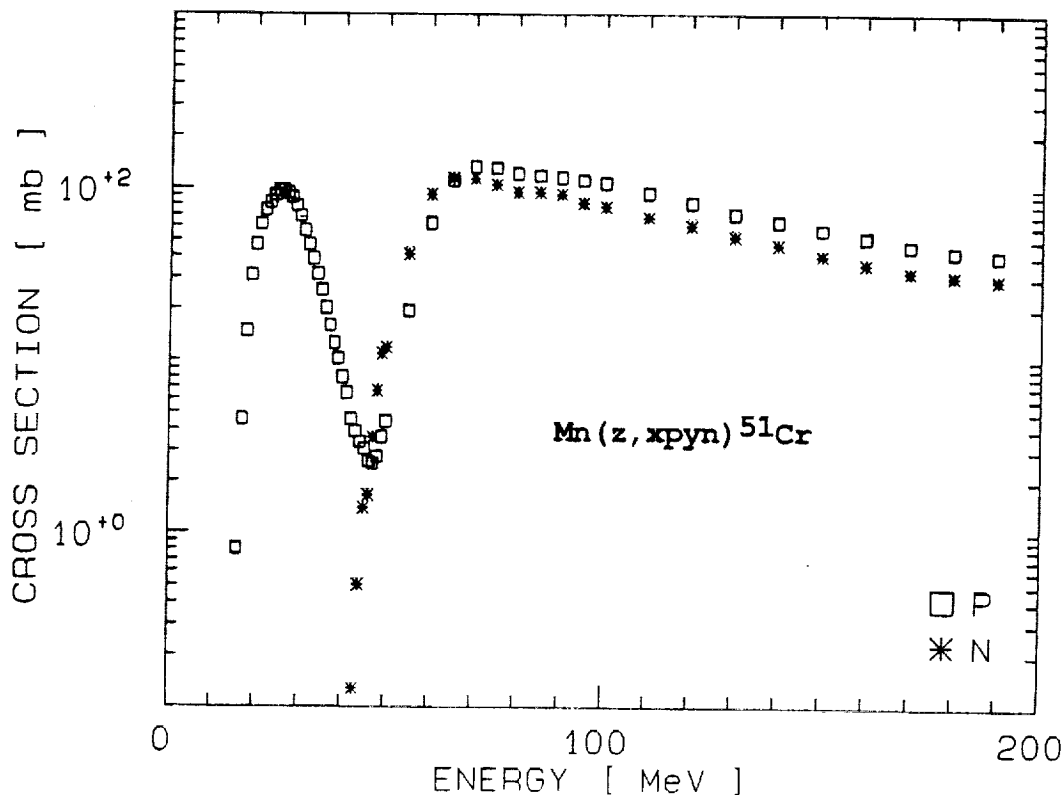


Fig. 4: Comparison of calculated excitation functions for the proton- and neutron-induced production of ^{51}Cr from Mn.

References: [1] R. Michel et al., LPS XX (1989) . [2] S.F. Mughabghab and D.I. Garber, BNL-325/ED3 V-1+2 (1973). [3] P. Eberhardt et al., Helv. Phys. Acta 34 (1961) 460. [4] R.E. Lingenfelter et al., EPSL 16 (1972) 355. [5] V.N. Manokhin et al., in: IAEA, Handbook of Nuclear Activation Data, IAEA Technical Reports Series No. 273, IAEA, Vienna (1987) 305. [6] S. Cierjacks (ed.) Neutron Sources for Basic Physics and Applications (Neutron Physics and Nuclear Data in Science and Technology;2), Pergamon Press, 1983. [7] M. Blann, Phys. Rev. Lett. 27 (1972) 337. [8] R. Michel and R. Stück, J. Geophys. Res. (Suppl.) 89 B (1984) 673. [9] R. Michel et al., Nucl. Phys. A 441 (1985) 617. [10] R. Michel and F. Peiffer, in: P.G.Young et al. (eds.) Nuclear Data for Basic and Applied Science, Gordon and Breach Sci. Publ., NY (1986) 1647. [11] R. Michel and F. Peiffer, KCK-NSIG-86, unpublished (1986). [12] M. Blann and J. Bisplinghoff, UCID-19614 (1982). [13] R. Michel et al., Nucl. Instr. Meth. Phys. Res. B16 (1985) 61 and B42 (1989) 76. [14] D. Aylmer et al., Jül-2130 (1987). [15] M. Blann, priv. comm. (1987). [16] M. Blann and H.K. Vonach, Phys. Rev. C28 (1983) 1475. [17] A. Cesana et al., 6th ASTM-Euratom Symposium on Reactor Dosimetry, 31 May - 5 June 1987, Jackson Hole, Wyoming. **Acknowledgment** This work was supported by the Deutsche Forschungsgemeinschaft.

517-90
351035
p-5

Thin-Target Cross Sections for the Production of Cosmogenic Nuclides by Charged-Particle-Induced Reactions; R. Michel, R. Bodemann, M. Lüpke, Zentraleinrichtung für Strahlenschutz, Universität Hannover, F.R.G.; U. Herpers, B. Dittrich, Abteilung Nuklearchemie, Universität zu Köln, F.R.G.

Thin-target cross sections for charged-particle-induced reactions provide the basis for a quantitative description of the production of cosmogenic nuclides by solar cosmic ray (SCR) particles. Combining reliable excitation functions of the underlying nuclear reactions with depth-dependent SCR particle spectra resulting from simple stopping calculations, SCR effects can be accurately described. Also any modelling of the interactions of galactic cosmic rays (GCR) with terrestrial and extraterrestrial matter depends on accurate reaction data, though the occurrences of GCR interactions with matter are much more complex and in spite of the fact that charged particles in most cases only contribute to a minor degree to the GCR production of cosmogenic nuclides.

Solar and galactic cosmic ray particles consist of about 90 % protons and 10 % alpha-particles, both particle types having roughly the same spectra as function of energy per nucleon. Thus, protons are the most important ones. But for an accurate modelling the complete knowledge of the cross sections of both proton- and alpha-induced reactions is necessary. A survey on the cosmogenic nuclides of interest and the target elements to be considered is given in table 1 without claiming completeness for this compilation.

Unfortunately, up to now the cross section data base is neither complete nor accurate. For many cosmogenic nuclides of interest no data exist at all. Moreover, many of the experimental data reported in the past suffer from severe lack of accuracy, so that often there are uncertainties of up to an order of magnitude when looking for non-evaluated experimental data. Such uncertainties do neither allow for tests of nuclear reaction models nor are they tolerable for the various applications of high-energy integral cross sections, in particular for an accurate modelling of cosmic ray interactions with matter.

Therefore a research program was initiated to measure the required excitation functions and to establish a consistent set of cross sections for the p- and alpha-induced production of cosmogenic nuclides from most relevant target elements. Irradiations and measurements are done in collaboration of groups from Ahmedabad, Cologne, Hannover, Jülich, Philadelphia, Studsvik, Zürich, and Uppsala. Thin-target cross sections for the production of stable and radioactive nuclides by proton-induced reactions on O, Mg, Al, Si, Ca, Ti, V, Mn, Fe, Co, Ni, Cu, Zr, Rh, Ba, and Au are measured up to 2600 MeV using accelerators at GWI/Uppsala ($E_p < 200$ MeV), CERN/Geneve ($E_p = 600$ MeV), LANL/Los Alamos ($E_p = 800$ MeV), and Saclay ($E_p = 1200$ and 2600 MeV). For alpha-induced reactions former measurements [1] are extended with respect to target element and product nuclide cover-

THIN-TARGET CROSS SECTIONS FOR THE PRODUCTION OF ...: Michel R. et al.

Table 1: Survey on target elements to be considered for the production of cosmogenic nuclides in meteoroids by charged-particle-induced reactions. All cross sections must be cumulative with regard to shortlived progenitors. This table neglects nuclides as ^{46}Sc , ^{48}V , ^{51}Cr , ^{54}Mn , ^{56}Co , ^{57}Co , ^{58}Co , which can be importance in freshly fallen meteorites. * of interest for alpha-induced reactions only.

PRODUCTS	$T_{1/2}$	TARGET ELEMENTS								
^{22}Na	2.6 a	Na	Mg	Al	Si	S	Ca	Fe	Ni	
^{60}Co	5.26 a	Ni								
^3H	12.3 a	C	O	Mg	Al	Si	S	Ca	Fe	Ni
^{44}Ti	47.3 a	Ca	Ti	Fe	Ni					
^{14}C	5.73 ka	O	Mg	Al	Si	S	Ca	Fe	Ni	
^{59}Ni	75. ka	Fe*	Ni							
^{36}Cl	300. ka	K	Ca	Fe	Ni					
^{26}Al	716. ka	Na*	Mg	Al	Si	S	Ca	Ti	Fe	Ni
^{41}Ca	103. ka	K	Ca	Ti	Fe	Ni				
^{81}Kr	210. ka	Sr	Y	Zr						
^{10}Be	1.6 Ma	C	O	Mg	Al	Si	S	Ca	Fe	Ni
^{53}Mn	3.7 Ma	Mn	Fe	Ni						
^{129}I	15.7 Ma	Ba	La	REE						
^{40}K	1.28 Ga	K	Ca	Ti	Fe	Ni				
He	stable	C	O	Mg	Al	Si	S	Ca	Fe	Ni
Ne	stable	Na	Mg	Al	Si	S	Ca	Fe	Ni	
Ar	stable	S*	Cl	K	Ca	Ti	Fe	Ni		
Kr	stable	Br	Rb	Sr	Y	Zr				
Xe	stable	Ba	La	REE						

age in order to establish production cross sections for stable and long-lived cosmogenic nuclides by irradiations at PSI/Würenlingen and at KFA/Jülich.

The stacked-foil technique is used to investigate proton- and alpha-energies up to 200 MeV. Above 200 MeV single energy points are investigated in order to minimize interferences from secondary particles. Gamma- and X-spectrometry as well as conventional and accelerator mass spectrometry are used to measure the residual nuclides, in particular all relevant cosmogenic nuclides. Up to now, final results were obtained for short- and medium-lived nuclides. The measurements for longlived nuclides as well as the data evaluation still are going on. Also the mass spectrometric measurements are not yet finished. First data for a p-energy of 600 MeV were already pub-

THIN-TARGET CROSS SECTIONS FOR THE PRODUCTION OF ...: Michel R. et al.

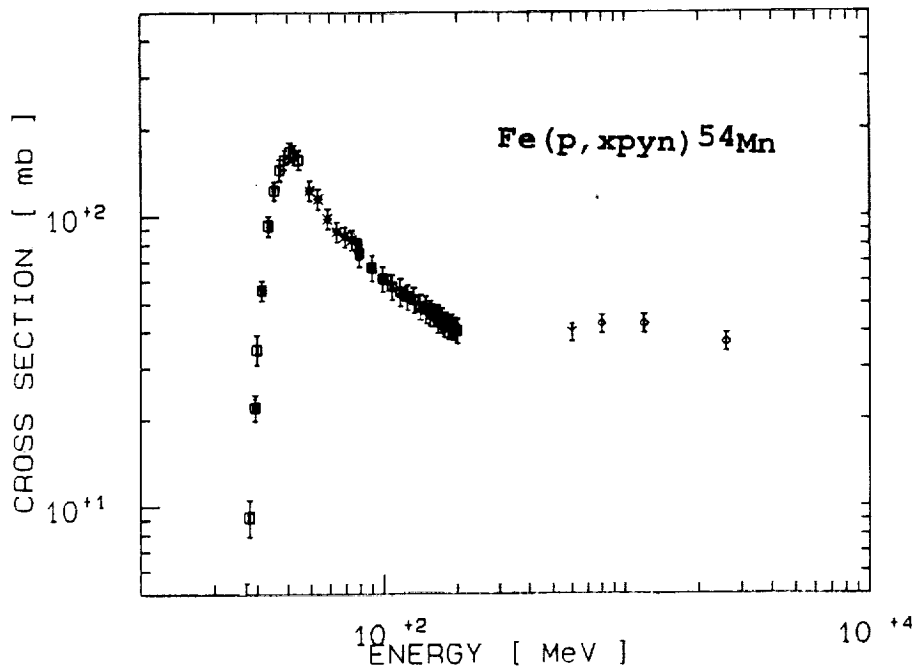


Fig. 1: Excitation function for the reaction $\text{Fe}(p, 2pxn) {}^{54}\text{Mn}$ measured by our group. For the data below 800 MeV see [1, 4] and refs. therein.

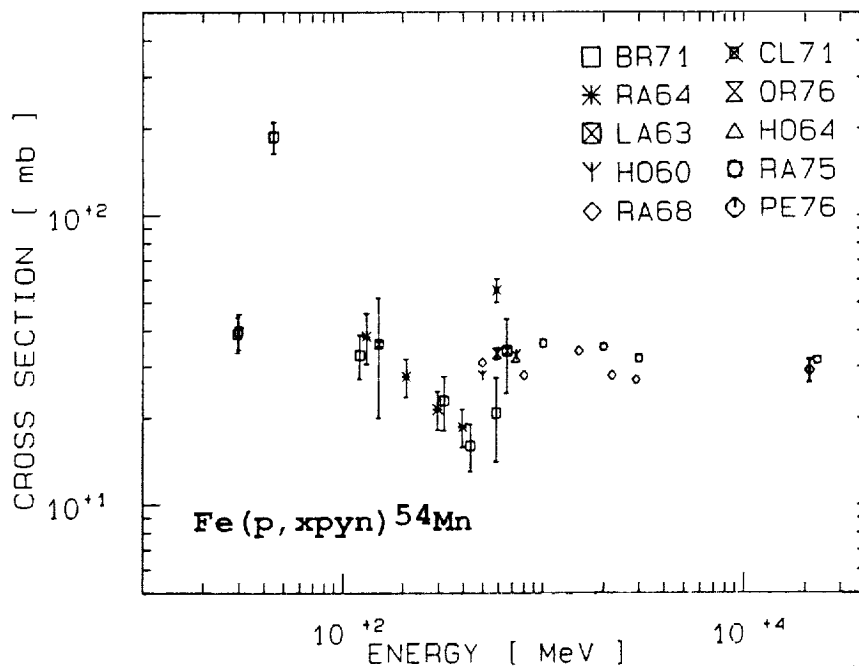


Fig. 2: Survey on cross sections reported by other authors for the reaction $\text{Fe}(p, 2pxn) {}^{54}\text{Mn}$.

THIN-TARGET CROSS SECTIONS FOR THE PRODUCTION OF ...: Michel R. et al.

lished [2,3]. The new data represent a consistent data set of thin-target cross sections of more than 300 individual spallation reactions. Together with the cross sections for proton energies up to 200 MeV measured earlier by our group [4,5], and references therein, they give the complete excitation functions from the thresholds up to 2600 MeV. As an exemple, the excitation function for the production of ^{54}Mn from iron measured by our group is presented in fig. 1. A comparison with all the data reported up to now by other authors for this reaction (fig. 2) emphasizes the advantage of a consistent data base and demonstrates the necessity to use only evaluated data for model calculations.

Though not all experimental cross sections are available right now, it is possible to perform a critical review of earlier experimental data and to do some comparison of the new data with the results of model calculations. The existing data already now allow for a discussion of the quality of parametric models [6,7], which are often used for the calculation of spallation cross sections. However, a comparison of the new experimental data with those calculated by Rudstam's CDMDG formula [6] and by the formula proposed by Silberberg and Tsao [7] using the code SPALL by Routti and Sandberg [8] in the energy range from 600 to 2600 MeV showed partial discrepancies. Though considerable improvements have been achieved in the more recent formula [7], in particular with respect to the production of light fragments, for many nuclides theory and experiment deviate by more than a factor of two (figs. 3 and 4). It has to be emphasized that the calculational accuracy obtained so far by the semiempirical formulas is not sufficient for model calculations of cosmogenic nuclides.

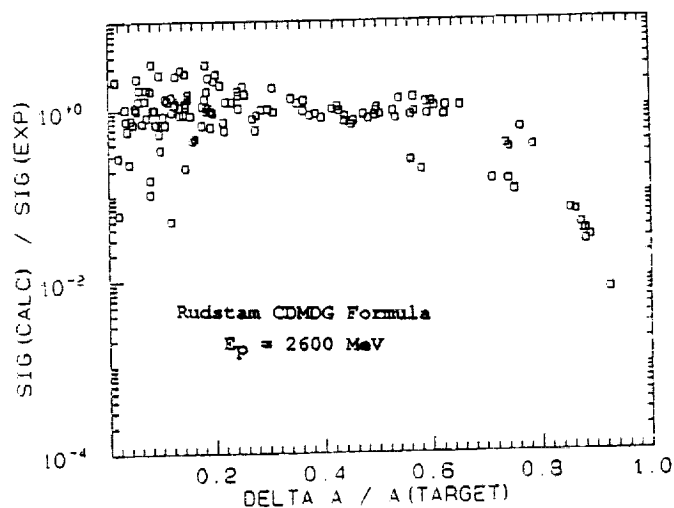


Fig. 3: Ratios of theoretical to experimental cross sections for proton-induced reactions at 2600 MeV as function of mass difference between target and product nuclei. The theoretical data were calculated by Rudstam's CDMDG formula [6], the experimental data are exclusively from our work.

THIN-TARGET CROSS SECTIONS FOR THE PRODUCTION OF ...: Michel R. et al.

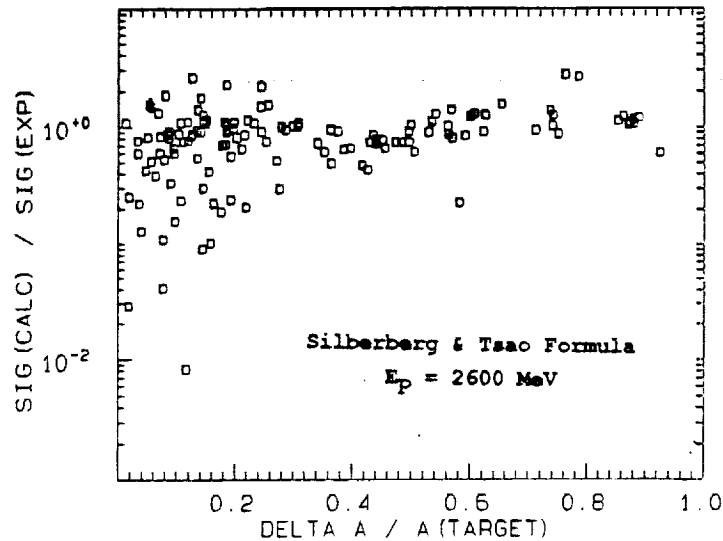


Fig. 4: Ratios of theoretical to experimental cross sections for proton-induced reactions at 2600 MeV as function of mass difference between target and product nuclei. The theoretical data were calculated by the semiempirical formula by Silberberg and Tsao [7], the experimental data are exclusively from our work.

Further, the question of theoretical predictions of thin-target cross sections on the basis of theories of nuclear reaction theories is addressed. For this purpose hybrid model calculations using the code ALICE LIVERMORE 87 [9] for p-energies up to 200 MeV were performed, which demonstrated the same excellent quality of a priori calculations as observed before [5]. For higher energies Monte Carlo calculations of the intranuclear cascade were performed using the high energy transport code HETC/KFA-2 within the newly developed HERMES code system [10]. Absolute production cross sections were obtained by evaluating the history of residual nuclei. First results on the target element Fe look very promising [2]. Presently, these calculations are extended to other target elements in order to obtain a systematic survey on the quality of such calculations and on the possibility to reliably predict unknown excitation functions.

References: [1] R. Michel et al., *Radiochimica Acta* 32 (1983) 173. [2] R. Michel et al., *The Analyst* 114 (1989) 287 and *Nucl. Instr. Meth. Phys. Res.* B42 (1989) 76. [3] R. Michel et al., in: *Progress Report on Nuclear Data Research in the Federal Republic of Germany for the Period April, 1st, 1987 to March, 31st, 1988*, NEANDC(E)-292 U Vol. V INDC(Ger)-32/LN+Special (1988) 25. [4] R. Michel, R. Stück, *J. Geophys. Res. (Suppl.)* 89 B (1984) 673. [5] R. Michel et al., *Nucl. Phys. A* 441 (1985) 617. [6] G. Rudstam, *Z. Naturf.* 21a (1966) 1027. [7] R. Silberberg, C.H. Tsao, *Astrophys. J. Suppl.* 25 (1973) 315. [8] J.T. Routti, J.V. Sandberg, *Comp. Phys. Comm.* 23 (1981) 411. [9] M. Blann, J. Bisplinghoff, J., UCID-19614 (1982) and M. Blann, priv. comm. (1987). [10] P. Cloth et al., Jül-2203 (1988). **Acknowledgment** This work was supported by the Deutsche Forschungsgemeinschaft.

518-90
321036
P-5

Monte Carlo Modelling of the Production of Cosmogenic Nuclides in Extraterrestrial Matter by Galactic Cosmic Ray Particles; R. Michel, Zentraleinrichtung fuer Strahlenschutz, Universitaet Hannover, Hannover, F.R.G., P. Dragovitsch, G. Dagge, P. Cloth, D. Filges, Institut fuer Kernphysik, KFA Juelich, Juelich, F.R.G.

Monte Carlo (MC) techniques provide a tool to describe quantitatively the complex occurrences of high energy hadronic interactions with matter on the basis of current nuclear physics models and have been successfully applied in various fields of basic and applied sciences. In particular, MC calculations with the HERMES code system [1] have been extremely successful in describing the production of residual nuclides in a number of 600 MeV thick-target irradiation experiments performed in order to simulate the production of cosmogenic nuclides in meteoroids [2,3]. Based on the experience from this validation a new model for the production of cosmogenic nuclides in extraterrestrial matter by galactic cosmic ray particles was proposed [4].

In this model the size- and depth-dependent production rates of cosmogenic nuclides are calculated for meteoroids as well as for planetary surfaces by combining the depth- and size-dependent spectra of primary and secondary particles resulting from MC calculations with composition-weighted thin-target production cross sections of the contributing nuclear reactions. The advantage of this method is that it strictly distinguishes between two completely different physical quantities, namely the spectra of the primary and secondary GCR particles in the respective material on the one hand and the cross sections of the underlying nuclear reactions on the other. This allows to derive from one set of MC calculations the depth- and size-dependent production rates of all cosmogenic nuclides wanted. Moreover, the calculations can easily be extended to a new nuclides if the respective cross sections are at hand. Presently, the cross sections for p-induced reactions are based on an evaluated set of experimental data and on our own recent data [2,3,5]. Those for n-induced reactions are calculated ones [6] using the code ALICE LIVERMORE 87 [7]. Still existing gaps in the experimental cross sections were closed in the same way.

MC calculations using the HERMES system were performed for GCR protons irradiating stony meteoroids, some selected irons and the lunar surface (compare also [8, 9]). The spectra of primary protons, secondary protons and secondary neutrons as function of size of and depth inside an extraterrestrial body were derived for energies between 1 MeV and 10 GeV in case of protons, while the neutrons were followed from 10 GeV to thermal energies. However, for a complete description of GCR interactions galactic He-nuclei must be taken into account, because their contribution makes up 30 % of the total GCR interactions with respect to both the number of nucleons as well as to the energy input. In our present calculations He-nuclei are

MONTE CARLO MODELLING OF THE PRODUCTION OF ...: Michel R. et al.

only taken into account by assuming them to break up immediately in the first collision and further to act in the same way as primary GCR protons. Thus, all production rates due to proton-induced reactions have to be scaled up by a factor of 1.3. The exact calculations for GCR He-nuclei will be performed in due course.

As primary GCR proton spectrum an average of the observed spectra during times of a quiet sun (1965, $M = 450$ MV) and an active sun (1969, $M = 900$ MV) was taken for the calculations. M is the force field parameter as used in the parameterization of the GCR spectra by Castagnoli and Lal [10]. The influence of solar modulation onto primary and secondary GCR particle spectra and consequently onto production rates in meteoroids was investigated performing independent MC calculations for the 1965 and 1969 primary spectra. The results describe the sensitivity of the production rates of different cosmogenic nuclides to changes in the GCR spectrum and allow for a discussion of the constancy of GCR fluxes in the past. A detailed analysis of the ^{26}Al and ^{53}Mn depth profiles in Apollo-15 drill-cores yielded a mean integral flux of primary GCR protons at 1 A.U. with energies above 10 MeV of $3.63 \text{ cm}^{-2} \text{ s}^{-1}$ (e.g. fig. 1), which is equivalent to a mean GCR p-spectrum with a force field parameter $M = 470$ MeV during the last 10 Ma. From an analysis of ^{26}Al and ^{53}Mn in Knyahinya a GCR-flux gradient of 10 % between 1 A.U. and the meteoroid orbits was derived.

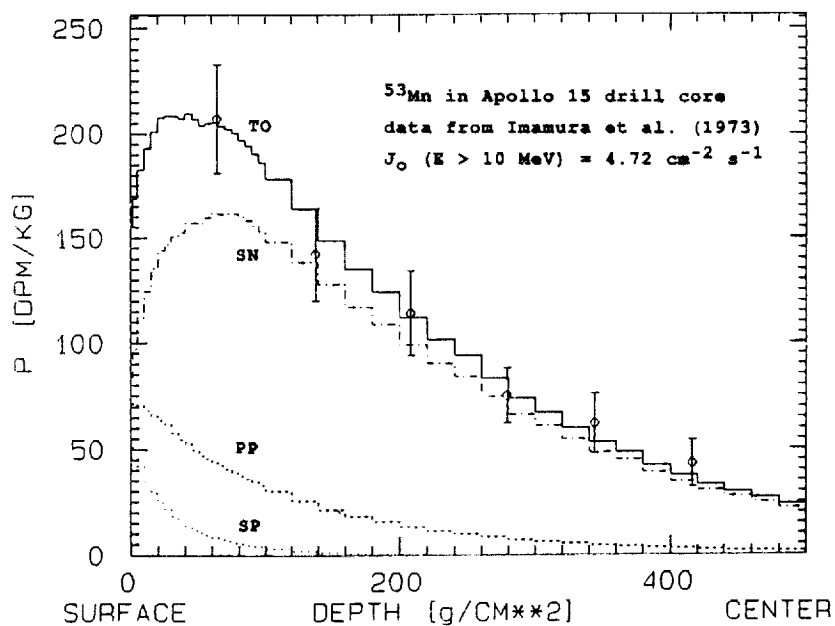


Fig. 1: Experimental depth profile of ^{53}Mn in Apollo-15 drill core [11] and a theoretical depth profile calculated with an integral flux of primary GCR protons at 1 A.U. of $3.63 \text{ cm}^{-2} \text{ s}^{-1}$. Galactic ^4He -nuclei are considered as described in the text.

MONTE CARLO MODELLING OF THE PRODUCTION OF ...: Michel R. et al.

The particle spectra in meteoroids as well as the depth and size dependences of integral particle fluxes are strongly different for protons and neutrons, the latter being the dominant species (compare [6, 8]). The highest n-fluxes were found for meteoroid radii of 65 cm, while the p-fluxes show a maximum at radii around 30 cm. While the results for meteoroids are in contrast to earlier calculations, the data obtained for the lunar surface [9] agree well with those reported earlier by Armstrong and Alsmiller [12]. A detailed survey on the particle spectra and fluxes is given and the influences of the chemical composition of the irradiated body on primary and secondary particle fields are quantitatively described.

Up to now, depth profiles for the production of ^{26}Al , ^{53}Mn and $^{20,21,22}\text{Ne}$ have been calculated for stony meteoroids with radii up to 65 cm, for the lunar surface and for an iron meteorite with 40 cm radius. Exemplarily, in figs. 2 - 4 the depth and size dependence of the production rates of ^{26}Al , ^{53}Mn , and ^{21}Ne in L-chondrites are presented. Fig. 5 gives the $^{22}\text{Ne}/^{21}\text{Ne}$ isotope ratio as function of depth and size for L-chondrites. The results are compared with experimental depth profiles and discussed with respect to the depth and size dependences of elementary production rates, production rate ratios and average production rates of different meteoroid classes.

References: [1] P. Cloth et al., JUEL - 2203 (1988). [2] R. Michel et al., Nucl. Instr. Meth. Phys. Res. B16 (1985) 61 and B42 (1989) 76. [3] D. Aylmer et al., Jül-2130 (1987). [4] R. Michel et al., LPSC XX (1989) 693. [5] R. Michel et al., The Analyst 114 (1989) 287. [6] M. Blann, J. Bisplinghoff, UCID-19614 (1982) and M. Blann, priv. comm. (1987). [7] R. Michel, H. Lange, Prediction of Thin-Target Cross Sections of Neutron-Induced Reactions up to 200 MeV, this report. [8] P. Dragovitsch et al., Applications of the HERMES Code System in Meteoritics, this report. [9] G. Dagge et al., Studies of the Cosmic Ray Induced Gamma-Emission at Planetary Surfaces Using Monte-Carlo Techniques in Respect of the Mars Observer Mission, this report. [10] G. Castagnoli, D. Lal, Radiocarbon 22 (1980) 133. [11] M. Imamura et al., Earth Planet. Sci. Lett. 20 (1973) 107. [12] T.W. Armstrong, R.G. Alsmiller, Proc. 2nd Lunar Sci. Conf. (1971) 1729.

Acknowledgment This work was supported by the Deutsche Forschungsgemeinschaft.

MONTE CARLO MODELLING OF THE PRODUCTION OF ...: Michel R. et al.

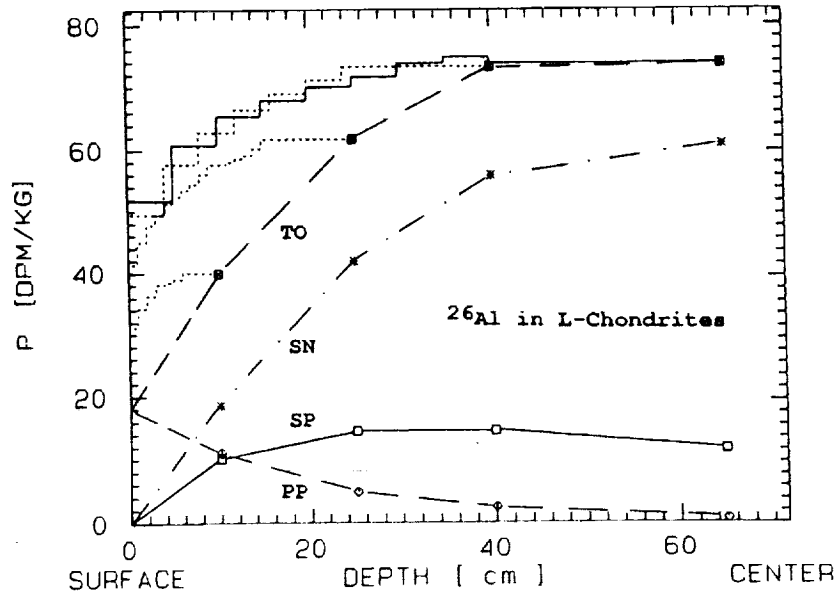


Fig. 2: Calculated production rates of ^{26}Al in L-chondrites irradiated with an $M = 470$ MeV primary GCR proton-spectrum. Galactic ^4He -nuclei and the flux gradient between 1 A.U. and the meteoroid orbits are taken into account as described above.

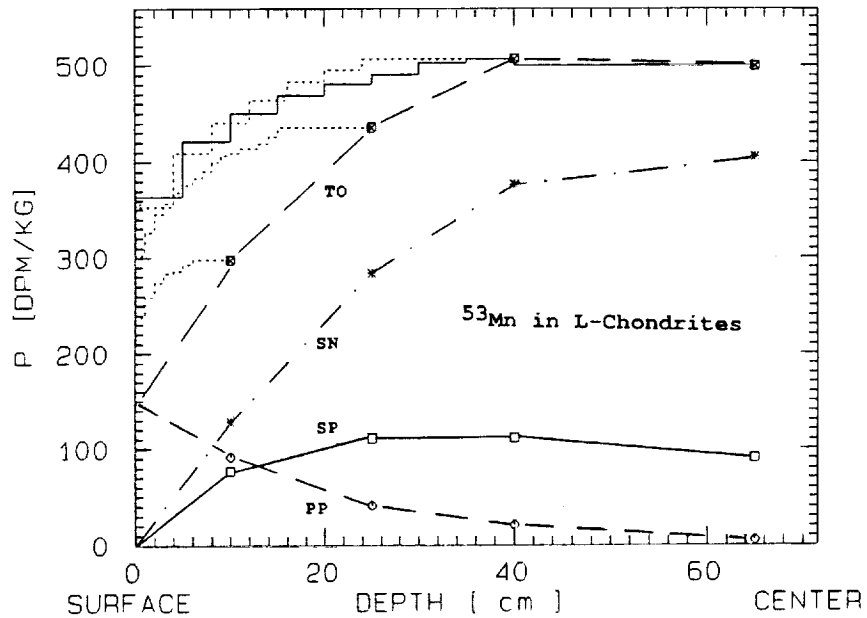


Fig. 3: Calculated production rates of ^{53}Mn in L-chondrites irradiated with an $M = 470$ MeV primary GCR proton-spectrum. Galactic ^4He -nuclei and the flux gradient between 1 A.U. and the meteoroid orbits are taken into account as described above.

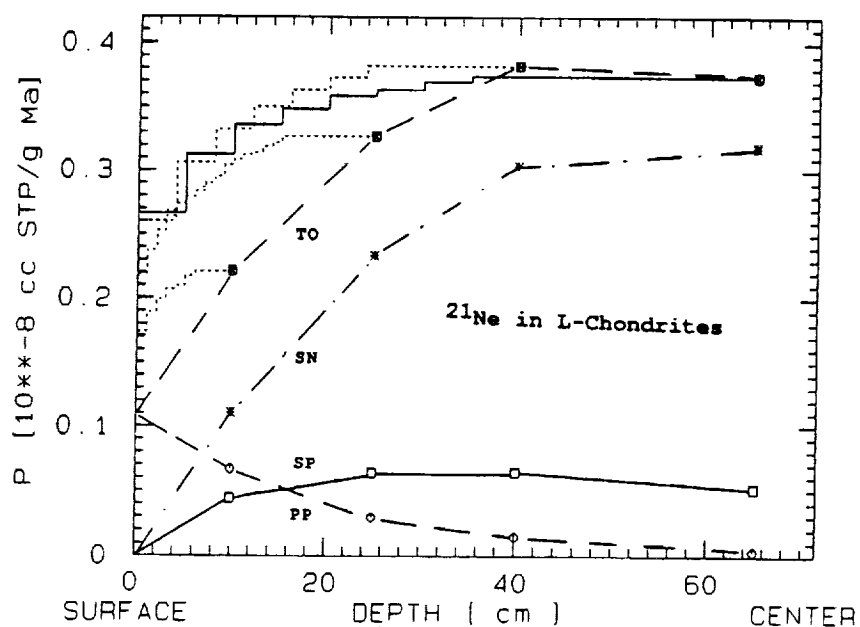


Fig. 4: Calculated production rates of ^{21}Ne in L-chondrites irradiated with an $M = 470$ MeV primary GCR proton-spectrum. Galactic ^4He -nuclei and the flux gradient between 1 A.U. and the meteoroid orbits are taken into account as described above.

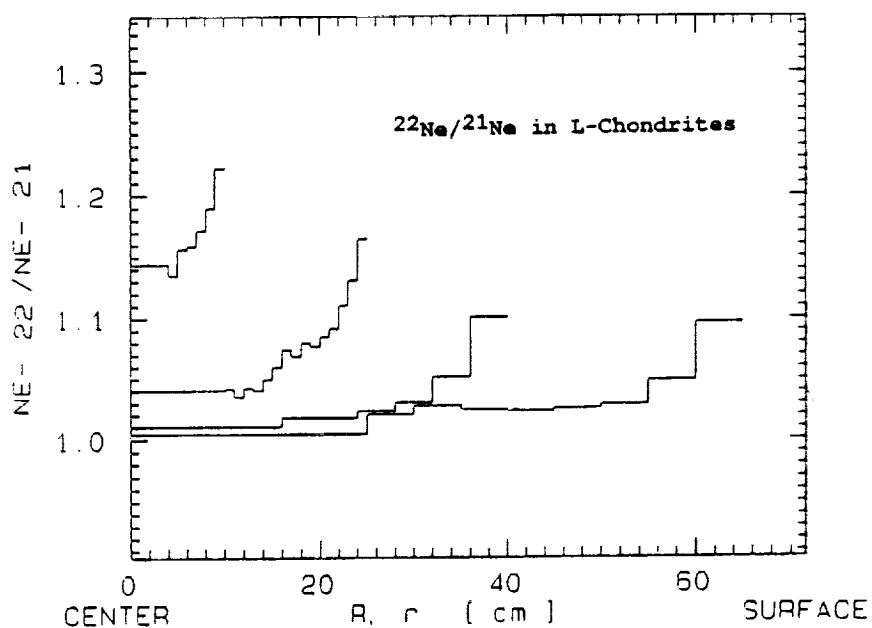


Fig. 5: $^{22}\text{Ne}/^{21}\text{Ne}$ isotope ratios in L-chondrites as revealed by the model calculations.

519-90
321637 91
p-5

BE-10 AND AL-26 IN METAL AND STONE PHASES OF METEORITES.

H.Nagai, M.Honda, Coll.of Humanities and Sci.,Nihon Univ.,Tokyo
M.Imamura, Inst.Nuclear Study, Univ.Tokyo
K.Kobayashi,Res.Cent.,Nuclear Sci.Tech.,Univ.Tokyo
H.Ohashi, Inst.Cosm.Ray Res.,Univ.Tokyo

Cosmogenic ^{10}Be and ^{26}Al were determined in separated metal and stone fractions of meteorites by AMS, accelerator mass-spectrometry. The tandem van de Graaf accelerator at the Univ. of Tokyo was employed for these measurements by applying the internal beam monitor method (1). Enriched ^{17}O was added to the sample as the monitor for ^{10}Be and enriched ^{10}B for ^{26}Al determinations respectively. The monitoring beam of $^9\text{Be}^{17}\text{O}^-$ is injected in the accelerating tube along with the main beam of $^{10}\text{Be}^{16}\text{O}^-$. On the other hand, the monitoring beam of $^{10}\text{B}^{16}\text{O}^-$ is introduced along with the $^{26}\text{Al}^-$ beam.

Chondrites, including antarctic chondrites and fragments of the Jilin chondrite, and stony irons were processed to separate their metal and stone phases. Because of higher ^{26}Al contents in their stone phases, extensive purifications for the metal grains had to be performed. The contamination levels must be lower than 1% stone in metals, and small stone corrections can be made. The sample sizes were 50-400 mg of metals and ca.100 mg of stones. The metal sample size was limited mainly by the shortage of available samples. Smaller amounts of the carriers were added for metal samples, down to 200 and 500 micro g.Be and Al respectively, and the observed atomic ratios of $^{10}\text{Be}/\text{Be}$ and $^{26}\text{Al}/\text{Al}$ of the samples were approximately 10^{-11} .

Some examples of recent determinations are shown in Table 1 (2,3). The fragments of the Jilin are characterized by the contents of ^{21}Ne and other products. They reflect the depth profile of the 1st stage irradiation, by 2 pi geometry for 8 million years and the smaller contributions near the surface of the 2nd stage, 4 pi for about 0.4-0.6 million years. The latter can be estimated from the deepest samples for stable and long-lived activities and are used for corrections to the net contributions in the first stage. These are expected to be exponentially distributed with depths except near the surface.

In general, the following equation, or the equivalent expression, can be applied for the statistical estimations of

^{10}Be AND ^{26}Al IN METAL AND STONE. NAGAI H. et al

production rates, P , of various high energy reaction products in iron and stone meteorites (4).

$$P(A,Z) = f(A,Z) * k_1' * (\Delta A + a)^{-k_2'}$$

where $a=4$ can be used as an empirical term; f is a partial yield of product, A,Z , among isobars, A ; k_1' indicates a production level in Fe target; ΔA is a mass difference between 56 and A , covering $A=54--20$. This formula has been developed originally for iron meteorites. In extensive applications of the formula for ^3He and ^4He in Fe, and for the products in the targets other than iron, the f value is generally used as a proportional coefficient and the equivalent ΔA can be assigned as an effective parameter.

The two sets of linear relations are obtained by plotting $\log[P(^{10}\text{Be})/P(^{53}\text{Mn})]$ vs. shielding index, k_2' , for stones and metals. An effective ΔA for ^{10}Be in metal is estimated at 18 (and $f=0.11$), in a wide range of $k_2'=1.8$ to higher than 3. This is the same as ^{38}Ar and ^3He . Therefore $P(^{10}\text{Be})$ is relatively constant, 5dpm/kg, within the chondrite group. For ^{10}Be in stones, $\Delta A=8$ (and $f=0.12$) can be assigned, in the range $k_2'=1.8-2.4$, as reported previously(2). A similar relation is seen in achondritic targets as has been shown in mesosiderites. This pattern is extended to the Jilin and to the lunar samples. The distributions of net ^{53}Mn and ^{10}Be in the 1st stage of the Jilin can be referred to the galactic productions near the lunar surface.

Similar relations were observed for ^{26}Al . Production ratios of $(^{26}\text{Al}/^{53}\text{Mn})$ can also be compared with k_2' s. In the stone phases of chondrites of ordinary sizes, the ratios were essentially constant at about 0.13. In other words, the ΔA for ^{26}Al in the stone phases is assigned to be 3 which is equal to that of ^{53}Mn . The ratio of $^{53}\text{Mn}/^{26}\text{Al}$ in metals is considered to be the most sensitive indicator for the shielding throughout stony and iron meteorites. A general relation between two parameters, k_1' and k_2' , is illustrated in Fig.1.

Ref. (1) H.Nagai et al(1987)Nucl.Instr.Method, B29,266-270; (1987) Meteoritics 22,467-469. (2) H.Nagai et al(1988) 13th Symp. Antarctic Meteorites, Jun.Tokyo. (3) H.Nagai et al(1989) 14th Symp. Antarctic Meteorites, Jun.Tokyo. (4) M.Honda(1985) EPSL 75,77-80; (1988) Meteoritics 23,3-12.

^{10}Be AND ^{26}Al IN METAL AND STONE. NAGAI H. et al.

BE-10 & AL-26 IN METAL & STONE. NAGAI H. et al

TABLE 1 BE-10 AND AL-26 FOUND IN METAL AND STONE FRACTIONS(1988-1989)

SAMPLE	CLASS ID	-----METAL FRACTION-----			-----STONE FRACTION-----			dpm/kgFe atom/ abbrev.				
		sample	mg.	%	sample	mg.	%	dpm/kg	dpm/kgFe	atom/ abbrev.		
ANTARCTIC CHONDRITES:												
ALH77299	H3 -19	116	4.58±.25	3.41±.26	13	31	17.7±1.1	42.4±3.7	317	1.9	15	299
Y7301	H5 -75	115	3.93±.22	2.83±.14	.04				102			
Y74001	H5 -71	118	5.31±.30	3.78±.21	.25	548W	18.9±.7		351	2.1	29	01
Y74117	L6 -73	145	4.64±.19			108	16.4±.9	47.7±1.8	240	2.0	22	117
Y74155	H4 -88	362	5.08±.08			101	17.0±.8	52.9±1.9	257	2.05	26	155
Y74156	H4 -73	439	4.56±.14			115	17.8±1.0	53.0±2.1	257	2.05	26	155
Y74192	H6 -78	169	5.51±.26	3.56±.19	.19	280	27.3±0.9		578	2.4	78	192
Y74364	H4 -74	119	6.26±.25		.19				407	2.0	25	
Y74418	H6 -71	112	6.06±.27		.06				275	2.1	31	418
Y74455	L6 -62	235	5.94±.27	3.4 ±.2	.15	106	18.3±1.1	49±2	278	1.8	13	455
Y74663	L6 -61	129	5.55±.27	3.0 ±.2	.03	114	18.1±1.1	39±1	255	1.75	12	663
Y75029	H3 -51	73		4.17±.27	.32				237	2.1	30	29
NON-ANTARCTIC CHONDRITES:												
BARWISE	H5 H30.12	473	6.26±.33			433	14.6±0.8		248	2.2	47	
BEARDSLEY	H5	320	4.35±.15						306	2.5	70	BDL
BRUDERHEIM	L6 16-2	483	4.71±.33	5.48±.80	1	1296	25.4±1.7		530	2.25	50	
	B156	154	5.07±.28	3.34±.38	1.3	477	23.1±1.0	56.2±4	491	2.22	45	
ETTER	L6 H47.260	430	2.36±.13	1.88±.15	.46	119	16.6±.7		(158)	2.6	75	ET
KESEN	H4	80	6.1 ±.4						347	2.2	47	KS
LA CRIOLLA	L6	1985	227	2.26±.12	.01	107	20.0±.7	63±2		2.5	63	
NEW CONCORD	L6	1860	178	2.70±.12	.12	100	17.0±.6	69±3	(174)	2.35	55	NC
NUEVO MERCUR.	H5	1978	402	2.78±.13	.20	120	22.4±1.4	64 ±4	(506)	2.3	63	NM
PEACE RIVER	L6 NO.4	422	5.01±.42	6.00±.53	.7	542	21.2±.8	55.9±4.1	400	2.1	30	
		344	4.99±.23	4.48±.62	.08							
TSAREV-	L5	87	0.58±.14	0.50±.05	.12	107	5.21±.46	15.9±0.7		2.8	46	TSAR

W: whole rock data. * Data compilation by K.Nishiizumi, Nucl. Tracks Rad. Meas., 13, 209-273(1987). Sources: ** L.SCHULTZ, + T.KIRSTEN, + F.BEGEMANN, + G.TU and Z.OUYANG, " M.HARRISON, & H.WANKE. In Fig.1 other data are also plotted: Admire(ADM); Y75108(108). Those of Lunar Core(in g/cm²) and Derrick Peak 78 series(DRP) are from Nishiizumi et al(1984;1987).

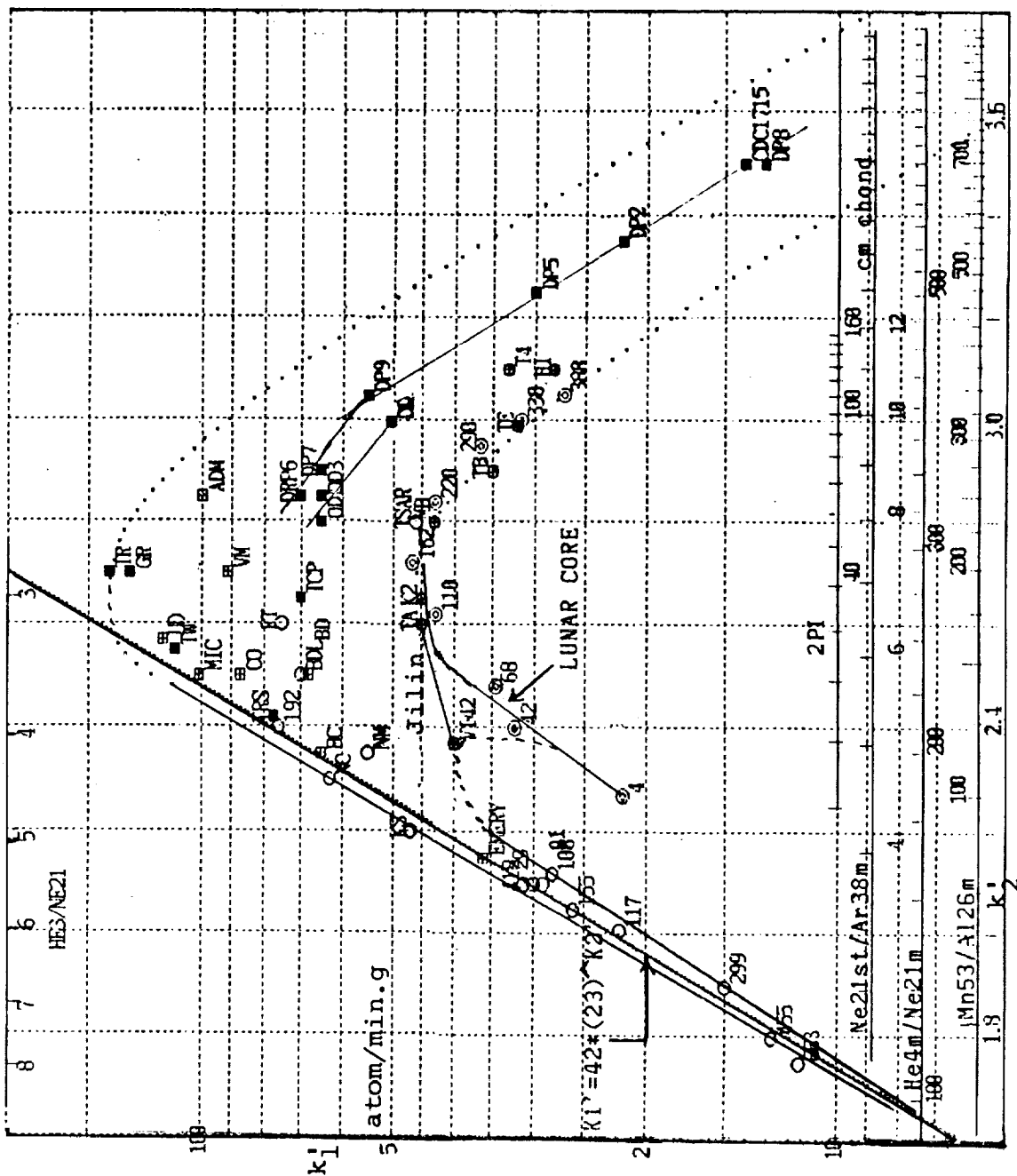


Fig.1 RELATION BETWEEN k_1' , INTENSITY PARAMETER, AND k_2' , SHIELDING PARAMETER

Abbreviations for samples can be referred to the Table 1. Plots for chondrites are in circle, stony irons in square with cross, irons in closed square, lunar core in double circle, Jilin data in circle with cross, respectively.

Approximate formula for small meteorites is $k_1' = 42 \cdot (23)^{k_2'}$ atom/min.kg.

520-90 321838

P-2

DEPTH PROFILES OF RADIONUCLIDE PRODUCTION IN SOLIDS WITH 2π GEOMETRY
 K. Nishiizumi, R. C. Reedy*, and J. R. Arnold
 Department of Chemistry, B-017, University of California, San Diego, La Jolla, CA92093
 *Earth and Space Science Division, MS-D438, Los Alamos National Lab, Los Alamos, NM87545

The lunar surface presents, in many ways, an ideal case for cosmogenic nuclide study. The surface of the moon has been bombarded by both SCR (solar cosmic rays) and GCR (galactic cosmic rays) for a few million to a few hundred million years at the same geometry and the same location in the solar system (1 A.U.). The cosmic ray bombardment geometry for lunar samples can be determined on a mm scale, a precision which can't be obtained with meteorites. Complications are caused by surface gardening and by erosion by micrometeorite impact, which change the static production profile. However, the knowledge of these effects, which can be gained from lunar studies, can be applied to model asteroid regolith and cometary surfaces. The moon is a limiting case for cosmogenic nuclide production since its radius is effectively infinity and the samples therefore experience a 2π geometry to cosmic ray bombardment. However, as we obtain a more precise understanding of the 2π bombardment case, we also learn more about bombardment in meteorites since the lunar model calculations can be extended to them fairly easily. The 2π lunar case can also apply to model development for bombardment at the surface of the earth, except for the importance of muon reactions in the earth's atmosphere in contrast to the importance of pion reactions for a solid body.

SCR: Production by solar particles (SCR) is confined to bodies without a significant atmosphere or magnetic field, and to a thin surface layer ($< \text{few g/cm}^2$). It is visible in all lunar surface material because of the absence of ablation. Other than in lunar material, SCR produced nuclides have been observed only in some cosmic spherules and in a very few meteorites. The Reedy-Arnold production model [1] fits the experimental data very well in those cases where all proton cross section data are available. Presently there is a lack of low energy (below 100 MeV) proton cross section data for production of ^{10}Be , ^{14}C , and ^{36}Cl . The knowledge of these low energy proton excitation functions is needed to pin down the SCR history during the last few million years. Figure 1 shows ^{53}Mn and ^{10}Be profiles in rock 68815 [2,3]. The depths of the samples measured in this study are the most carefully determined to date. The SCR production in lunar soil has not been emphasized in past discussions except for studies of gardening [4], but its integral value is useful for SCR studies of production in rocks and meteorites since the erosion problem is eliminated (but replaced by the gardening problem).

GCR: Production by galactic cosmic rays (GCR) extends to a depth of meters in solid matter. The most extensive studies to determine GCR production profiles were those of the Apollo 15 long core (up to 400 g/cm^2). Figure 2 shows ^{10}Be , ^{26}Al , ^{36}Cl , and ^{53}Mn depth profiles measured for this core [5,6]. These data represent the test for all production models, as well as the constant-flux model that underlies them. The Reedy-Arnold model fits the measured profiles very well except that a normalization is required to adjust the absolute activity levels due (we believe) to the lack of neutron cross sections. There is also a small discrepancy for the ^{36}Cl profile due to the exclusion of the $^{35}\text{Cl}(n,\gamma)$ reaction in the Reedy-Arnold model. For a nuclide produced only by neutron capture (such as ^{60}Co), the depth profile would look very different, with little production near the surface [7]. Mixing in the lunar regolith is not rapid enough to affect the profile of these radionuclides except close to the surface ($\sim 10 \text{ g/cm}^2$). The exposure time of lunar soil is also long enough to saturate all cosmogenic radionuclides (with the hypothetical exception of ^{40}K in metal or anorthite).

Each lunar core has a different chemical composition. The production rates from different target elements can be obtained by comparing several core samples with different chemical

RADIONUCLIDE PRODUCTION IN SOLIDS WITH 2π GEOMETRY: Nishiizumi, K. et al.

compositions if the samples come from the same shielding depth, because the exposure geometry has been precisely measured for these lunar samples.

Only lunar samples preserve a record of the details of the SCR history and provide accurate determination of 2π GCR production profiles from 0 to 400 g/cm^2 . Measurements of ^{14}C , ^{41}Ca , and ^{129}I in long lunar cores are in progress. We need low energy proton and neutron cross section data to improve the model. Profile measurements on a longer core (6-8m) would extend the data into a region not yet investigated and provide a check on the model calculations. Obtaining such a sample should be one goal of a future mission.

One limitation of all studies on *in situ* bombardment effects in extraterrestrial matter is that the measurements are "integral", that is, that they reflect the entire history of the bombardment for each sample under study. Given the slow evolution of lunar (or meteoritic) surfaces, effects are averaged over long periods, in contrast for example to ^{14}C studies of tree rings on earth. There is at least one possible way to approach a differential record more closely. This is to collect a core at the bottom of a narrow rille or cleft into which material is steadily being transported by gardening, but which is more or less shielded from further bombardment and material loss by impact. A returned core from such a "sediment" would be a fascinating object of study.

REFERENCES

- [1] Reedy, R. C. and Arnold, J. R. (1972) *J. Geophys. Res.*, **77**, 537-555.
- [2] Kohl, C. P., Murrell, M. T., Russ, G. P. III and Arnold, J. R. (1978) *Proc. Lunar Planet. Sci. Conf. 9th*, 2299-2310.
- [3] Nishiizumi, K., Imamura, M., Kohl, C. P., Nagai, H., Kobayashi, K., Yoshida, K., Yamashita, H., Reedy, R. C., Honda, M. and Arnold, J. R. (1988) *Proc. Lunar Planet. Sci. Conf. 18th*, 79-85.
- [4] Langevin, Y., Arnold, J. R. and Nishiizumi, K. (1982) *J. Geophys. Res.*, **87**, 6681-6691.
- [5] Nishiizumi, K., Elmore, D., Ma, X. Z. and Arnold, J. R. (1984) *Earth Planet. Sci. Lett.*, **70**, 157-163
- [6] Nishiizumi, K., Klein, J., Middleton, R. and Arnold, J. R. (1984) *Earth Planet. Sci. Lett.*, **70**, 164-168.
- [7] Wahlen, M., Finkel, R. C., Imamura, M., Kohl, C. P. and Arnold, J. R. (1973) *Earth Planet. Sci. Lett.*, **19**, 315-320.

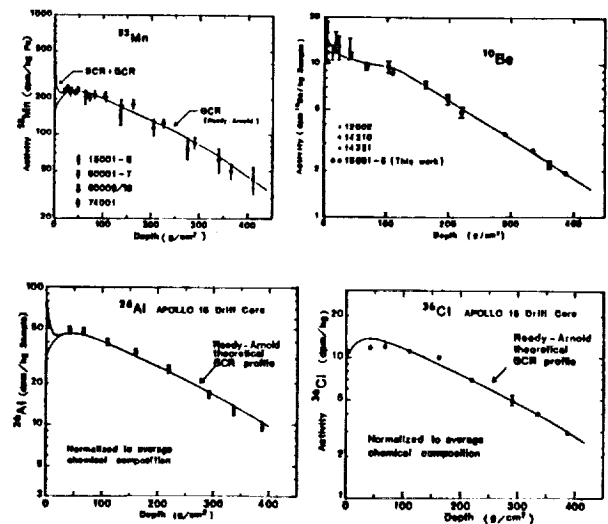
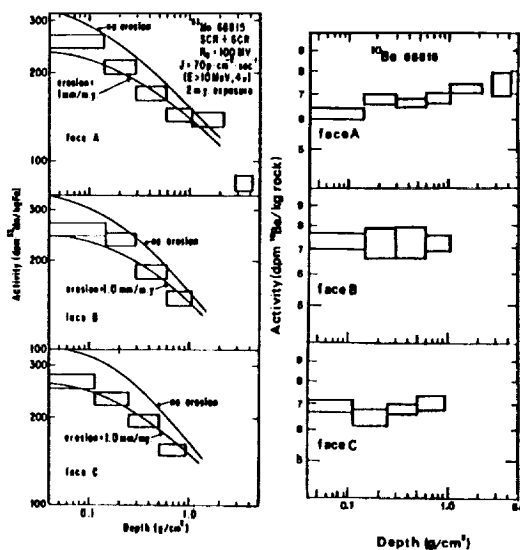


Fig. 1. ^{53}Mn and ^{10}Be depth profiles in rock 68815 [2,3].

Fig. 2. ^{53}Mn , ^{10}Be , ^{26}Al , and ^{36}Cl depth profiles in 15001-7 [5, 6]

521-90
321039
p-2

COSMOGENIC-NUCLIDE PRODUCTION RATES CALCULATED USING PARTICLE FLUXES AND CROSS SECTIONS*; Robert C. Reedy, Earth and Space Sciences Division, Mail Stop D438, Los Alamos National Laboratory, Los Alamos, NM 87545.

There have been several approaches used to predict the production rates of cosmic-ray-produced nuclides in extraterrestrial matter. The method reviewed here uses fluxes of cosmic-ray particles and cross sections for nuclear reactions. It is used both for particles in or made by the galactic cosmic rays (GCR) as well as for solar-cosmic-ray (SCR) particles. The use of derived energy spectra for the cosmic rays coupled with cross sections was first well developed by Arnold, Honda, and Lal (1) in 1961 for iron meteorites. The model was extended to the Moon in 1972 by Reedy and Arnold (2) and later to stony meteorites (e.g., 3). It is also the basic approach used to predict cosmogenic nuclide production rates in small particles in space (e.g., 4) and for production by the protons and alpha particles in the solar cosmic rays (e.g., 2).

The basic model. The production rate for a cosmogenic nuclide at depth d in an object of radius R , $P(R, d)$, can be calculated as the sums over target elements, i , and cosmic-ray particles, j , and the integral over energy, E , of

$$P(R, d) = \sum_i N_i \sum_j \int \sigma_{ij}(E) F_j(E, R, d) dE \quad (1)$$

where N_i is the abundance of the i th element, $\sigma_{ij}(E)$ is the cross section as a function of energy for making the nuclide from element i with particle j , and $F_j(E, R, d)$ is the flux of particle j with energy E at depth d in an object of radius R . Both the GCR and SCR consist mainly of protons, some α particles and $\sim 1\%$ of heavier nuclei. For SCR particles, which mainly have energies of ~ 10 - 100 MeV, only the primary particles are considered (2). For the high-energy (~ 1 - 10 GeV) GCR particles, many secondary particles can be made, such as neutrons and pions, and all of these primary and secondary particles should be considered in Eqn. (1). Uses of this type of model will be briefly reviewed in order of both greater particle energy and increasing target size. The main concerns in this model are getting the two key terms in Eqn. (1), the particle fluxes, $F_j(E, R, d)$, and the cross sections, $\sigma_{ij}(E)$, for all important energies.

Solar Cosmic Rays. Most of the relatively-low energy SCR particles are stopped in matter by ionization energy losses (2). The few SCR particles that react tend to produce few secondary particles; most SCR calculations ignore these secondaries. As α particles constitute only $\sim 2\%$ of the SCR, they usually are ignored and only the protons are considered. The main exception is ^{59}Ni in the Moon, which is made almost entirely by solar α particles via the $^{56}\text{Fe}(\alpha, n)^{59}\text{Ni}$ reaction (5).

The fluxes of solar protons and α particles as a function of depth can be calculated quite well using known relations for ionization energy loss, and there is little disagreement among authors on the SCR-particle fluxes determined as a function of depth (e.g., 2,6). The main problem has been the lack of measured excitation functions, cross sections as a function of energy, for the major reactions. As the SCR-particle flux decreases rapidly with increasing energy, most reactions are induced by particles with energies slightly above the reaction thresholds. For many solar-proton-produced nuclides, cross sections, especially near thresholds, need to be measured (7).

Small Objects in Space. In objects that are much smaller than the interactions lengths of cosmic-ray particles (~ 100 g/cm²), few secondary particles are produced and those that are produced usually escape to space. Thus only the primary cosmic-ray particles need to be considered for cosmic dust and spherules and other such small objects in space (e.g., 4). Near the Sun, SCR particles are important sources of cosmogenic nuclides in these small objects, and, as above, cross sections are often the limiting factor in calculating production rates. For the high-energy GCR particles, the cross sections for protons are usually known but there are few for the $\sim 13\%$ of α particles in the GCR (cf. 8). The energy spectra for GCR particles are fairly well measured in the solar system but are very poorly known in interstellar space (4,8).

Galactic Cosmic Rays. The versions of this model usually used for GCR particles in meteorites (1,3) and the Moon (2) don't consider these cosmic-ray particles separately in Eqn. (1), but combines them, using

$$P(R, d) = \sum_i N_i \int \sigma_i(E) F(E, R, d) dE \quad (2)$$

where the flux term $F(E, R, d)$ now includes all types of particles. The justification for this inclusion of all primary and secondary particles into one term is that primary and secondary particles at higher energies ($\gtrsim 100$ MeV) tend to have similar cross sections while most particles with $E \lesssim 100$ MeV are neutrons (1,2). For the high energies, cross sections for proton-induced reactions are usually used and assumed to apply to other energetic species (e.g., primary α particles and secondary neutrons and pions) with the same energies. The scarcity of high-energy cross sections for these other particles has been a major factor in adopting this assumption. Thus, in a sense, the use of Eqn. (2) is somewhat like using Eqn. (1) with only two types of particles: lower-energy neutrons and higher-energy strongly-interacting particles. Because of the great complexity in the cascade of particles produced by high-energy cosmic rays in large objects, such as the large variety of secondary particles and the huge range of energies, assumptions like those above have been a feature of almost all models for predicting rates of GCR-produced nuclides.

Getting both the flux and cross-section terms in Eqn. (2) have been difficult. For the fluxes of GCR particles in iron meteorites, Arnold *et al.* (1) mainly used measurements of GCR particles in the Earth's atmosphere and only considered three fluxes that varied in shape above 100 MeV. In extending this model to the Moon, Reedy and Arnold (2) made the flux term a continuous function of depth and had the flux shapes both below and above 100 MeV vary as a function of a "shielding" parameter. When the Reedy-Arnold model was shown to work reasonably well for the Moon, it was modified for stony meteorites by getting flux models that fit cosmogenic nuclide data for several meteorites, such as St. Severin (9). This model was later generalized to spherical meteoroids of any radius (3), although the flux models and calculated production rates have often been poor, especially for fairly small ($R \lesssim 20$ g/cm²) and large ($R \gtrsim 150$ g/cm²) objects.

There also is often a lack of cross sections to use in GCR calculations, usually for neutron-induced reactions. This lack is especially true for the higher neutron energies, as very few neutron cross sections have been measured above 20 MeV. Often measured cross sections for proton-induced reactions are assumed for neutrons. There is good evidence that this assumption of equality for proton-induced and neutron-induced reactions is not valid for many target/product pairs. In some cases, the reactions for the two types of incident particles are known to be different, such as $^{24}\text{Mg}(n,\alpha)^{21}\text{Ne}$ versus $^{24}\text{Mg}(p,n3p)^{21}\text{Ne}$ (9).

Discussion. One virtue of this flux/cross-section approach to calculating cosmogenic-nuclide production rates is its flexibility. If one wants to calculate rates for a new nuclide, one only needs excitation functions for making that product and can use the established particle fluxes. It also can be used for simulation experiments if particle fluxes in the irradiated object are measured or calculated (e.g., 10). For SCR particles and/or small objects, it is the main approach for calculating production rates. It has worked very well for the top ~ 300 g/cm² of the Moon, although absolute rates calculated with the model and the presently adopted excitation functions often need to be normalized by factors of as much as ~ 40 %.

The model's limitations are the need for both good fluxes and excitation functions. The fluxes for interstellar GCR particles are very poorly known (4,8). The flux models for meteorites are poor, especially for small and large objects, and only have been developed for spherical meteoroids (3). Applications to SCR-produced nuclides has been limited by the lack of good excitation functions (Re+89). For GCR calculations, a serious problem is the lack of cross sections for neutron-induced reactions.

References: (1) Arnold J. R. *et al.* (1961) *J. Geophys. Res.* **66**, 3519. (2) Reedy R. C. and Arnold J. R. (1972) *J. Geophys. Res.* **77**, 537. (3) Reedy R. C. (1985) *PLPSC 15th, J. Geophys. Res.* **90**, C722. (4) Reedy R. C. (1987) *PLPSC 17th, J. Geophys. Res.* **92**, E697. (5) Lanzerotti L. J. *et al.* (1973) *Science* **179**, 1232. (6) Michel R. and Brinkmann G. (1980) *J. Radioanal. Chem.* **59**, 467. (7) Reedy R. C. *et al.* (1989) *Lunar Planet. Sci.* **XX**, 890. (8) Reedy R. C. (1989) *Lunar Planet. Sci.* **XX**, 888. (9) Reedy R. C. *et al.* (1979) *Earth Planet. Sci. Lett.* **44**, 341. (10) Michel R. *et al.* (1986) *Nucl. Instrum. & Methods* **B16**, 61. * Work supported by NASA and done under the auspices of the US DOE.

522-93
321040
R 2

PRODUCTION RATES OF COSMOGENIC PLANETARY GAMMA RAYS.*

R. C. Reedy¹ and P. A. J. Englert.² (1) Earth and Space Sciences Division, Mail Stop D438, Los Alamos National Laboratory, Los Alamos, NM 87545; (2) Department of Chemistry, San Jose State University, San Jose, CA 95192-0101.

Planetary gamma rays are energetic ($E \sim 0.2\text{--}10$ MeV) photons that can be used to determine the elemental composition of a planet's surface (1,2). The γ rays are made during the de-excitation of atomic nuclei, and their energies usually indicate uniquely which nucleus and excited level produced them. Such γ rays were used to determine the abundances of several elements in the Moon by gamma-ray spectrometers on Apollos 15 and 16 (e.g., 3,4). There are four main sources of the γ rays used to determine the elemental compositions of planets: (1) natural decay of ^{40}K , thorium, uranium, and their daughters; (2) capture of thermal neutrons, such as $^{56}\text{Fe}(n,\gamma)$; (3) nonelastic scatter of low-energy ($E \sim 0.4\text{--}15$ MeV) neutrons, e.g., $^{56}\text{Fe}(n,n\gamma)^{56}\text{Fe}$; and (4) reactions by higher-energy ($E \gtrsim 15$ MeV) particles, such as $^{28}\text{Si}(p,p\alpha\gamma)^{24}\text{Mg}$. The latter three sources use particles in or made by the galactic cosmic rays. Gamma-ray spectroscopy can be used for planets with no (e.g., Moon) or very thin (e.g., Mars) atmospheres and also for smaller objects like asteroids and comets. Planetary gamma-ray spectroscopy can be used to determine a wide range of elements, ranging from most major elements, some important minor elements (such as the radioactive ones like uranium), and certain volatile elements, such as hydrogen (5) and carbon (6). A gamma-ray spectrometer is scheduled to be part of the Mars Observer mission (7).

In many ways, the determination of production rates of the planetary γ rays made by cosmic rays is similar to determining production rates of cosmogenic nuclides by galactic-cosmic-ray (GCR) particles. Sometimes, the same reaction can make both γ rays and a cosmogenic nuclide, such as the $^{56}\text{Fe}(n,2n\gamma)^{55}\text{Fe}$ or $^{35}\text{Cl}(n,\gamma)^{36}\text{Cl}$ reactions. However, there are some differences, such as most γ rays tending to be made by much lower-energy ($E \lesssim 15$ MeV) reactions than those making most cosmogenic nuclides. Two main approaches have been used in helping to determine production rates of cosmogenic γ rays: simulation experiments and calculations using particle fluxes and cross sections.

Fluxes and Cross Sections. If the flux of cosmic-ray particles in a planet's surface is known as a function of depth and particle energy, then the rate that a γ ray is produced can be calculated by integrating over energy the product of flux times cross section (1,2). The distributions of cosmic-ray particles from thermal to GeV energies are well known in the Moon, but not for other planets. On Mars, the presence of a thin atmosphere and possibly high concentrations of volatiles containing hydrogen and carbon cause the cosmic-ray-particle flux to deviate significantly from a lunar-like one (e.g., 6-8). An additional complication for large planets is that thermal neutrons are gravitationally bound and thus thermal neutrons that escape can return to the surface (9). Measurements of the neutrons that escape from a planet will help in mapping various elements such as hydrogen and carbon (8,9) and will provide information on particle fluxes and nuclear interactions occurring in the planet's surface. When samples are returned from Mars or a comet, a knowledge of these cosmic-ray-particle fluxes will be needed to help in the interpretation of the cosmogenic nuclides observed in these samples.

Many γ -ray-producing cross sections have been measured, especially inelastic-scattering reactions induced by neutrons having energies below ~ 15 MeV, but many cross sections for reactions of interest to planetary gamma-ray spectroscopy have not been measured (e.g., 2,7). Reactors are used in measuring yields for the production of capture γ rays. Some $(n,x\gamma)$ and $(p,x\gamma)$ cross sections as a function of energy are being measured. These irradiations often can be done at the same accelerators as used to determine cross sections for the production of cosmogenic nuclides. One advantage of measuring prompt γ rays instead of activation products is that time-of-flight techniques can be used to identify the energy of the neutron inducing the reaction or to reduce backgrounds in the γ -ray detector.

Simulation Irradiations. Cosmogenic nuclides have often been measured in thick targets irradiated by energetic particles. This approach simulates the bombardment of the Moon or meteorites by the GCR, and some of our earlier understanding of the distribution of cosmogenic nuclides came from such irradiations. Similarly, γ rays can also be measured from targets irradiated by energetic

particles. This is also a good simulation of what happens when a gamma-ray spectrometer is operated near a planet. The incident projectiles used in such γ -ray simulations have ranged from 6-GeV protons (10) to neutrons with energies of as much as 78 MeV (11) down to 0-14 MeV (12). These simulations have helped to confirm theoretically calculated γ -ray fluxes, such as those from iron by nonelastic (10) and thermal (12) reactions. More simulation irradiations are planned. Cosmogenic nuclides measured in samples from inside these targets would help to confirm how well natural conditions have been simulated (e.g., 13).

Simulation experiments have been good help in planning for planetary gamma-ray spectrometer missions. The γ -ray spectra from thick-target irradiations should be similar to those observed from a planet. Many features in these spectra, such as γ -ray line widths or backgrounds, can be identified and studied. Most γ rays are emitted with energy spreads that are narrower than the few keV widths seen in pulse height spectra from high-resolution germanium detectors. Among the γ rays that have a broad spread of energies as emitted from planets are those from inelastic-scattering reactions with carbon (e.g., 12). Simulations showed that energetic neutrons escaping from the target produce relative broad background peaks as a result of inelastic-scattering reactions with nuclei in the germanium detector (10,12). However, on the whole, simulation experiments have confirmed that planetary gamma-ray spectroscopy should work well in determining the abundances of many elements in the top few tens of centimeters of a planet's surface.

Discussion. Planetary gamma rays are often made by reactions very similar to those that make cosmogenic nuclides. Results from the study of cosmogenic nuclides have helped in predicting γ -ray fluxes, as was the case for the Moon. Work on understanding and measuring γ rays from Mars and comets will help us to predict the production rates of cosmogenic nuclides in samples from these different and often volatile-rich objects. Similar models are used to calculate rates for making γ rays and cosmogenic nuclides, and similar irradiations are done to measure their production cross sections. Simulations experiments, like those that were valuable in predicting rates and profiles for cosmogenic nuclides, are now being used in planning for planetary gamma-ray spectroscopy missions. The overlap of the planetary-gamma-ray and the cosmogenic-nuclide communities has been, and will continue to be, beneficial to both.

References: (1) Reedy R. C. *et al.* (1973) *J. Geophys. Res.* **78**, 5847. (2) Reedy, R. C. (1978) *Proc. Lunar Planet. Sci. Conf. 9th*, p. 2961. (3) Bielefeld M. J. *et al.* (1976) *Proc. Lunar Sci. Conf. 7th*, p. 2661. (4) Etchegaray-Ramirez M. I. *et al.* (1983) *PLPSC 13th, J. Geophys. Res.* **88**, A529. (5) Haines E. L. and Metzger A. E. (1984) *Nucl. Instrum. & Methods* **226**, 509. (6) Evans L. G. and Squyres S. W. (1987) *J. Geophys. Res.* **92**, 9153. (7) Reedy R. C. (1988) in *Nuclear Spectroscopy of Astrophysical sources*, AIP Conf. Proc. 170, p. 203. (8) Drake D. M. *et al.* (1988) *J. Geophys. Res.* **93**, 6353. (9) Feldman W. C. *et al.* (1989) *J. Geophys. Res.* **94**, 513. (10) Metzger A. E. *et al.* (1986) *PLPSC 16th, J. Geophys. Res.* **91**, D495. (11) Englert P. *et al.* (1987) *J. Radioanal. Nucl. Chem.* **112**, 11. (12) Brückner J. *et al.* (1987) *PLPSC 17th, J. Geophys. Res.* **92**, E603. (13) Englert P. *et al.* (1987) *Nucl. Instrum. & Methods* **A262**, 496.

* Research supported by NASA. Los Alamos work done under the auspices of US DOE.

523-93
321041
P2

CROSS SECTIONS FOR GALACTIC-COSMIC-RAY-PRODUCED NUCLIDES.*

R. C. Reedy,¹ K. Nishiizumi,² and J. R. Arnold.² (1) Earth and Space Sciences Division, Mail Stop D438, Los Alamos National Laboratory, Los Alamos, NM 87545; (2) Department of Chemistry, B-017, University of California, San Diego, La Jolla, CA 92093-0317.

One of the most commonly used approaches for predicting the production rates of nuclides made by galactic-cosmic-ray (GCR) particles in extraterrestrial matter (1) is one that uses fluxes of cosmic-ray particles and cross sections for nuclear reactions. This use of GCR-particle fluxes coupled with cross sections was first developed by Arnold, Honda, and Lal (2) in 1961 for iron meteorites, then was extended to the Moon in 1972 by Reedy and Arnold (3) and later to stony meteorites (e.g., 4). This family of models has worked well, but one of their limitations is the lack of good measured cross sections for the production of many nuclides. This lack of cross sections for GCR-induced reactions is also a problem for the approach of using theoretically calculated particle fluxes in studies of artificially or naturally irradiated targets (e.g., 5). Needed cross sections for solar-proton calculations were presented in (6).

In this approach (2,3), the production rate for GCR particles making a cosmogenic nuclide at depth d in an object of radius R , $P(R, d)$, is calculated as the sum over target elements, i , and the integral over energy, E , of

$$P(R, d) = \sum_i N_i \int \sigma_i(E) F(E, R, d) dE \quad (1)$$

where N_i is the abundance of the i th element, $\sigma_i(E)$ is the cross section as a function of energy for making the nuclide from element i , and $F(E, R, d)$ is the flux of GCR particles with energy E at depth d in an object of radius R . The primary particles in the GCR consist mainly of protons, $\sim 13\%$ α particles, and $\sim 1\%$ of heavier nuclei (7). From the high-energy (~ 1 – 10 GeV) GCR particles, many secondary particles can be made, such as neutrons and pions. All of these primary and secondary particles should be considered in the flux and cross-section terms of Eqn. (1). The main concerns in applying this model have been getting the two key terms in Eqn. (1), the GCR particle fluxes, $F(E, R, d)$, and the cross sections, $\sigma_i(E)$, for all important energies. This type of model and some weaknesses in the flux models are reviewed in another paper presented at this Workshop (8). Below is discussed the need for cross sections for use in calculating rates for the GCR production of cosmogenic nuclides.

At high energies ($E \gtrsim 100$ MeV), cross sections for proton-induced reactions are usually used and assumed to apply to other energetic species (e.g., primary α particles and secondary neutrons and pions) with the same energies, mainly because of the scarcity of high-energy cross sections for these other particles. At energies below a few hundred MeV, cross sections for neutron-induced reactions are used in Eqn. (1), as neutrons are the dominant particle at such energies because lower-energy charged particles are fairly rapidly stopped by ionization energy losses (3). The energy above which neutrons cease being over $\approx 50\%$ of all particles depends on the depth and the target's size but is ~ 200 – 400 MeV (2,9) for deep in large objects.

In the discussions below, it is usually assumed that existing measurements are correct or that the measurement uncertainties are not too large. However, a few old measurements may be incorrect, for example the beam flux was poorly monitored. In some cases, the product of interest might not have been quantitatively separated from the target, as was possibly the case for the $^{16}\text{O}(p,3p)^{14}\text{C}$ cross sections of (10). Sometimes two measurements of a cross section differ by an amount much greater than the quoted errors, for example for ^{26}Al from silicon (cf., 1) or ^{10}Be from oxygen at 135 MeV (cf., 11). Thus it is good to have independent measurements of important cross sections, or additional ones if there are disagreements among existing results.

High-Energy Cross sections. At energies above a few hundred MeV, there usually are adequate cross sections for most cosmogenic nuclides. Except for a few proton energies (e.g., ~ 200 – 600 MeV or $\gtrsim 3$ GeV), there are usually several accelerators available for such cross-section measurements. Cross sections for proton-induced reactions usually are used at such energies, and there are few indications that adopting such proton cross sections is a poor assumption, especially at energies $\gtrsim 1$ GeV. One case where proton-induced cross sections are very poor for energies above 100 MeV is for ^{10}Be from oxygen, for which neutron-induced cross sections appear to be much higher than

NEEDED GCR CROSS SECTIONS

Reedy R. C. *et al.*

proton-induced ones up to energies of ~ 1 GeV (11). Another case might be ^{14}C from oxygen, another example of a very neutron-rich product.

Usually cross sections at high energies are missing for cosmogenic nuclides that are rarely studied. Often this is a case for nuclides for which new measurement techniques have been fairly recently developed. Recently, the use of accelerator mass spectrometry (AMS) to measure long-lived radionuclides has often created the need for cross section measurements. This need is especially true for radionuclides that recently or are just "coming on line" for routine AMS measurements, such as ^{36}Cl , ^{41}Ca and ^{129}I . Often there are few cross sections for minor target elements, such as nickel for calculations involving nuclides made in iron meteorites or metallic phases of chondrites. Sometimes there is a large gap between energies for measured high energy cross sections. While cross sections at high (≥ 100 MeV) energies almost always behave smoothly with energy, interpolations across large energy gaps can yield relatively poor cross sections, especially if the cross section was still increasing at the lower energy.

Low-Energy (Neutron) Cross sections. There is usually a lack of cross sections for neutron-induced reactions. This lack is especially true for the higher neutron energies, as very few neutron cross sections have been measured above 20 MeV. Often measured cross sections for proton-induced reactions are assumed for neutrons. There is good evidence that this assumption of equality for proton-induced and neutron-induced reactions is not valid for many target/product pairs. In some cases, the reactions for the two types of incident particles are known to be different, such as $^{24}\text{Mg}(n,\alpha)^{21}\text{Ne}$ versus $^{24}\text{Mg}(p,n3p)^{21}\text{Ne}$ (12), or are strongly believed to be different, such as for ^{14}C (3) or ^{10}Be (11) from oxygen.

There are only a very few cases where there are adequate cross sections for neutron-induced reactions. These are usually where production occurs at low energies ($E_n \lesssim 20$ MeV) and for cosmogenic nuclides with relative short half-lives. Cases where there are a number of neutron cross sections include $^{40}\text{Ca}(n,\alpha)^{37}\text{Ar}$, $^{39}\text{K}(n,p)^{39}\text{Ar}$, and $^{23}\text{Na}(n,2n)^{22}\text{Na}$. Usually such neutron cross sections can be found in data compilations like (13), but not always, such as the $\text{Mg}(n,\alpha)\text{Ne}$ measurements of (12). Even in these cases it would be good to have some additional cross sections for neutron energies ≥ 15 –20 MeV. The list of needed cross sections for neutron production of cosmogenic nuclides would be long. The best approach here would be to first concentrate on the commonly studied product nuclides, such as ^{26}Al and ^{21}Ne .

The major problem in getting such neutron-induced cross sections is locating good sources of energetic neutrons. Two approaches, using mono-energetic neutrons or sources with a continuum of neutron energies, should be used. Below ≈ 20 MeV, monoenergetic neutrons often are made by reactions involving deuterons and tritons, but when neutrons with $E \geq 20$ MeV are made by such reactions there are also lower-energy neutrons made by break-up reactions. Other reactions, such as $^7\text{Li}(p,n)^7\text{Be}$, can be used to produce neutrons that are quasi-monoenergetic in that most neutrons occur at the highest neutron energy. Above 20 MeV, it is usually hard to get intense mono-energetic neutron sources. Thus spallation or other reactions are used to get "white" neutrons with a broad continuum of energies. Such spallation sources usually produce high intensities of neutrons. However, some mono-energetic cross-section measurements are needed to get cross sections for monitor reactions or a few known cross sections for the cosmogenic nuclides of interest prior to unfolding the measurements made using "white" sources.

References: (1) Reedy R. C. (1987) *Nucl. Instrum. & Methods* B29, 251. (2) Arnold J. R. *et al.* (1961) *J. Geophys. Res.* 66, 3519. (3) Reedy R. C. and Arnold J. R. (1972) *J. Geophys. Res.* 77, 537. (4) Reedy R. C. (1985) *PLPSC 15th, J. Geophys. Res.* 90, C722. (5) Michel R. *et al.* (1986) *Nucl. Instrum. & Methods* B16, 61. (6) Reedy R. C. *et al.* (1989) *Lunar Planet. Sci.* XX, 890. (7) Simpson J. A. (1983) *Annu. Rev. Nucl. Part. Sci.* 33, 323. (8) Reedy R. C. (1989) this Workshop. (9) Armstrong T. W. and Alsmiller, R.G. (1971) Oak Ridge National Laboratory report ORNL-TM-3267. (10) Tamers M. A. and Delibrias G. (1961) *C. R. Acad. Sci.* 253, 1202. (11) Tuniz C. *et al.* (1984) *Geochim. Cosmochim. Acta* 48, 1867. (12) Reedy R. C. *et al.* (1979) *Earth Planet. Sci. Lett.* 44, 341. (13) McLane V. *et al.* (1988) *Neutron Cross Sections, Volume 2, Neutron Cross Sections Curve* (San Diego: Academic Press). * Research supported by NASA. Los Alamos work done under the auspices of US DOE.

524-90
331042
p-5

**A new semi-empirical formula for spallation and
fragmentation reactions induced by high energy protons**

H. SAUVAGEON, CENBG, URA 451, 33170 Gradignan, France

I - General Principle of the calculation

Spallation and fragmentation are nuclear reactions which may be described in the well known framework of the two-step model. If the cascade-evaporation model rather well works for spallation, the question of fragmentation remains open and the nature of the second step is not well understood. However, one generally considers that the second step of fragmentation includes an evaporation-like mechanism. This fact has an important consequence : Isotopic distributions are very similar for spallation and for fragmentation. The universality of these isotopic distributions may also be called complete loss of memory. As noted by Hüfner (1), it suggests that some process is involved in the production of the isotopes where the system has to come to thermal equilibrium.

Roughly speaking, spallation rather leads to products relatively closed to the target while fragmentation concerns products with mass $A_p < 30$. So, an important parameter to distinguish these two mechanisms is the ratio $\Delta A/A_T$ where ΔA is the mass difference between target (A_T) and product (A_p).

$$\frac{\Delta A}{A_T} \lesssim 0.4 \text{ for spallation and } \frac{\Delta A}{A_T} \gtrsim 0.5 \text{ for fragmentation}$$

The principle of the calculation is very simple and includes two parts :

- The first part consists to fit experimental isotopic distributions at saturation energy which is reached when cross section

SPALLATION AND FRAGMENTATION REACTIONS: H. Sauvageon

remains constant (6 GeV for spallation and 3-10 GeV for fragmentation according to the product mass).

- The second part of the calculation consists to fit experimental excitation functions between 300 MeV and saturation energy.

With all the set of experimental cross sections available in literature, it is quite possible now to exhibit some clear and simple behaviours and so to get trustworthy fit characteristics.

II - Calculation at saturation energy

As mentioned above, we have to fit the evolution of experimental isotopic distributions of independtly formed spallation and fragmentation nuclides by a gaussian curve of which the expression is :

$$\sigma = \sigma_{\text{Max}} \exp [-(A - A_{\text{Max}})^2 / 2 S^2]$$

where σ is the cross section of the nuclide of mass A obtained in the interaction and index Max refers to the maximum of the distribution. S is related to the FWHM (Full-Width at Half-Maximum), ΔA , of the gaussian $S = \Delta A / 2.35$; σ_{max} is the cross section of the maximum of the isotopic distribution at saturation energy (fig. 1 and 2).

This calculation consequently requires the knowledge of three types of data :

- The position of the maximum of isotopic distributions in the N-Z plane (A_{Max});
- The evolution of the widths of the distributions (Γ);
- The evolution of the values of maximum cross sections (σ_{Max} versus A_T);

All these parameters have been obtained from experimental results (figs. 1 and 2) with a good precision and their variations give a coherent description of the main characteristics of the cross sections for spallation and fragmentation nuclides.

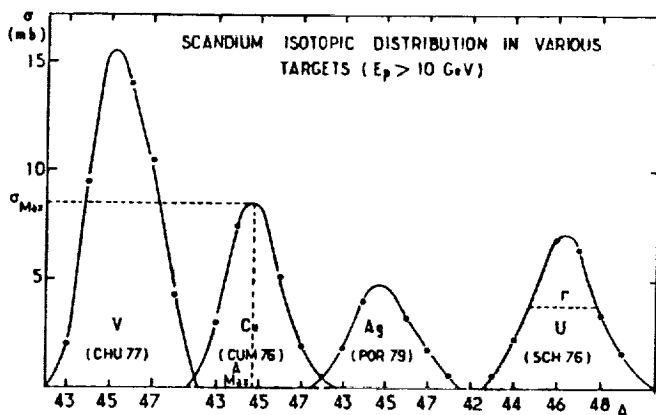


Figure 2
Evolution of scandium isotopic distributions with increasing target mass. Experimental points are represented by empty circles.

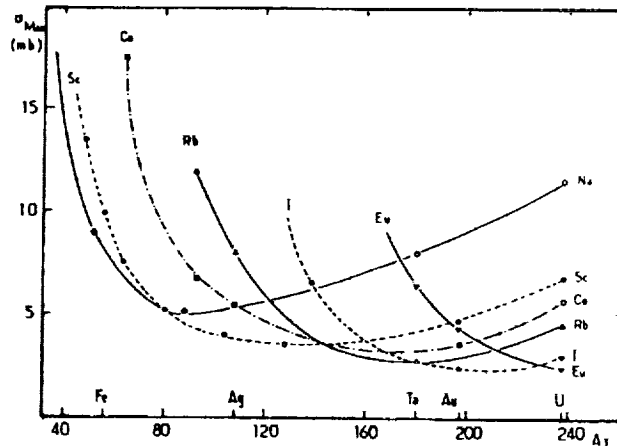


Figure 3
Variation versus target mass of the maximum of isotopic distribution for Na, Sc, Co, Rb, I and Eu nuclides. Various symbols (o, o, etc...) correspond to experimental points.

III - Excitation functions

1) Spallation

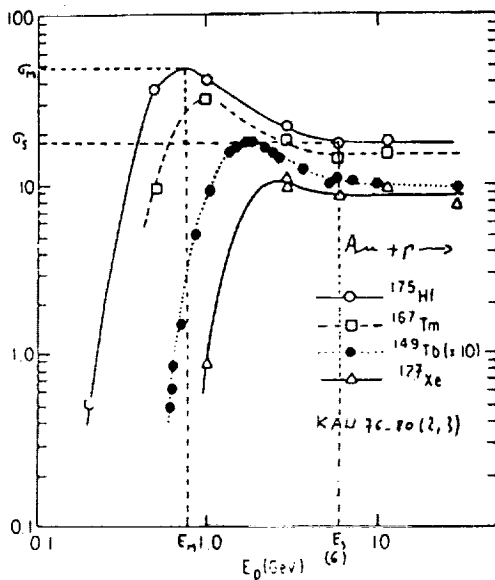


Figure 3: Spallation excitation functions of different products formed in gold.

Figure 3, from Kaufman et al (2,3) gives an excellent representation of spallation excitation functions.

From this figure, it is easy to get several interesting informations :

- the spallation excitation functions may be decomposed in 3 parts : an increasing part from threshold to E_M corresponding to the maximum cross section σ_M ; a decreasing part from E_M to E_s , saturation energy which is 6 GeV for spallation; at last, a constant part (saturation regime) above 6 GeV where cross section remains equal to σ_s .

- the value of E_M increases with ΔA , the mass difference between target and product.

- the value of the ratio σ_M/σ_s decreases when ΔA increases. It is quite easy to fit these two variations.

SPALLATION AND FRAGMENTATION REACTIONS: H. Sauvageon

In summary, the increasing part of the excitation function ($0,3 \text{ GeV} < E < E_M$) can be fitted by the expression :

$$\sigma(E) = \sigma_M \left(\frac{E}{E_M} \right)^\alpha \frac{E_M}{E} \quad \text{where } \sigma_M, E_M \text{ and } \alpha \text{ are functions of } Z_T \text{ and } \frac{\Delta A}{A_T}$$

The decreasing part of the excitation function ($E_M < E < 6 \text{ GeV}$) is given by :

$$\sigma(E) = \frac{6}{6 - E_M} \frac{E_M}{E} (\sigma_M - \sigma_S) \left(\frac{1}{E} - \frac{1}{6} \right) + \sigma_S$$

2) Fragmentation

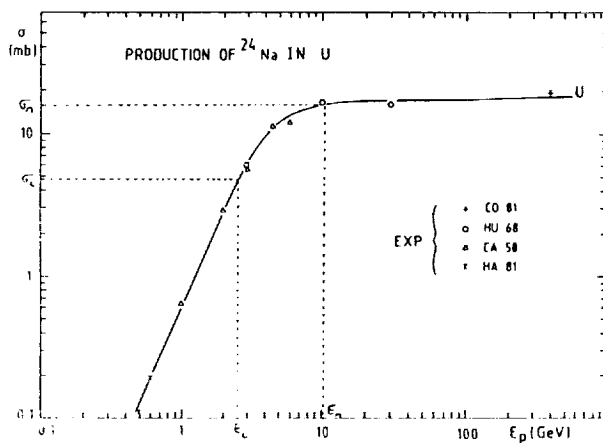


Figure 4 :
Production of ^{24}Na in
U target.

Figure 4 exhibits a characteristic fragmentation excitation function in which we distinguish three regions :
- An increasing (exponential) part from threshold to E_L corresponding to σ_L . This part can be fitted by the following expression :

$$\sigma(E) = \sigma_L \left(\frac{E}{E_L} \right)^\beta$$

where β is a function of Z_T , $\Delta A/A_T$ and $(N/Z)_p$

- A slightly increasing part of the excitation function from E_L to E_M corresponding to σ_M , the maximum of excitation function (which is also the value at saturation regime for fragmentation products)

$$\sigma(E) = K_1 + \frac{K_2}{E^\gamma} \quad \text{where } K_1, K_2 \text{ and } \gamma \text{ are functions of } Z_T, \Delta A/A_T \text{ and } (N/Z)_p$$

SPALLATION AND FRAGMENTATION REACTIONS: H. Sauvageon

IV - Comparison with experimental results and conclusion

In this paragraph, we are going to compare our calculation (curves) with experimental data (points). Figures 5 and 6 concern spallation products (in copper and gold) while figure 7 concerns fragmentation (^{24}Na produced in Au).

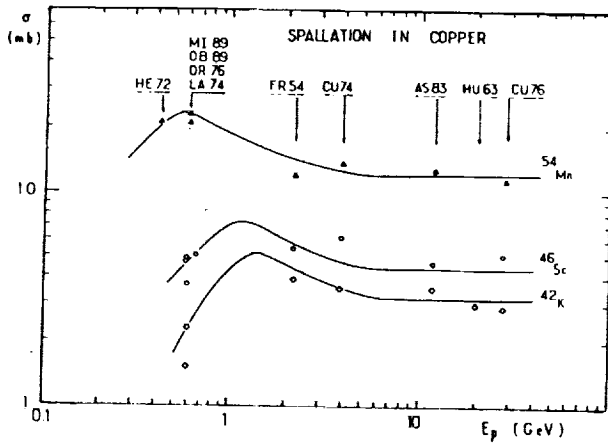


Figure 5; Spallation of copper
(—This work; Δ, \circ, \square experimental points).

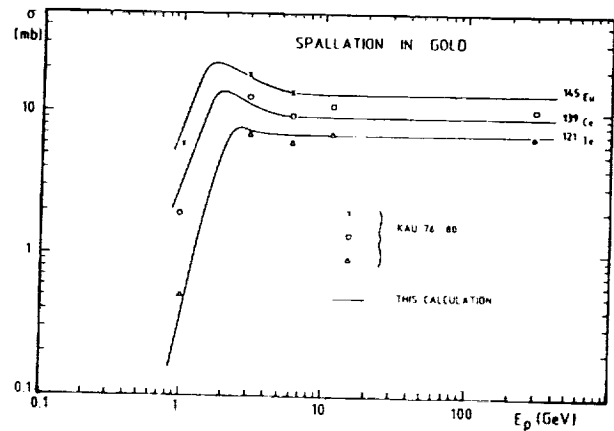


Figure 6; Spallation of gold
(—This work; \times, \circ, Δ experimental points).

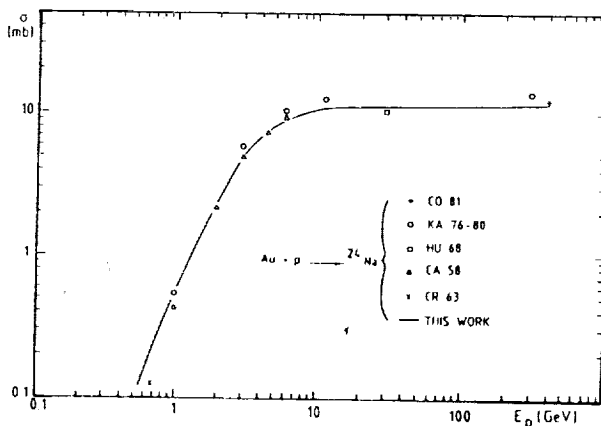


Figure 7; Production of ^{24}Na
in gold.

In conclusion we can affirm that the agreement is good between this calculation and the experimental data. There are still some discrepancies in the transition region (between spallation and fragmentation), but in the coming months, these difficulties will be solved and this calculation will be quite finished and available in particular for cosmochemistry and astrophysics applications.

- (1) Hüfner J. (1985) Physics Reports, **125**, p. 129-185
- (2) Kaufman S.B., Weisfield M.W., Steinberg E.P., Wilkins B.D., and Henderson D. (1976) Physical Review **C14**, p. 1121-1132
- (3) Kaufman S.B., and Steinberg E.P. (1980) Physical Review, **C22**, p. 167-178

PRODUCTION RATES OF NOBLE GASES IN METEORITES - A REVIEW;
Ludolf Schultz, Max-Planck-Institut für Chemie, D-6500 Mainz

Introduction

Meteoroids as meter-sized bodies interact with cosmic radiation during their flight in space. As a result cosmogenic stable and radioactive nuclides are produced within the meteoroid by the primary radiation and also by secondary particles of lower energy. The production rates of cosmogenic isotopes depend mainly on (1) the chemical composition of the irradiated material, (2) the size of the meteoroid and (3) the location of the analyzed sample within the meteoroid. The two last parameters are difficult to determine in meteoritic samples because during atmospheric transit a considerable part of the meteoroids mass is lost.

Stable cosmogenic noble gas isotopes in extraterrestrial materials are cumulated over the time of irradiation and can be used to study the history of these objects. For this purpose production rates must be obtained either via measured cosmogenic radionuclides or basic calculations. The production rate of cosmogenic radionuclides is equal to their saturation activity. Those of stable nuclides cannot be measured directly but must be calculated from their concentration and the exposure age of the meteorite. In this paper our present knowledge of cosmogenic noble gas production rates is reviewed.

Absolute ²¹Ne production rates

Noble gases in meteorites are a mixture of different components: Radiogenic, trapped and cosmogenic gases as well as possible atmospheric contaminations. Besides ³He (which could be affected by diffusive loss) and ³⁶Ar (where large trapped concentrations mask the cosmogenic component), cosmogenic ²¹Ne can be obtained best. Therefore, this isotope is widely used for the calculation of exposure ages.

The production rate of ²¹Ne in meteoritic samples is calculated using exposure ages which have been determined via activities of radionuclides. This is possible for meteorites with low exposure ages where the radionuclide is not yet in saturation; however, in this case the saturation activity is needed and must be taken from other meteorites. Furthermore, an exposure age can be calculated if a radioactive and a stable cosmogenic nuclide are measured and the production rate ratio of these two nuclides is known from other sources. This method yields good results for isotope pairs like ⁴⁰K-⁴¹K or ⁸¹Kr-⁸²Kr.

A summary of ²¹Ne production rates has been given recently by Eugster [1]. Absolute values for production rates in stone meteorites of L-group chemistry can be divided into two groups: While ²⁶Al-derived rates group around 0.47x10⁻⁶ ccSTP/gMa those calculated from other radionuclides are found between 0.30 to 0.33 x 10⁻⁶ccSTP/gMa. The reason for this discrepancy is not known.

PRODUCTION RATES OF NOBLE GASES: L. Schultz et al.

Shielding corrections

Due to the size and depth effect ("shielding"), the ^{21}Ne production rates can vary by more than a factor of two within a single meteorite. For stony meteorites with considerable Mg contents the cosmogenic $^{22}\text{Ne}/^{21}\text{Ne}$ ratio has been applied as a shielding parameter, which, however, cannot account for both factors, size and depth. It should be kept in mind that the use of this ratio as shielding correction still gives production rates with uncertainties of $\pm 20\%$, which, for extreme shielding ($1.07 < ^{22}\text{Ne}/^{21}\text{Ne} > 1.20$), might be even higher.

Commonly used is the shielding correction formula of the production rate of ^{21}Ne $P(21)$ given by Nishiizumi et al. [2]:

$$P(21) = P(21)_{1.11} F [21.77(^{22}\text{Ne}/^{21}\text{Ne}) - 19.32]^{-1}$$

with $P(21)_{1.11}$ as the ^{21}Ne production rate under the shielding condition given by $^{22}\text{Ne}/^{21}\text{Ne} = 1.11$ and F a correction factor for different chemical compositions.

Chemical composition

Elemental production rates are needed to account for the different chemical composition of meteorite groups. In meteorites such production rates are obtained by analyzing mineral separates with different chemical composition from one meteorite. The dependence of the average production rate of ^{21}Ne , $P(21)$, as function of the concentration of the for Ne-production important elements is (e.g. [3]):

$$P(21) = 1.63[\text{Mg}] + 0.6[\text{Al}] + 0.32[\text{Si}] + 0.22[\text{S}] + 0.33[\text{Fe+Ni}]$$

([X] - weight fraction of element X).

This production rate, however, depends also on the bulk composition of the meteorite because a meteorite with high concentrations of FeNi has higher production rates for isotopes which are mainly produced by low-energy secondary particles [4]. The higher multiplicity for the production of secondary neutrons from elements like Fe as compared to O or Si is the reason and limits the value of a production rate formula as given above.

In summary: The calculation of precise cosmic ray exposure ages from stable cosmogenic nuclides is limited. This is due to differences of absolute production rates calculated from different radionuclides. Furthermore, equations used for shielding corrections and adjustments to different chemical compositions are approximations only.

References: [1] O. Eugster, Geochim. Cosmochim. Acta 52, 1649, 1988. [2] K. Nishiizumi, S. Regnier and K. Marti, Earth Planet. Sci. Lett. 50, 156, 1980. [3] L. Schultz and M. Freundel, In Isotopic Ratios in the Solar System (eds. CNES), 27, 1985. [4] F. Begemann and L. Schultz, Lunar Planet. Sci. XIX, 51, 1988.

526-90

ABS. ONLY

351044

EVOLUTION OF METEORITIC BODIES IN SPACE; G.K.Ustinova, V.A.Alexeev, and A.K.Lavrukhina; Vernadsky Institute of Geochemistry and Analytical Chemistry, USSR Academy of Sciences, Moscow, 117975 USSR P-1

Determination of the pre-atmospheric sizes of meteorites by using the depth profiles of cosmogenic radionuclides allows to evaluate the average sizes of the meteorites for different time periods before their fall to the earth according to the half-lives of these radionuclides (1). Namely, short-lived radionuclides give us information about the sizes of meteorites just before their entering to the earth atmosphere, while stable cosmogenic isotopes as well as tracks characterize the average sizes of meteorites for all cosmic age. Such approach allows to investigate the evolution of the meteorites in space and their complex radiation history.

The pre-atmospheric sizes of some stony meteorites have been investigated. The average sizes of the chondrites Bruderheim, Innisfree, Malakal, Peace River and St. Severin turned out constant over at least ~6 million years. On the contrary, the average sizes of the chondrites Harleton and Gorlovka for the last ~400 years and those of the Ehole chondrite for the last ~8 years were less of their average sizes for the last ~6 million years. In the case of the other chondrites under consideration the results are uncertain due to the large range of the errors, and higher precision of the measurements of radioactivity of the radionuclides is required to elucidate the evolution of these chondrites.

(1) Ustinova G.K., Alexeev V.A., and Lavrukhina A.K. (1988) Geokhimiya, No.10, p.1379-1395.

527-90
321045
R-1

COSMOGENIC RADIONUCLIDE PRODUCTION RATES IN METEORITES
S. Vogt, Rutgers University, Department of Chemistry, New Brunswick, NJ 08903

The production rate of cosmogenic nuclides depends systematically on size and depth, usually referred to as "shielding", and on composition of meteorites. The variation attributed to shielding and compositional effects are ordinarily considered in relation to the *average* values for a group of meteorites. Accordingly, first the ways in which these average production rates are obtained will be discussed, followed by the elaboration on the variations.

Methods for Determining Average Production Rates - Under a constant cosmic ray bombardment, the activity of a cosmogenic radionuclide in a freshly exposed meteoroid will grow according to the relation $P = P_0(1 - e^{-\lambda t})$ where λ is the decay constant, t the exposure age and P_0 is the production rate. P can be measured and in the limit of $\lambda t \gg 1$ its value approaches the production rate. The determination of P_0 thus requires that P is measured in meteorites known to have large exposure ages.

A priori, it is not known whether a particular meteorite satisfies this condition. Fuse and Anders [1969] solved the problem by plotting the radionuclide contents (^{26}Al) of many meteorites against their contents of a stable cosmogenic nuclide (^{21}Ne). The asymptotic, horizontal level of the plot gave an average production rate for the isotope ^{26}Al , P_{26} .

This approach can be generalized so as to yield both the production rate of a radionuclide and that of a stable isotope by setting t equal to S/P_s . Here S is a measurable, stable cosmogenic nuclide content (e.g. ^{21}Ne) and P_s is its average production rate [Hampel et al., 1980; Moniot et al., 1988]. The data can then be fit with a two-parameter (P_r and P_0) curve of the form given above.

Another method for the determination of production rates is based on measurements of cosmogenic krypton isotopes [Nishiizumi et al., 1980; Schultz and Freundel, 1985]. As the element krypton has a long-lived radioisotope (^{81}Kr , $t_{1/2} = 0.2 \text{ Ma}$), an age can be calculated from the measurement of ^{81}Kr and of one stable cosmogenic Kr isotope such as ^{79}Kr . The measurement of other cosmogenic krypton isotopes (^{80}Kr and ^{82}Kr) makes it possible to correct for shielding effects on the $^{81}\text{Kr}/^{83}\text{Kr}$ production rate ratio. The net result, a $^{81}\text{Kr}/\text{Kr}$ age, can be used to obtain production rates for other nuclides from the equations given above. Eugster [1988] gives a detailed discussion of this important method.

Average Production Rates in Stony Meteorites - Eugster [1988] has used $^{81}\text{Kr}/\text{Kr}$ ages to obtain average production rates for stable noble gases in certain stony meteorite classes. He also compiles production rates derived from other methods. With one important exception, they agree within $\pm 10\%$. The set of production rates based on ^{26}Al fitting described above is about 50% higher than for the other methods. The reason for this discrepancy is not known; it may originate in unrecognized need for shielding corrections or that the gases accumulated only during the most recent period of exposure to cosmic rays. Table 1 presents the average radionuclide production rates observed in meteorites.

The mean production rates for the long-lived radionuclides ^{26}Al and ^{53}Mn in ordinary chondrites (H, L and LL chondrites) are averages of 200 and 100 analyses, respectively. Nishiizumi et al. [1980] also compiled ^{26}Al and ^{53}Mn data. They report production rates as a function of the shielding parameter $^{21}\text{Ne}/^{21}\text{Ne}$ (see also next chapter). Several studies include estimates of a mean value for the ^{10}Be production rate in somewhat smaller groups ($N < 30$) of ordinary chondrites. The numerical values agree within limits of error. The treatments of Sarafin et al. [1984] and Vogt [1988] allow for shielding effects.

The average production rates in eucrites are consistent with expectations based on compositional systematics and on calculations. Production rates for ^{10}Be and ^{26}Al in ureilites are about 20% lower than in other groups even after allowing for composition. Recent studies indicate that shielding effects probably caused this unusual pattern [Aylmer et al., 1990], rather than a change in the cosmic ray flux [Wilkening et al., 1973].

Begemann and Vilcsek [1969] derived an average ^{36}Cl production rate in the metal phase of meteorites from their analyses of 22 metal separates from stony meteorites. Nishiizumi et al. [1983] studied the ^{36}Cl activities in the metal phase of a set of Antarctic meteorites and confirmed the older ^{36}Cl production rate, which was also adopted for small iron meteorites.

Table 1 : Average Radionuclide Production Rates in Meteorites

Class	^{10}Be [dpm/kg]	^{26}Al [dpm/kg]	^{36}Cl ^a [dpm/kg]	^{41}Ca ^a [dpm/kg]	^{54}Mn [dpm/kg _w]
H	20.6 ± 1.0 ¹ 18.4 ± 1.8 ^{2,3}	56.1 ± 1.0 ¹ 56 ± 7 ⁴	22.8 ± 3.1 ¹		434 ± 28 ⁶ 414 ± 50 ^{4,8}
L, LL	22.1 ± 1.1 ¹ 19.8 ± 2.0 ^{2,3}	60.2 ± 0.8 ² 60 ± 7 ^{4,8}	22.8 ± 3.1 ¹		434 ± 28 ⁶ 414 ± 50 ^{4,8}
Eucrite	21.8 ± 2.2 ⁷	93 ± 14 ⁷			
Ureilite	20.3 ± 1.0 ¹	42.3 ± 2.2 ³			
Iron	4 - 5 ⁹	3 - 4 ⁹	22.8 ± 3.1 ¹	23.8 ± 0.6 ¹⁰	350 - 550

Notes: ^a activities in dpm/kg metal; ^b values for mean shielding of $^{21}\text{Ne}/^{21}\text{Ne} = 1.11$.
Refs.: [1] Vogt [1988]; [2] Hampel et al. [1980]; [3] Nishiizumi et al. [1989]; [4] Englert [1979]; [5] Sarafin et al. [1984]; [6] Nishiizumi et al. [1980]; [7] Aylmer et al. [1988a]; [8] Aylmer et al. [1990]; [9] Aylmer et al. [1988b]; [10] Fink et al. [1989].

production rate after correcting for terrestrial age. Fink et al. [1989] report an average ^{41}Ca production rate for iron meteorites based on analyses of four small iron falls. Their result for Bogou disagrees by more than a factor of two with one presented by Kubik et al. [1986].

Comprehensive listings of radionuclide and light noble gas data are provided by Nishiizumi [1987] and Schultz and Kruse [1989], respectively.

Depth and Size Dependence of Production Rates - Variations of 5-30% from the average production rate values occur regularly in meteorites because the samples come from different depths in bodies of various sizes. To attain a precision of 10% in an exposure age, one must allow for these variations. The depth and size dependence of the production of many cosmogenic nuclides have been investigated in great detail during the last decade.

Direct measurements of the depth are impossible as ablation removes an unknown part of material from the meteorite during its passage through the earth's atmosphere. In certain cases, the depth at which a sample was irradiated can be estimated from the densities of nuclear tracks, trails of irradiation damage induced by heavy cosmic ray particles in dielectric media such as pyroxenes. Track determinations have

Aylmer et al. [1988b] measured ^{10}Be and ^{26}Al production rates in iron meteorites. The activities correlate well with the shielding indicator $^{4}\text{He}/^{21}\text{Ne}$, as suggested by Voshage and Feldmann [1979]. The average ^{10}Be production rate was 10-20% lower than that derived by Chang and Waenke [1969] from decay-counting measurements.

The measurement of ^{41}Ca by AMS is a recent development. Fink et al. [1987] reported the spatial distribution of ^{41}Ca activities in the iron meteorite Grant and estimated a ^{41}Ca

COSMOGENIC RADIONUCLIDE PRODUCTION RATES: S. Vogt

been used to establish the depth scales for cosmogenic nuclide profiles [Bhandari et al., 1980]. Relative sample depths in large meteorites can also be obtained from measurements of cosmogenic radionuclides produced by thermal neutrons, e.g. ^{60}Co .

For ordinary chondrites the cosmogenic $^{22}\text{Ne}/^{21}\text{Ne}$ ratio serves widely as shielding indicator [Eberhardt et al., 1966; Graf et al., 1990]. The ratio decreases with increasing depth and size as secondary particle production enhances the importance of the $^{24}\text{Mg}(n,\alpha)^{21}\text{Ne}$ reaction. By plotting various cosmogenic nuclide contents against the $^{22}\text{Ne}/^{21}\text{Ne}$ ratio, a number of correlations have been established that serve as a basis for shielding corrections [e.g. Englert, 1979; Nishiizumi et al., 1980]. Unfortunately, observations and theoretical calculations show that production rates are not uniquely determined by the $^{22}\text{Ne}/^{21}\text{Ne}$ ratio. Voshage [1984] discusses the use of empirical shielding monitors, especially the $^4\text{He}/^{21}\text{Ne}$ ratio for iron meteorites.

Table 2 provides a compilation of production rates of long-lived cosmogenic radionuclides in meteorites of various sizes. Median production rates are provided where meteorites revealed no detectable variation with depth, production rate ranges are given for those where a depth dependency was experimentally verified. Some detailed comments follow.

Table 2: Production Rates of Long-Lived Radionuclides in Meteorites of Different Preatmospheric Radii.

Meteorite	Class	Radius [cm]	^{10}Be [dpm/kg]	^{26}Al [dpm/kg]	$^{36}\text{Cl}^*$ [dpm/kg]	$^{41}\text{Ca}^*$ [dpm/kg]	^{55}Mn [dpm/kg _{Fe}]
Madhipura	L	6.5 ¹	16.8 ²	40.2 ²			295 ¹
Udaipur	H4	9 ¹	17.6 ²	44.8 ²			314 ¹
Bansur	L6	15 ¹	19.2 ²	49.5 ²			377 ¹
ALHA 78084 ^a	H4	14 ³	19.2 ²	52.9 ¹			360 ³
Keyes ^c	L6	25 ¹		50.9-68.9 ⁵			380-530 ^a
St. Severin	LL6	25 ¹	19.8-28.2 ⁷		19.7-23.3 ^a		364-495 ^a
Knyahinya	L5	45 ¹⁰	19.9-26.6 ⁷	59.7-77.1 ¹			378-537 ²
Dhurmsala	LL6	50 ¹¹	22.9 ¹¹	58.9 ¹¹			379 ¹¹
Grant ^c	Om	40 ¹²	2.7-4.3 ¹²	2.2-4.0 ¹²		16.2-18.0 ¹⁴	
Allende	C3V	>55 ¹⁷	19.5 ¹⁷	52.8 ¹⁸	27.2 ¹³		304 ¹⁴

Notes: * activities in dpm/kg metal; ¹ meteorite find; ^a corrected for a terrestrial age of 0.14 Ma [Nishiizumi et al., 1983]. **Refs.:** [1] Bhattacharya et al. [1980]; [2] Vogt [1988]; [3] Sarafin et al. [1985]; [4] Vogt et al. [1986a]; [5] Cressy [1975]; [6] Englert [1984]; [7] Tuniz et al. [1984a]; [8] Nishiizumi et al. [1989]; [9] Englert and Herr [1980]; [10] Graf [1988]; [11] Englert et al. [1986]; [12] Graf et al. [1987]; [13] Fink et al. [1987]; [14] Fink et al. [1989]; [15] Nishiizumi et al. [1986]; [16] Nishiizumi [1978]; [17] Tuniz et al. [1984b]; [18] Cressy [1972].

Small Stones: For cosmogenic radionuclides, no significant variation of GCR production rates with depth has yet been seen in a meteorite with a radius less than 15 cm. Small variations must exist, however, as the $^{22}\text{Ne}/^{21}\text{Ne}$ ratio correlates weakly with depth. The increase in average production rates as the meteoroid radius increases from 5 cm upward demonstrates the influence of the build-up of the secondary particle cascade even in bodies smaller than 10 cm.

Medium Size Stones: St. Severin and Keyes had roughly the same size in space (radius \approx 25 cm) and show depth related variations in their

production rates of about 20%. The correlation of P_{33} with the shielding parameter $^{22}\text{Ne}/^{21}\text{Ne}$ for each meteorite has a steeper slope than does the corresponding multi-meteorite plot. A similar observation was reported earlier for P_{26} in the Keyes chondrite [Cressy, 1975]. Absolute production rates for ^{55}Mn , up to 530 dpm/kg_{Fe}, exceed the average value of P_{33} (see Table 1) by about 20%. The constancy of the

$^{55}\text{Mn}/^{26}\text{Al}$ production rate ratio with depth in the Keyes chondrite confirms previous results by Herpers and Englert [1983]. Because of its shielding independence for ordinary chondrites with preatmospheric radii less than 35 cm [Herpers and Englert, 1983], this ratio has been used to calculate exposure ages up to about 10 Ma [Herpers and Englert, 1983] as well as terrestrial ages for some Antarctic chondrites [e.g. Herpers and Sarafin, 1987]

A depth-dependent variation of the radionuclide ^{10}Be was first reported in St. Severin [Tuniz et al., 1984a]. A large increase ($\approx 30\%$) of the production rate seems to occur within the outermost 15 cm. A similar observation was reported by Vogt et al. [1986b] for the depth dependence of ^{10}Be in the L5 chondrite Knyahinya (radius 45 cm, Graf [1988]).

Nishiizumi et al. [1988] observe a moderate depth dependence for the radionuclide ^{36}Cl in the metal phase of the St. Severin chondrite. The small variation of P_{36} with depth in this meteorite helps validate the use of ^{36}Cl in calculating terrestrial ages in the range 0.2 to 1 Ma.

Barton et al. [1982] scanned the ^{26}Al contents of a 30 x 40 cm slab from the H6 chondrite Estacado. The ^{26}Al profiles have flat maxima in the center (≈ 60 dpm/kg) with reductions of about 30% toward the edges. The results are consistent with calculations that assume a pre-atmospheric radius of 35 cm.

Large Stones: As mentioned above, P_{10} in Knyahinya increases most steeply in the outermost 15 to 20 cm, whereas the production rate remains constant at greater depths. The absolute ^{10}Be concentrations exceed the averaged production rate significantly, by up to 30%. Graf et al. [1990] show that the $^{10}\text{Be}/^{21}\text{Ne}$ production rate ratio varies little with depth and provides a new tool for the calculation of exposure ages for chondrites. The small variations which do exist correlate well with the $^{22}\text{Ne}/^{21}\text{Ne}$ ratio and can be corrected.

The ^{55}Mn and ^{26}Al profiles of Knyahinya [Vogt, 1988] show about the same relative variations as found in Keyes and St. Severin. The average absolute level of P_{26} in Knyahinya is about 15% higher than that found in any other depth profile study. At its maximum P_{26} reaches almost 80 dpm/kg. Within 10 cm or so of the center of the meteorite the profiles of ^{26}Al and ^{55}Mn gradually flatten out; there is even a hint that the maximum in the profile has been passed [Vogt, 1988].

A search in the LL6 chondrite Dhurmsala, (radius ≈ 50 cm) yielded no firm evidence for variations of the radionuclide production rates due to shielding [Englert et al., 1986]. The significance of this study is somewhat limited, as all data were derived from a one-kg specimen. The high shielding depth of this specimen, however, suggests that average production rates for radionuclides decrease in meteoroids with radii greater than about 45 cm, the size of Knyahinya.

Average radionuclide contents in the carbonaceous chondrite Allende (radius > 55 cm) are consistent with this conclusion. The levels of the production rate are similar to average values from ordinary chondrites (Table 1) after allowance is made for the effects of composition. Surprisingly, the ^{10}Be and ^{26}Al contents vary not at all with depth, even in the outermost regions. The contents of the neutron-induced isotopes ^{36}Cl and ^{60}Co show the expected trends, i.e. activities increase with depth.

Iron Meteorites: Systematic variations of light noble gases in iron meteorites were extensively studied by Signer and Nier [1960, 1962] and Voshage [c.g.1984]. Graf et al. [1987] report new measurements of the spatial distribution of the light noble gases and radionuclides ^{10}Be and ^{26}Al in a slab of the iron meteorite Grant. The radionuclides indicate that production rates decrease by about 25% from the edge to the center and correlate well with the shielding indicator $^4\text{He}/^{21}\text{Ne}$. More surprisingly came the depth independence of the $^{10}\text{Be}/^{21}\text{Ne}$ production rate ratio, which can be used to obtain better exposure ages for iron meteorites, as well. The activities are lower than the averages in iron meteorites (Table 1), perhaps because Grant's terrestrial age and/or shielding.

Composition Dependence of Production Rates - Production rates depend appreciably on the absolute abundance of the target elements from which the isotopes are made. This dependence is reflected in the variation of average production rates among meteorite classes (Table 1). Even within one meteorite class, the target element concentrations may vary 10% in very small samples (mg range). Any reasonably precise calculation of exposure ages takes composition into account.

Estimates of elemental production rates are usually obtained by regression methods. For data, one turns either to analyses of several meteorites with different composition or to several minerals from single meteorites. Studies of elemental production rates for ^{26}Al [Fuse and Anders, 1969; Cressy, 1971; Hampel et al., 1980] and ^{10}Be [Moniot et al., 1988].

By analyzing certain nuclides in mineral separates rather than in bulk material, one can sometimes reduce composition-related adjustments, in order to obtain terrestrial or exposure ages. For example, nuclear reactions on locally small and/or variable concentrations of Cl, K and Ca in bulk chondrites strongly influence ^{36}Cl production. In calculating the terrestrial ages of stony meteorites by using the ^{36}Cl -method, it is therefore better to measure ^{36}Cl in the metal phase.

In carrying out the regression analyses mentioned above, one assumes that the production rate, for instance, of ^{36}Cl depends linearly on the concentration of Cl, K, Ca etc.. In fact, the development of the secondary cosmic ray flux that is responsible for much ^{36}Cl production should reflect to some extent the composition of the matrix. Thus, a meteorite richer in iron may develop a secondary flux with more low-energy neutrons. If so, the production rate of ^{36}Cl attributable to Cl, $P_{\text{Cl}}/g \text{ Cl}$, could change from meteorite to meteorite. Begemann and Schultz [1988] argue for just such an effect for the isotope ^{39}Ar in mesosiderites and in other meteorites as well. Curiously, P_{Cl} in irons and in stones seem comparable.

Multiple Exposure Histories and Cosmic Ray Flux - Frequently, the exposure ages calculated by different methods disagree and the measured cosmogenic nuclide contents form pattern that differs from those observed in any well-studied meteorite. Under these circumstances, multiple episodes of exposure (complex irradiation history) or temporal and spatial variations of the cosmic ray flux in the past may be invoked to explain the disparities.

Complex Histories: Complex irradiation histories can be divided into two groups according whether the first stage(s) occurred well before, or just prior to, the most recent one. The case of multiple exposures that are regarded as separated in time is discussed in detail by e.g. Caffee et al. [1988]. The second case, complex recent irradiation histories of meteoroids may be quite common [e.g. Wetherill, 1985] and has been suggested for about 30% of the iron meteorites [Schaeffer et al., 1981]. Surprisingly, the percentage for stony meteorites is much smaller. It is not yet clear whether the scarcity is real or reflects inadequate assessment techniques. In any event, only few meteorites show signs of complex irradiation: Yamato 7301 and Allan Hills 76008 [Nishiizumi et al., 1979]; Torino [Bhandari et al., 1989] and Bur Gheluai [Wieler

et al., 1990]. A curious pattern of cosmogenic nuclide contents in Sierra de Mage once ascribed to multiple exposure [Carver and Anders, 1970], was later shown to be the result of heavy shielding [Nishiizumi et al., 1984; Aylmer et al., 1988a].

Most remarkable is the complex irradiation history for the H5 chondrite Jilin (Kirin) [Heusser et al., 1979], the largest known stony meteorite. Jilin had a two-stage-exposure [Honda et al., 1980, 1982]. The ^{60}Co activities in documented samples imply a preatmospheric (2nd stage) radius of about 85 cm [Heusser et al., 1985]. In this geometry, Jilin was exposed for 0.4 - 0.6 Ma [Heusser et al., 1985; Pal et al., 1985]. A previous exposure as part of a much larger body (a "2 π " exposure) lasted for 6.2 to 10 Ma [Begemann et al., 1985; Heusser et al., 1985]. The exposure ages were obtained from combined determinations of ^{21}Ne , ^{10}Be , ^{26}Al and ^{55}Mn . Unexpectedly, measurements of the ^{10}Be and ^{26}Al activities as a function of the depth in the main fragment of Jilin (about 100 cm, edge to edge) indicate only a small increase towards the surface [Vogt, 1988]. The ^{36}Cl activities, measured in the metal phase of adjacent samples, likewise show a small variation with depth [Nishiizumi et al., 1989].

Variations in Cosmic Ray Intensity: Short term variations of the cosmic ray flux intensity have been verified through studies of short-lived radionuclides such as ^{22}Na and ^{54}Mn . Measurements in freshly fallen meteorites showed a significant correlation with the 11-year solar cycle [e.g. Evans et al., 1982, 1986] and were attributed to the low-energy GCR flux.

Long term variations were inferred from measurements in iron meteorites. Irons have exposure ages of 0.01 to 1 Ga [e.g. Voshage, 1984]. Disparities in the $^{26}\text{Al}/^{21}\text{Ne}$ and $^{40}\text{K}/^{41}\text{K}$ exposure ages led Hampel and Schaeffer [1979] to the conclusion that the cosmic-ray flux might have increased in the last few million years by about 50%. Marti et al. [1984] and Aylmer et al. [1988b] suggested a possible change within the last few hundred million years of about +35%. The variation could be attributed to either an increase in the cosmic ray flux during the last ≈ 10 Ma or an increased modulation of galactic cosmic rays by the solar wind 10 or more Ma ago [Caffe et al., 1988].

References: Aylmer et al. (1988a), *Geochim. Cosmochim. Acta*, **52**, 1691-1698; Aylmer et al. (1988b), *Earth Planet. Sci. Lett.*, **88**, 107-118; Aylmer et al. (1990), *Geochim. Cosmochim. Acta*, in press; Barton et al., *Geochim. Cosmochim. Acta*, **46**, 1963-1967; Bhandari et al. (1980), *Nuclear Tracks*, **4**, 213-262; Bhandari et al. (1989), *Meteoritics*, **24**, 29-34; Bhattacharya et al. (1980), *Earth Planet. Sci. Lett.*, **51**, 45-57; Begemann and Vilcsek (1969), in: *Meteorite research*, edited by P. Millman, 355-362, D.Reidl, Dordrecht; Begemann and Schultz (1988), *Lunar Planet. Sci.*, **XIX**, 51-52; Caffee et al. (1988), in: *Meteorites and the Early Solar System*, Univ. Arizona Press, 205-245; Carver and Anders (1970), *Earth Planet. Sci. Lett.*, **8**, 214-220; Chang and Waenke (1969), in: *Meteorite Research*, edited by P. Millman, pp. 396-401, D. Reidel, Dordrecht; Cressy (1971), *Geochim. Cosmochim. Acta*, **35**, 1283-1296; Cressy (1972), *J. Geophys. Res.*, **77**, 4905-4911; Cressy (1975), *Earth Planet. Sci. Lett.*, **22**, 275-283; Eberhardt et al. (1969), *Z. Naturforsch.*, **21a**, 414-426; Englert (1979), *Inaugur. Diss.*, Univ. Koeln, pp. 139; Englert and Herr (1980), *Earth Planet. Sci. Lett.*, **47**, 361-369; Englert (1984), *Lunar Planet. Sci.*, **XV**, 248-249; Englert et al. (1986) *Geochim. Cosmochim. Acta*, **50**, 1593-1598; Eugster (1988), *Geochim. Cosmochim. Acta*, **52**, 1649-1659; Evans et al. (1982), *J. Geophys. Res.*, **87**, 5577-5591; Evans et al. (1986), *Meteoritics*, **21**, 243-250; Fink et al. (1987), *Nucl. Instrum. Methods*, **B29**, 275-280; Fink et al. (1989), *Meteoritics*, **24**, 266; Fuse and Anders (1969), *Geochim. Cosmochim. Acta*, **33**, 653-670;

- Graf et al. (1987), *Nucl. Instrum. Methods*, **B29**, 262-265; Graf (1988), *Inaug. Diss., ETH-Zuerich*, pp. 132; Graf et al. (1990), *Geochim. Cosmochim. Acta*, in press;
- Hampel and Schaeffer (1979), *Earth Planet. Sci. Lett.*, **42**, 348-358; Hampel et al. (1980), *Geochim. Cosmochim. Acta*, **44**, 539-547; Herpers and Englert (1983), *Proc. Lunar Planet. Sci. Conf.*, **14th**, *J. Geophys. Res.*, Part 1, **88**, B312-B318; Herpers and Sarafin (1987), *J. Radioanalyt. Nucl. Chemistry*, **110**, 191-195; Heusser et al. (1979), *Meteoritics*, **14**, 412-414; Heusser et al. (1985), *Earth Planet. Sci. Lett.*, **72**, 263-272; Honda et al. (1980), *Geochim. J.*, **14**, 83-89; Honda et al. (1982), *Earth Planet. Sci. Lett.*, **57**, 101-109;
- Kubik et al. (1986), *Nature*, **319**, 568-570;
- Marti et al. (1984), *Lunar Planet. Sci.*, **XV**, 511-512; Moniot et al. (1983), *Geochim. Cosmochim. Acta*, **47**, 1887-1895; Moniot et al. (1988), *Geochim. Cosmochim. Acta*, **52**, 499-504;
- Nishiizumi (1978), *Earth Planet. Sci. Lett.*, **41**, 91-100; Nishiizumi et al. (1979), *Mem. Natl. Inst. Polar Res.*, Spec. Issue **12**, 161-177; Nishiizumi et al. (1980), *Earth Planet. Sci. Lett.*, **50**, 156-170; Nishiizumi et al. (1983), *Earth Planet. Sci. Lett.*, **62**, 407-417; Nishiizumi et al. (1984), *Meteoritics*, **19**, 283; Nishiizumi et al. (1986), *Lunar Planet. Sci.*, **XVII**, 619-620; Nishiizumi (1987), *Nucl. Tracks Radiat. Meas.*, **13**, 209-273; Nishiizumi et al. (1988), *Proc. Lunar Planet. Sci. Conf.*, **19th**, Cambridge Univ. Press, 305-312; Nishiizumi et al. (1989), *Earth Planet. Sci. Lett.*, **93**, 299-313;
- Pal et al. (1985), *Earth Planet. Sci. Lett.*, **72**, 273-275;
- Sarafin et al. (1984), *Nucl. Instrum. Methods*, **B5**, 411-414; Sarafin et al. (1985), *Earth Planet. Sci. Lett.*, **73**, 171-182; Schaeffer et al. (1981), *Earth Planet. Space Sci.*, **29**, 1109-1118; Schultz and Freundel (1985), in: *Isotopic ratios in the Solar System*, Centre Nationale d'Etudes Spatiale, Cepadues-Editions, Toulouse, France, 27-33; Schultz and Kruse (1989), *Meteoritics*, **24**, 155-172; Signer and Nier (1960), *J. Geophys. Res.*, **65**, 2947-2964; Signer and Nier (1962), *Researches on Meteorites*, 7-35;
- Tuniz et al. (1984a), *Geochim. Cosmochim. Acta*, **48**, 1867-1872; Tuniz et al. (1984b), *Third Intern. Symp. Accelerator Mass Spectrometry*, 89;
- Vogt et al. (1986a), *LPI Tech. Rpt.* 86-01, 55-57; Vogt et al. (1986b), *Meteoritics* **21**, 257; Vogt (1988), *Inaugur. Diss., Univ. Koeln*, pp. 150; Voshage and Feldmann (1979), *Earth Planet. Sci. Lett.*, **71**, 181-194; Voshage (1984), *Earth Planet. Sci. Lett.*, **71**, 181-194;
- Wetherill (1985), *Meteoritics*, **20**, 1-22; Wieler et al. (1990), *Lunar Planet. Sci.*, **XXI**, 1335-1336; Wilkening et al. (1973), *Geochim. Cosmochim. Acta*, **37**, 1803-1810.

528-90

321046

P-4

**STUDY OF HIGH ENERGY PARTICLE PROPAGATION INSIDE
SOLID MATTER AND DERIVATION OF COSMOGENIC NUCLIDE
PRODUCTION RATES IN IRON METEORITES** B. Zanda

Muséum National d'Histoire Naturelle - 61, rue Buffon - 75005 Paris. FRANCE

Institut d'Astrophysique de Paris - 98, bis Bd Arago - 75014 Paris. FRANCE

Different approaches may be used in order to derive cosmogenic nuclide production rates as a function of depth inside irradiated bodies of various sizes. One main approach is a comparison with simulation experiments through the irradiation of thick targets. In these experiments, the transposition of the available beam geometry to the isotropic irradiation conditions in space has been obtained in different ways from mathematical corrections to rotating spherical targets in the beam [1]. A second type of approach consists in evaluating particle fluxes as a function of depth in the irradiated bodies. These fluxes are used together with nuclear reaction cross section data to derive production rates. In this approach, fluxes have traditionally been derived in a semiempirical way through the study of meteoritical and thick target data or of stars induced in nuclear emulsions [2-4]. A physical alternative to these approaches lies in the study of the processes involved in particle propagation. The transport equations for each type of particles are established and can be solved to derive particle fluxes either through the following of intranuclear and internuclear cascades by a Monte Carlo method [5-7] or with the use of a deterministic computation as in the model presented here.

1 - Basic features of the model

Only the main characteristics of this model are recalled here, details being given elsewhere [8,9]. Particle losses in nuclear interactions and slowing down of charged particles are studied together with secondary particle production. Secondary particle production is a fundamental process and its evaluation constitutes a stumbling block to any physical model studying high energy particle propagation inside solid matter. Due to the lack of data in this field, this evaluation has been performed through the use of results from intranuclear cascades calculations (see section 2). Different types of particles can be taken into account (we have so far considered protons and neutrons) and the simultaneous solution of the linked transport equations is achieved through iterations. Two different deterministic methods have been developed in order to solve these equations. The first one is based on the characteristics method and consists in solving the transport equation along a line corresponding to the trajectory of the particles inside the meteoritical matter. The distance between two points of the mesh may become large with regards to the range for protons: this limitates the use of this method at energies above ≈ 300 MeV. The second method is based on the diamond numerical scheme and does not suffer from this limitation. The results obtained with this method being still preliminary, only results obtained with the characteristics method in iron spheres of various radii will be presented here.

Production rates as a function of depth inside spherical meteoroids are derived from the particle fluxes with the use of spallation reactions cross sections (see section 2): neutrons have so far been treated simultaneously with protons due to the data available in the energy range considered.

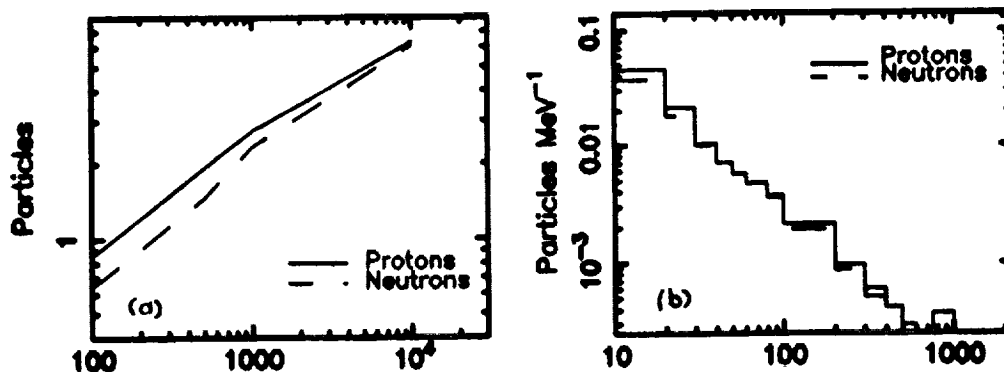
2 - Nuclear data used as input

(a) *Secondary particle production:* Monte Carlo intranuclear cascades calculations allow to estimate the total number of protons and neutrons produced per reaction (ν) as a function of the type of incident particle and of its energy (E'). They also allow to derive the energetic and angular spectrum of the emitted particles (Fig. 1). Results from the HETC code have been shown to stand satisfactorily comparison with experimental data [10]. The estimation of the energy spectrum of the emitted particles is of great incidence over the derived fluxes as it is clearly very different to distribute the incident particle energy over a bunch of secondaries or to have a few fast ones taking most of it. This spectrum can be described as a function $KE^{-\beta(E')}$ where E is the energy of the emitted particles. The value of K is obtained from the normalization: $\int_{E_0}^{E'} KE^{-\beta(E')} dE = 1$, where E_0 is the lower energy cutoff used for the computation. An estimation of $\beta(E')$ can be obtained from the total energy taken out by the different types of emitted particles which is a side result of the Monte Carlo code: $\int_{E_0}^{E'} \nu(E') KE^{-\beta(E')} E dE = q(E')$ where $q(E')$ is the total amount of energy taken away by the secondary particles. From $\nu(E')$ and $q(E')$ for emitted neutrons and protons both from proton and neutron induced reactions, we have derived $\beta(E')$ for the same four cases (Fig. 2).

(b) *Reaction cross sections:* The production cross sections clearly constitute the major source of uncertainty over the computed production rates. We have used experimental data whenever available and results from semiempirical formulae elsewhere. The formulae used are from Silberberg and Tsao (see [11] and references therein). The "adopted values" of [12] have also been considered. Our adopted values are shown in Fig. 3 for the most important reactions considered (namely production of ^{10}Be , ^{21}Ne , ^{26}Al and ^{38}Ar from Fe) and details can be found in [9]. The whole situation of available cross sections is currently changing as new set of data become available [13,14].

3 - Application to meteoritical data

Production rates have been computed at various depths in a set of spheres having the chemical composition of the iron meteorite Grant and with radii ranging from 30 to 60 cm. Production ratios of ^{26}Al (P_{26}) and ^{21}Ne (P_{21}) versus ^{10}Be (P_{10}) are shown in Fig. 4 (each dot corresponds to different shielding conditions). Only the 35 cm radius sphere and the two extreme points of the set are represented in the case of ^{26}Al : $P_{26} = (0.70 \pm 0.13)P_{21}$ close to the surface of objects. Data from Graf et al. [15] for P_{26} and P_{10} in Grant are also shown: the covered range is very similar but the data are mostly located in the part corresponding to the outer region of the sphere. This may either mean that the most shielded samples have not been measured so far or that the two production rates are slightly underestimated. The production rate ratio $P_{21}/P_{10} = (1.5 \pm 0.3)$ can be seen to remain constant over a large range of shieldings. This ratio and the data in Graf et al. allow to estimate a ^{21}Ne age of 600 ± 140 Ma in the case of an irradiation by the present GCR flux. This age can be compared with the 590 ± 50 Ma estimate from [16] and it has been used to compute the ^{21}Ne and ^{38}Ar shown in Fig. 5. Computed abundances agree with data close to the surface of a 30 cm radius object, but the abundances computed with this radius become too low when depth increases. Such a discrepancy may well be explained by the uncertainties of the model, mainly geometry of meteoroid, exposure duration, particle and nuclide production cross sections and present low energy cutoff.



E' = Energy of incident proton (MeV) E = Energy of emitted particles (MeV)
 Figure 1 (a) - Average number of protons and neutrons emitted with $E \geq 10$ MeV per reaction induced on Fe nuclei as a function of the incident proton energy E' . (b) - Energy spectrum of these particles in the case when the incident proton energy $E' = 1$ GeV.

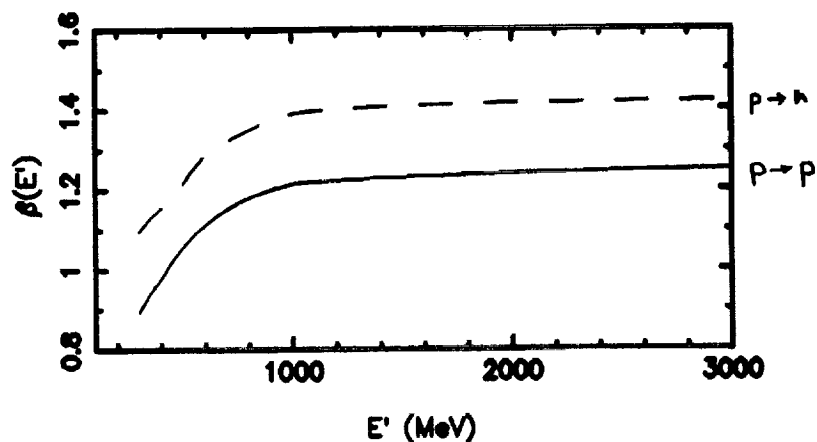


Figure 2 Spectral shape of the emitted particles deduced from the total amount of energy they take away as a function of the incident particle energy.

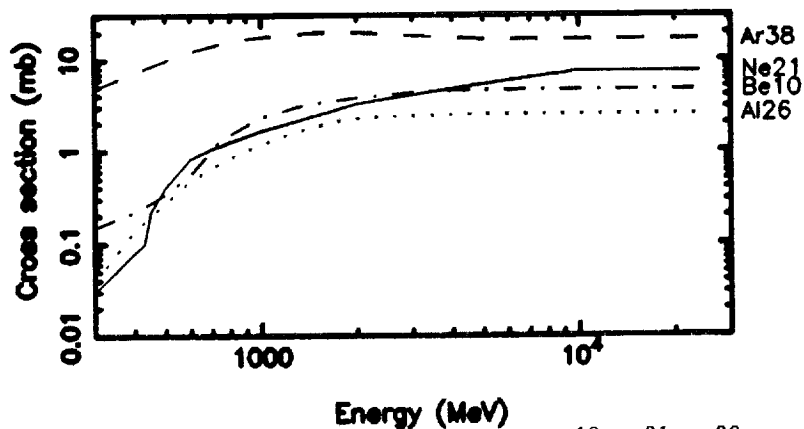


Figure 3 Adopted cross sections (mb) for the production of ^{10}Be , ^{21}Ne , ^{26}Al and ^{38}Ar from Fe (figures given in [9]).

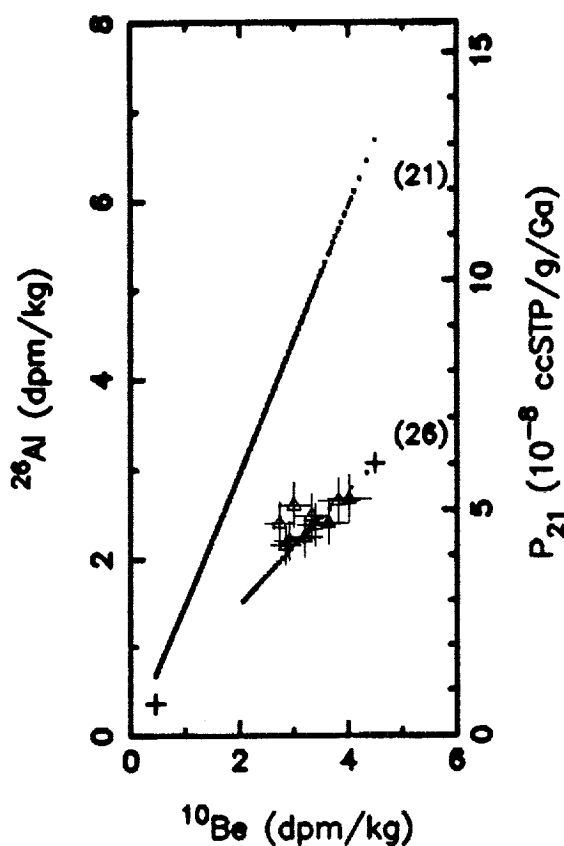


Figure 4 Production rate correlation for ^{10}Be , ^{21}Ne and ^{26}Al . All dots correspond to different shielding conditions.

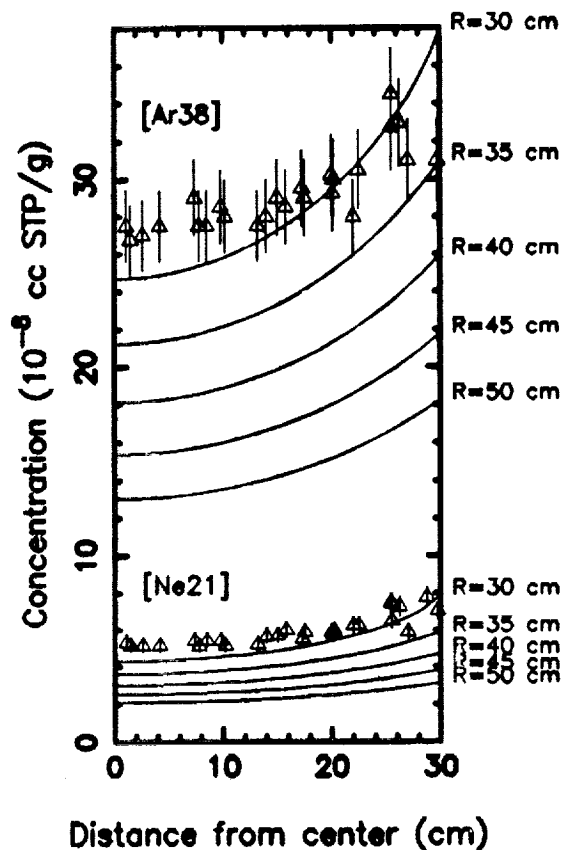


Figure 5 Concentration profiles of ^{21}Ne and ^{38}Ar . Data from [15] are displayed with admitted errors of 7%.

- [1] Michel, R., Peiffer, F., Theis, S., Begemann, F., Weber, H., Signer, P., Wieler, R., Cloth, P., Dragovitsch, P., Filges, D., and Englert, P.: 1989 *Nucl. Instr. Meth. Phys. Res.*, in press
- [2] Signer, P. et Nier, A.O.: 1960 *J. Geophys. Res.* **65**, 2947-2964
- [3] Arnold, J.R., Honda, M. and Lal, D.: 1961 *J. Geophys. Res.* **66** No 10, 3519-3531
- [4] Reedy, R.C.: 1985 *Proc. 15th Lun. Planet. Sci. Conf. part 2; J. Geophys. Res. suppl.* **90**, C722-C728
- [5] Armstrong, T.W. and Alsmiller, R.G.: 1971 *Proc. 11th Lun. Sci. Conf.* **2**, 1729-1745
- [6] Masarik, J., Emrich, P., Povinec, P. and Tokár, S.: 1986 *Nucl. Instr. Meth. Phys. Res. B* **17**, 483-489
- [7] Dragovitsch, P.: 1987 *PhD Thesis, Cologne University*
- [8] Zanda, B.: 1988 *PhD Thesis, Université de Paris VII*
- [9] Zanda, B., Malinie, G. and Audouze, J.: 1989 *Earth Planet. Sci. Lett.*, in press
- [10] Filges, D., Cierjacks, S., Hino, Y., Armstrong, T.W. and Cloth, P.: 1980 *Jülich internal report Jül-1960* — ISSN 0366-4003
- [11] Silberberg, R., Tsao, C.H. and Letaw, J.R.: 1985 *Astrophys. J. Suppl.* **53**, 873-881
- [12] Tobaillem, J. and de Lassus St-Genies, C.H.: 1975 *Note CEA-N-1466(3)*
- [13] Michel, R., Dittrich, B., Hergers, U., Peiffer, F., Schiffmann, T., Cloth, P., Dragovitsch, P., and Filges, D.: 1989 *The Analyst*, in press
- [14] Webber, W.R.: 1987 *Proc. 20th I.C.R.C., Moscow* **OG 10-2**, 463-466
- [15] Graf, T., Vogt, S., Bonani, G., Hergers, U., Signer, P., Suter, M., Wieler, R., and Wölfli, W.: 1987 *Nucl. Instr. Meth. Phys. Res.* **B29**, 262
- [16] Lipschutz, M.E., Signer, P. and Anders, E.: 1965 *J. Geophys. Res.* **70** No6, 1473

List of Workshop Participants

James R. Arnold
Chemistry Department, B-017
University of California, San Diego
La Jolla, CA 92093-0317

Friedrich Begemann
Max-Planck-Institut für Chemie
Saarstrasse 23
D-6500 Mainz
Federal Republic of Germany

N. Bhandari
Physical Research Laboratory
Navrangpura
Ahmedabad
India 380009

Janice Bishop
Box H
Department of Chemistry
Brown University
Providence, RI 02912

Elisabetta Boaretto
Racah Institute of Physics
91904 Givatram
Jerusalem
Israel

Klaus Bremer
Abteilung Nuklearchemie
Universität Köln
Zùlpicherstrasse 47
D-5000 Köln
Federal Republic of Germany

G. Dagge
Institut für Kernphysik
Postfach 1913
D-5170 Jùlich
Federal Republic of Germany

Beate Dittrich
Abteilung Nuklearchemie
Universität Köln
Zùlpicher Strasse 47
D-5000 Köln 1
Federal Republic of Germany

Peter Dragovitsch
Institut für Kernphysik
Postfach 1913
D-5170 Jùlich
Federal Republic of Germany

Peter Eberhardt
Physikalisches Institut
University of Bern
Sidlerstrasse 5
CH-3012 Bern
Switzerland

Mitsuru Ebihara
Department of Chemistry
Tokyo Metropolitan University
2-1-1, Fukasawa, Setagaya-ku
Tokyo 158
Japan

Peter A. J. Englert
Department of Chemistry
San Jose State University
San Jose, CA 95192

David Fink
Department of Physics
University of Pennsylvania
Philadelphia, PA 19104

Thomas Graf
Chemistry Department, B-017
University of California, San Diego
La Jolla, CA 92093-0317

Ralph P. Harvey
Department of Geology
University of Pittsburgh
Pittsburgh, PA 15260

Ulrich Herpers
Abteilung Nuklearchemie
Universität Köln
Zùlpicher Strasse 47
D-5000 Köln 1
Federal Republic of Germany

G. F. Herzog
Department of Chemistry
Rutgers University
New Brunswick, NJ 08903

Masatake Honda
Department of Chemistry
Nihon University
3-25-40 Sakura Josui
Setagaya, Tokyo 156
Japan

James E. Keith
Code SN3
NASA Johnson Space Center
Houston, TX 77058

Jeffrey Klein
Department of Physics
University of Pennsylvania
Philadelphia, PA 19104

Christian Koeberl
Institute of Geochemistry
Universität Wien
A-1010 Wien
Austria

- Devendra Lal**
Mail Stop A-020
Scripps Institution of Oceanography
University of California, San Diego
La Jolla, CA 92093-0220
- Bernard Lavielle**
Centre d'Etudes Nucleaire de Bordeaux-Gradignan
Le Haut Vigneau
33170 Gradignan
France
- L. Lindner**
Pr. Wilhelm van Oranjelaan 13
NL-1412 GJ Naarden
The Netherlands
- Marilyn M. Lindstrom**
Code SN2
NASA Johnson Space Center
Houston, TX 77058
- Michael E. Lipschutz**
Department of Chemistry
Purdue University
West Lafayette, IN 47907
- Kurt Marti**
Chemistry Department, B-017
University of California, San Diego
La Jolla, CA 92093-0317
- Thomas Meisel**
Institute of Geochemistry
Universitt Wien
A-1010 Wien
Austria
- Rolf Michel**
Zentraleinrichtung fr Strahlenschutz
Universitt Hannover
Hannover D-3000
Federal Republic of Germany
- Theo Michel**
Physikalisches Institut
University of Bern
Sidlerstrasse 5
CH-3012 Bern
Switzerland
- Robert K. Moniot**
Division of Science and Mathematics
Fordham University
College at Lincoln Center
New York, NY 10023
- Alfred O. Nier**
School of Physics and Astronomy
University of Minnesota
Minneapolis, MN 55455
- Kunihiko Nishiizumi**
Chemistry Department, B-017
University of California, San Diego
La Jolla, CA 92093-0317
- Robert C. Reedy**
Group SST-8, Mail Stop D438
Los Alamos National Laboratory
Los Alamos, NM 87545
- Robert Rssel**
Abteilung fr Nuklearchemie
Zlpicher Strasse 47
D-5000 Kln
Federal Republic of Germany
- Silvia Sartori**
Dip. di Fisica
G. Galilei University
Via Marzolo 8
Padova I-35131
Italy
- Henri Sauvageon**
Centre d'Etudes Nucleaire de Bordeaux-Gradignan
Le Haut Vigneau
33170 Gradignan
France
- Ludolf Schultz**
Max-Planck Institut fr Chemie
Otto-Hahn-Institute
Saarstrasse 23
D-6500 Mainz
Federal Republic of Germany
- S. Vogt**
Department of Chemistry
Rutgers University
New Brunswick, NJ 08903
- Hartwig Weber**
Max-Planck-Institut fr Chemie
Saarstrasse 23
D-6500 Mainz
Federal Republic of Germany
- Rainer Wieler**
Isotopengeochemie, NO C61
ETH-Zrich
CH-8092 Zrich
Switzerland
- Brigitte Zanda**
Laboratoire de Mineralogie
Museum National d'Histoire Naturelle
61, rue Buffon
Paris 75005
France